TEMPORAL AND SPATIAL TRENDS OF FINE PARTICULATE MATTER COMPOSITION IN FAIRBANKS, ALASKA

By

Kristian C. Nattinger, B.S.

A Thesis Submitted in the Partial Fulfillment of the Requirements

for the Degree of

MASTER OF SCIENCE

in

Chemistry

University of Alaska, Fairbanks

August 2016

Approved:

William R. Simpson, Committee Chair
Jennifer J. Guerard
Catherine F. Cahill
Thomas K. Green, Chair
Department of Chemistry and Biochemistry
Paul Layer, Dean
College of Natural Science and Mathematics
Michael Castellini, *Dean of the Graduate School*

Abstract

Fairbanks, AK experiences extreme winter pollution episodes that result in violations of the Fine Particulate ($PM_{2.5}$) National Ambient Air Quality Standards and pose significant health risks for inhabitants. We analyzed the 2006-2014 wintertime (November 1 to the end of February) $PM_{2.5}$ composition from four sampling sites in the Fairbanks North Star Borough (FNSB) to provide insight into sources and trends. We developed conversions for particulate carbon measurements that were sampled/analyzed with different methods to allow quantitative comparisons. Using these conversions, we found excellent mass closure between $PM_{2.5}$ mass concentration reconstructed from particulate composition and directly measured $PM_{2.5}$ mass concentration. The North Pole Fire Station #3 site (NPFS3) $PM_{2.5}$ mass concentration is nearly double the concentration at other sites in the FNSB and significantly different (t-test on log normalized data, 95% conf.). We observe significant differences (t-test, 95% conf.) in the $PM_{2.5}$ composition between the NPFS3 site and all other sites for most components. Comparison to source profiles indicates that the difference in $SO_4^{2-}/PM_{2.5}$ and organic carbon (OC)/$PM_{2.5}$ ratios is attributable to greater use of wood heat in the areas surrounding the NPFS3 site than in Fairbanks. This interpretation is supported by the results of the Home Heating Survey, which found a greater reported use of wood for heat in North Pole than in Fairbanks. Interannual variability is observed in the $PM_{2.5}$ composition. The increase in fuel oil price in 2009 is correlated with an increase in $OC/PM_{2.5}$ ratio and a decrease in the $SO_4^{2-}/PM_{2.5}$. The interannual variability of the $SO_4^{2-}/PM_{2.5}$ and $NH_4^+/PM_{2.5}$ ratios are correlated. The particles appear to be neutralized until 2010 when a drop in NH_4^+ is not accompanied by as large of a drop in anions leaving the particles acidic. The mean sulfur oxidation ratio is 5%, attributable to primary and possible secondary oxidation of SO_2. The results of our analysis supports modeling results that wood

smoke contributes a large fraction to the Fairbanks area $PM_{2.5}$. Our work also identified changes in the concentration, composition and spatial distribution of $PM_{2.5}$ that may help air quality managers in identifying effective $PM_{2.5}$ control strategies.

Table of Contents

Page

Page

Page

Page

Page

List of Figures

Page

List of Tables

Page

List of Appendices

Page

Glossary and Acronyms

ADEC: Alaska State Department of Environmental Conservation

Airshed: A portion of the atmosphere that disperses pollutants in a similar way. Used for air quality regulatory purposes.

AQS: Air Quality System. This is the source for almost all data used in this work. The AQS data is located on the EPA website at http://aqsdr1.epa.gov/aqsweb/aqstmp/airdata/download_files.html.

BAM: Beta attenuation monitor, an instrument that takes continuous ambient $PM_{2.5}$ concentration measurements

CALPUFF: Lagrangian atmospheric transport model (Scire et al., 2000)

CMAQ: Community Modeling and Analysis System https://www.cmascenter.org/cmaq/

CMB: Chemical mass balance, a receptor model produced by the EPA for conduction source apportionment from particulate speciation

CSN: Chemical Speciation Network

DRI: Desert Research Institute

$dsft^3$: Dry standard cubic feet, a unit used in (Ward, 2013), and in emission profiles

EC: Elemental carbon

EPA: US Environmental Protection Agency

FID: Flame ionization detector (used in thermal optical analysis methods)

FNSB: Fairbanks North Star Borough

FRM: Federal Reference Method, method used to determine NAAQS compliance (Frank, 2006)

GVEA: Golden Valley Electric Association

IGOR: Graphing and analysis software used in this thesis. Version 6.3.7.2, Wavemetrics Inc., Portland OR.

IMPROVE: Interagency Monitoring of Protected Visual Environments (Desert Research Institute, 2005)

MDL: Method detection limit

NAAQS: National Ambient Air Quality Standards, the EPA regulations for air quality

NCore: National Core, a set of air quality monitoring sites established by the EPA in 2011 (sampling site)

NIOSH: National Institute of Occupational Safety and Health (thermal optical analysis method) (Chow et al., 2001)

NPE monitor: North Pole Elementary (sampling site)

NPFS3: North Pole Fire Station #3 (sampling site)

NSS: Non-sulfate sulfur

NWS: National Weather Service

OC: Organic carbon

OCM: Organic carbon mass, includes bonded oxygen and hydrogen

OP: Pyrolized organic carbon (or organic pyrolysis fraction: the carbon that evolves after the introduction of O_2 and before the laser signal returns to its initial value

OPM: Other Primary $PM_{2.5}$ components synonymous with OPP.

$$OPM = 3.73 * \mathrm{Si} + 1.63 * \mathrm{Ca} + 2.42 * \mathrm{Fe} + 1.94 * \mathrm{Ti}$$

OPP: Other primary particulates. Synonymous with OPM

PMF: Positive Matrix Factorization, a receptor model for conducting source apportionment with particulate speciation data

$PM_{2.5}$: Fine particulate solid phase material less than 2.5 microns in diameter

RCM concentration: Reconstructed mass concentration

SANDWICH: Sulfate, Adjusted Nitrate, Derived Water, Inferred Carbonaceous Material Mass Balance Approach

SASS: MetOne Super Speciation Air Sampler System

SCC: Sharp Cut Cyclone. The cyclone separator used with the Super SASS sampler

Significant: Statistically significant. In this thesis statistical significance is determined using the t-test (95% conf.).

SIP: State Implementation Plan. The plan in place to address the non-attainment of the $PM_{2.5}$ NAAQS.

SOB: Fairbanks State Office Building (sampling site)

SOR: Sulfur Oxidation Ratio (Section 2.8.1)

STN: Speciated Trends Network, EPA approved method for carbon analysis

SASS: MetOne Super Speciation Air Sampler System NIOSH 5040 method. Many adaptations of the NIOSH method exist

SMAT: Speciated Modeled Attainment Test (used by ADEC to project future $PM_{2.5}$)

Thermal inversion: A meteorological condition when the change in temperature with elevation is positive, which facilitates stagnation of air and trapping of pollutants.

Thermal Optical Methods: Method used to analyze the particulate organic and elemental carbon. This method combusts the particulate carbon into CO2 which is measured with a flame ionization detector. The optical correction allows this method to separate organic from elemental carbon. (Desert Research Institute, 2005)

TOR: Thermal Optical Reflectance (optical correction method used in the thermal optical analysis) (Desert Research Institute, 2005)

TOT: Thermal Optical Transmittance (optical correction method used in thermal optical analysis) (Desert Research Institute, 2005)

$\mu g\ m^{-3}$: Micrograms of particulate per cubic meter of filtered air

URG: URG-3000N Sampler, used with the IMPROVE module http://www.urgcorp.com/index.php/systems/manual-sampling-systems/urg-3000n-carbon-sampler

VOC: volatile organic carbon

Volatile: Turns from liquid/solid to gas at ambient temperatures.

WSCP: Wood Stove Changeout Program

XRF: X-ray fluorescence, a form of spectroscopy

Acknowledgements

Without the help of many people the product in front of you would not exist. My first thank you goes to my advisor, Bill Simpson who put countless hours into writing code that made the analysis of such a large data set possible and ensured that our work was easily replicable. Along the way Bill took the time to teach me the process of critical and rigorous data analysis as we worked through the many puzzles addressed in this research. I know as I move forward into my next step as a science teacher, that I will bring with me a deeper understanding of the process of science, and a standard for rigor that will make me a better caretaker of knowledge.

Deanna Huff and others from the Alaska State Department of Conservation provided a ton of support as well. Despite their busy schedule, Dea and others took time to catch us up to speed on what is already known about these particles, explained EPA modeling, and provided us with the data that is not available through the EPA.

I have rarely in my life seen a data set of environmental samples with r^2 values that were so close to one, and I know we have many hardworking technicians to thank for collecting this data with such care.

And of course without the strong support of the University of Alaska, Fairbanks, College of Natural Sciences and Mathematics, and the Geophysical Institute for providing teaching and research assistantships this work could not have been possible. I am grateful for travel funding from both the College of Natural Sciences and Mathematics as well as the Biomedical Learning and Student Training program.

Dedication

I would like to dedicate this thesis to all the great people who I met while living in North Pole, Alaska during my first year in graduate school. Their friendship got me through the hardest academic challenge of my life, and their critical observations regarding air pollution management (and strong desire to share these observations!) motivated me to work hard to understand the complexity of air quality management. I hope that we can all work together using science to make the air we breathe cleaner, and keep our homes warm at night.

Chapter 1: Introduction

1.1 Motivation

Air pollution is estimated to annually cause seven million premature deaths worldwide, with over three million attributed to fine particulate matter (Holstius et al., 2014). As evidence continues to indicate that these particles present a serious threat to public health, the US Environmental Protection Agency (EPA) lowered the 24-hour National Ambient Air Quality Standard (NAAQS) limit to 35 micrograms of particulate matter with a diameter ≤ 2.5 μm ($PM_{2.5}$) per cubic meter of air (μg m^{-3}) in 2007 (EPA, 2014b).

Fairbanks currently violates this standard during thermal inversions that occur exclusively in the winter, exposing residents to some of the highest $PM_{2.5}$ levels in the U.S. (Ward, 2013). These violations create a legal requirement for Fairbanks to reduce wintertime $PM_{2.5}$. The portion of the Fairbanks North Star Borough (FNSB) that is considered in non-compliance with EPA $PM_{2.5}$ standard (referred to as the non-attainment area) is depicted in Figure 1.1.

Identification of trends in the concentration, composition and spatial distribution of $PM_{2.5}$ during these winter events may help determine the most effective actions to reduce $PM_{2.5}$. This information may also identify the locations and causes of the most serious levels of $PM_{2.5}$ and the effectiveness of current mitigation programs (Section 1.3.2).

Figure 1.1: Location of Fairbanks and the $PM_{2.5}$ non-attainment area in Alaska (Alaska Department of Environmental Conservation, 2015)

1.2 Review of Health Effects of Fine Particulates

Exposure to high levels of $PM_{2.5}$ for even short periods of time is associated with deleterious health impacts (Naeher et al., 2007). The EPA Integrated Science Assessment for Particulate Matter (EPA, 2014b) found increased mortality and respiratory illness correlated with exposure to increased $PM_{2.5}$ mass concentration. Specifically, cardio and cerebral-pulmonary illnesses are associated with long term exposure to fine particulates, and high concentrations can create severe illness in people who already suffer from these conditions (Zanobetti et al., 2014). A hospital visit study specific to Fairbanks found a 6% increase in hospitalizations due to these conditions during NAAQS $PM_{2.5}$ violations (Kossover, 2010). In addition, chronic exposure to low concentrations of $PM_{2.5}$ has been recently correlated with degenerative mental diseases including Alzheimer's (Jung et al., 2015). Based on these extensive epidemiological studies that assess the health effects of particles from a variety of sources and polluted airsheds the EPA has

chosen to use overall $PM_{2.5}$ mass concentration as the regulatory standard for particulates. NAAQS compliance is determined by drawing size sorted ambient air through a filter for twenty-four hours at breathing level. The filters are shipped to a lab and the gravimetric $PM_{2.5}$ mass is determined allowing calculation of the ambient gravimetric mass concentration by dividing the $PM_{2.5}$ mass by the total volume of air pulled through the filter. This method is reproducible and allows representative $PM_{2.5}$ mass concentration measurements to be make at sampling sites across the U.S. While some current research indicates that the toxicity of PM is affected by composition and source (Seagrave et al., 2006), (Kaivosoja et al., 2013) and (Naeher et al., 2007), there is currently insufficient data to support changing regulations, and no cost effective and reproducible test for composition that could be implemented on a regulatory scale.

1.3 Background

$PM_{2.5}$ is composed of solid or liquid phase particles that are smaller than 2.5 microns in diameter. These particles stay suspended for extended periods of time and travel through dispersion similar to gases, entering structures through door cracks and other openings.

The highest $PM_{2.5}$ gravimetric mass concentrations are measured on colder days due to increased emissions and thermal inversions that trap these pollutants at breathing level. Emissions are known to increase during cold weather from a variety of sources, in particular home heating. Thermal inversions occur when the atmospheric temperature increases with elevation and are common during the Fairbanks winter. A radiosonde from the Fairbanks international airport during an inversion (Figure 1.2) shows how the inverted temperature profile can start at ground level during the extreme cold of the Fairbanks winter, which traps pollution very effectively.

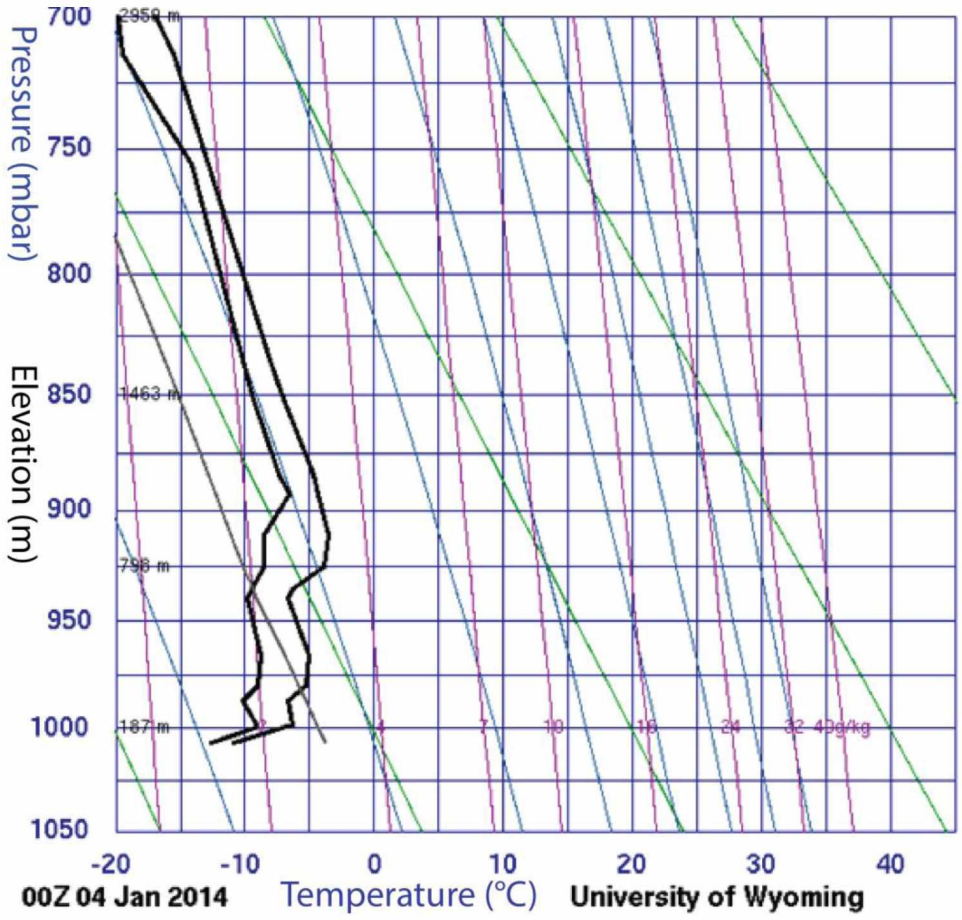

Figure 1.2: Radiosonde taken at the Fairbanks International Airport. Note that temperature is depicted with the black line on the right, and the dew point temperature is on the left. Both use units of °C, shown on the x-axis. Units for the y-axis are atmospheric pressure in mbar. In this radiosonde, temperature increases with elevation (secondary y-axis, units of meters) for the first about 187m above ground level indicating a strong thermal inversion (University of Wyoming Department of Atmospheric Science, 2015).

1.3.1 Fairbanks Emission Sources

Figure 1.3 depicts the $PM_{2.5}$ emissions that occur within the FNSB airshed. $PM_{2.5}$ is emitted either directly into breathing level, usually by non-point sources, or above breathing level, usually by point sources. In the Fairbanks area, point sources are almost entirely composed of electrical generators. $PM_{2.5}$ is measured at breathing level by samplers located on the roofs of buildings because this is where people are exposed to particulate pollution. The goal of this thesis and much

of the other research that has been completed on Fairbanks air pollution is to better understand breathing level particulates.

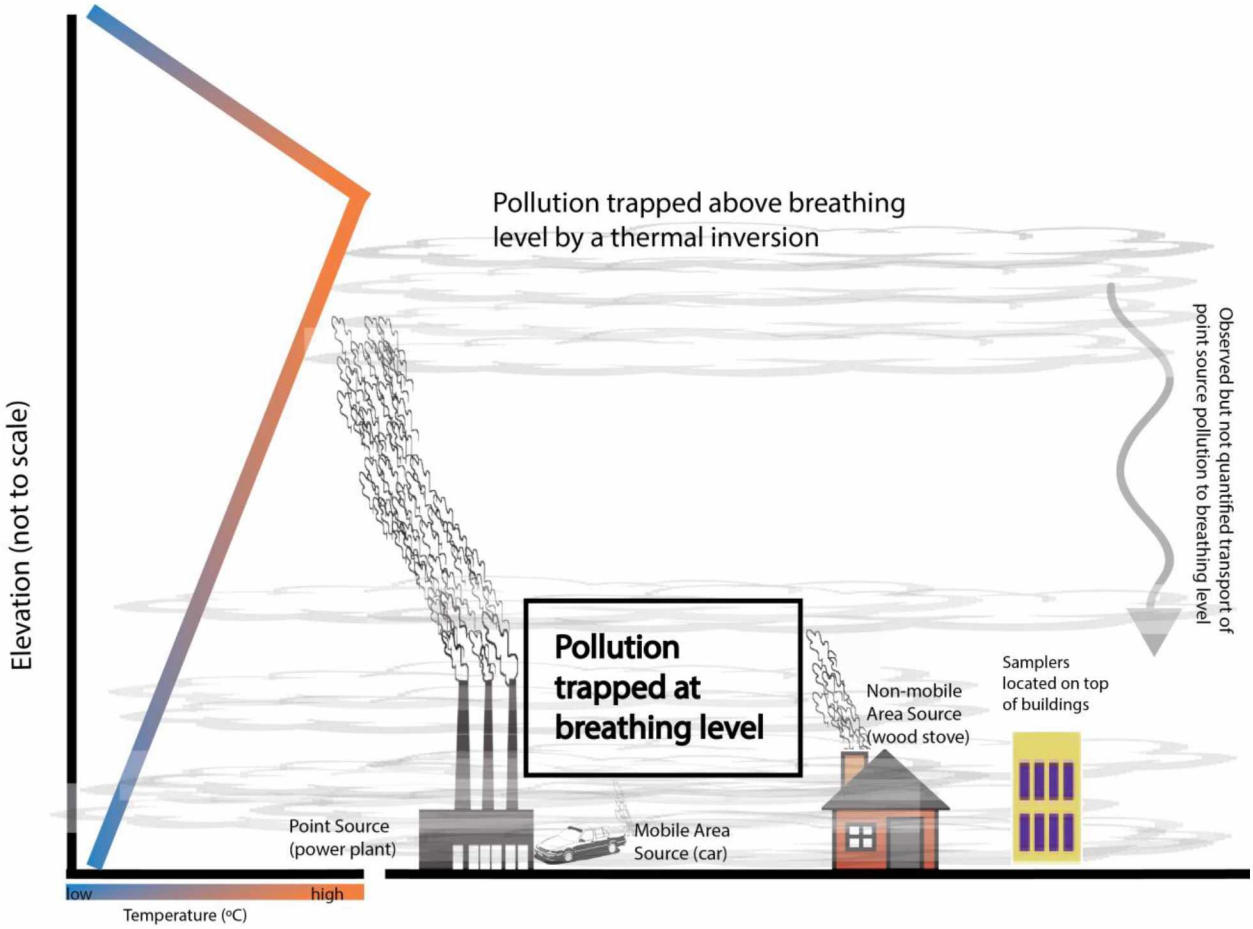

Figure 1.3: Diagram of the FNSB airshed. This diagram depicts a day with a strong thermal inversion, shown by the temperature profile on the right axis. The focus of this thesis is to better understand the pollution trapped at breathing level, using data from the rooftop ambient samplers. Credit for clip art: http://www.clipartbest.com/clip-art-factory

Emission inventory modeling uses measured emissions and the estimated total emissions from each source category to estimate the contribution of each source to the particulates in an airshed. Table 1.1 shows the emission data that is available in the Fairbanks area, and the form of this data. While the point source emissions are known to a high degree of certainty due to continuous monitoring, other sources are not known to this level of certainty. This variability is

one reason that other modeling approaches are needed to identify the sources of particulates in the airshed. Table 1.2 shows total emissions into the Fairbanks airshed calculated from emission inventory modeling, indicating that the majority of particulates are from home heating, specifically wood smoke. Emission inventory modeling does not separate particles that make it to breathing level from those that stay above the inversion, and thus has limited use for this thesis which is focused on breathing level $PM_{2.5}$.

Table 1.1: $PM_{2.5}$ source classifications and types of available emissions data for Fairbanks specific sources (Alaska Department of Environmental Conservation, 2015). In addition to this data, source profiles are available for all emission sources from locations other than the Fairbanks.

Source Type	Example	Data Available
Point Sources	Electrical Generation	Continuous monitoring
Area Sources	Home Heating	Fairbanks source profiles, emission factors
On Road Mobile Sources	Cars	Emission factors, vehicle warm up data
Non-Road Mobile Sources	Snowmobiles	Emission factors

Table 1.2: 2008 model based estimation of daily $PM_{2.5}$ emissions by source sector to total $PM_{2.5}$ (Alaska Department of Environmental Conservation, 2015). These values include emissions above and below the inversion layer. The term 'actual measurement' in reference to point source emissions indicates that these emissions have been directly measured.

Source Sector	Est. % of Total Emissions
Wood Space Heat, Area	54.9
Oil Space Heat, Area	1.1
Other Area Sources	1.2
Point (Actual Measurement)	28.6
On-Road, Running Exhaust	8.8
On-Road, Start and Idle Exhaust	4.9
Non-Road Exhaust	0.5

1.3.2 Current Mitigation

FNSB has implemented two programs designed to decrease the emissions from wood stoves based on the finding that a significant portion of breathing level $PM_{2.5}$ is from wood smoke (Section 1.7). The wood stove changeout program (WSCP) was implemented in 2010 and created a financial incentive for individuals to replace solid fuel heating appliances that emit large amounts of $PM_{2.5}$ with EPA certified appliances that meet model specific particulate emission limits (for example, 3.1g/hour for non-catalytic wood stoves). EPA stoves emit up to 87% less particulates than non-certified stoves (Broderick and Houck, 2005). Also implemented in 2010, the "Burn Wise" education program (http://burnwise.alaska.gov) educates local residents on the benefits of burning dry wood, specifically a reduction in particulates and increased heating efficiency. Both programs are still in use.

1.4 Particle Formation

$PM_{2.5}$ is the result of direct emissions of particle phase material, or formed as the result of transformation of primary gases to less volatile compounds that either condense onto existing particles or form new particles (Jacob, 1999).

Emissions that contribute to $PM_{2.5}$ can be due to combustion, biogenic emissions and dust. Due to the lack of biological activity and wind/dust in the Fairbanks winter, it is assumed in this thesis that the majority of this $PM_{2.5}$ is sourced almost entirely from combustion processes.

1.4.1 Primary Particles

Primary emission particulate composition measured from a specific source are referred to as source profiles (Section 1.6). Primary emissions are classified as either filterable emissions - particles emitted directly in the solid or liquid phase; or condensable emissions - substances emitted in the gas phase that condense quickly into the solid or liquid phase during cooling (Torvela et al., 2014). Elemental carbon (EC) is entirely the result of primary emissions (Turpin and Lim, 2001). Inorganic gases may condense during wood combustion onto zinc oxide (ZnO) particles to form primary condensable particulate, or ash (Torvela et al., 2014). This material is considered primary despite being the result of gas condensation, since it condenses so quickly that it is measured in source profiles.

1.4.2 Secondary Particle Formation

Secondary processes governing particle formation are complex and varied (Huff, 2014). Nitrogen dioxide (NO_2) oxidizes to nitric acid (HNO_3) and reacts with ammonia gas (NH_3) to form secondary ammonium nitrate (NH_4NO_3) aerosol. The combination of primary and secondary NH_4NO_3 aerosol makes up about 4% of the $PM_{2.5}$ mass concentration in Fairbanks. This estimation

includes particle bound water (PBW) that condenses with NH_4NO_3 (Huff, 2014). The association of NH_4NO_3 with PBW occurs when the relative humidity is greater than the critical relative humidity of NH_4NO_3. NH_4NO_3 has a critical relative humidity of about 60% (Adams and Merz, 1929). The relative humidity in Fairbanks during the winter is often close to 100% since extremely cold air is unable to hold any measureable amount of water, and a measurement for the PBW was not encountered in the literature. Volatile organic compounds (VOCs) and semi-volatile organic compounds (SVOCs) can contribute secondary mass to the organic carbon (OC) fraction of $PM_{2.5}$. After oxidation in the atmosphere, VOCs become more polar and less volatile due to an increase in their size and oxygen mass. These less volatile compounds can condense onto previously formed particulate matter, or nucleate new particles (Seinfeld and Pankow, 2003). Sulfur oxidation can contribute to secondary particle formation, and is described in Section 1.4.3.

1.4.3 Sulfur Oxidation

The combustion of fuel that contains sulfur releases gaseous sulfur dioxide (SO_2) and primary particulate sulfate (SO_4^{2-}). SO_2 may be oxidized in the gas or particle phase to form sulfuric acid (H_2SO_4). In the gas phase, photo-oxidation of SO_2 often takes place through hydroxyl radical ($\cdot OH$) mediated oxidation. Gaseous H_2SO_4 quickly condenses to the particle phase, either nucleating new particles or condensing onto existing particles. In the particulate phase, photo-oxidation generally takes place through hydrogen peroxide (H_2O_2) or ozone (O_3) mediated oxidation. Oxidation of SO_2 in the particle phase results in particle growth and not the creation of new particles (Alexander et al., 2009). Photochemical mechanisms may not occur during the Fairbanks winter due to the lack of photon flux and removal of ozone by NO_x (Joyce et al., 2014). However, evidence exists that secondary sulfur oxidation is taking place in the Fairbanks airshed, and alternative oxidative mechanisms have been proposed. Specifically, the Community Modeling

and Analysis System (CMAQ) atmospheric model used by the ADEC was unable to reproduce the observed particulate sulfate (SO_4^{2-}) without the addition of the water vapor necessary to allow transition metal catalyzed oxidation (a non-photochemical mechanism) (Alaska Department of Environmental Conservation, 2014). All other $PM_{2.5}$ components are accurately represented in the model, including oxidation products such as particulate nitrate (NO_3^-). The transition metals iron (Fe) and manganese (Mn) have been shown in laboratory studies to catalyze the oxidation of SO_2 (Brandt and van Eldik, 1995) providing evidence that this mechanism may exist in ambient conditions as well.

Chemical mass balance models (Section 1.7.3) are also unable to reproduce measured particulate SO_4^{2-} and this issue is dealt with by adding secondary SO_4^{2-} as a separate source profile (Ward, 2013). The lack of a known sulfur oxidation mechanism decreases the ability for models to predict how changing sulfur emissions will impact the production of particulate sulfate (Huff, 2014).

Joyce et al. (2014) notes that a very fast oxidative mechanism could result in secondary SO_4^{2-} appearing to be a primary pollutant. This is an example of what is referred to as "condensable emissions" by (Torvela et al., 2014), and this condensation may create errors in source profiles since the cooling methods used in measuring source profiles differ from the cooling that takes place as exhaust exits a source into ambient conditions (especially during the Fairbanks winter).

The combustion of heating oil is likely the most significant source of sulfur at breathing level. Heating oil sold in Fairbanks has 2,500 ppm sulfur (Leelasakultum et al., 2012) much higher than in other states. Home heating devices that combust this high sulfur oil emit gases and particles at breathing level.

Evidence is contradictory regarding whether emissions that occur above the inversion layer from point sources (which are known to contain sulfur) are transported to breathing Tran and Mölders (2011) observed that wind direction does not impact the ground level $PM_{2.5}$ measured at the Fairbanks State Office Building (SOB) during inversion events, and thus conclude that most of the emissions from point sources such as power plants remain above the inversion layer and do not heavily impact breathing level $PM_{2.5}$. The certainty of this result is limited by the difficulty inherent in determining wind direction during inversion events, which are characterized by low wind speed (Tran and Mölders, 2011), and by the limited number of sampling locations. In contrast, Peltier (2012) measured spikes in the trace metals mercury (Hg) and selenium (Se), known tracers of coal burning, in breathing level $PM_{2.5}$ during times when air motion suggested transport from a nearby coal power plant. These observations provide evidence that emissions from point sources are transported to breathing level.

The ADEC emission inventory determined that 64.4% of total SO_2 emitted in the airshed (both above and below inversion) is due to point sources. Atmospheric transport and chemistry models utilized by the ADEC estimate that 22% of breathing level SO_2 is from point sources, 78% from heating oil, and <1% from mobile sources (Alaska Department of Environmental Conservation, 2015). Peltier (2012) used this result to determine that 15% of breathing level particulate SO_4^{2-} is from point sources.

Particulate sulfur may be biogenic or anthropogenic. Shakya and Peltier (2013) used data from the 24 hour filter samples taken in Fairbanks, and observed 22% disagreement between SO_4^{2-} measured with ion chromatography (IC) and elemental sulfur measured with x-ray fluorescence (XRF) providing evidence for a non-sulfate (biogenic) sulfur source. Disagreement between sulfur measurements was largest in the summer. Peltier (2012) sampled submicron (10-15 nm range)

particles in Fairbanks during the winter using a particle-into-liquid sampler (PILS), and analyzed elemental sulfur with an inductively coupled plasma mass spectrometry (ICP-MS) and sulfate with IC. Peltier (2012) found almost perfect agreement between hourly SO_4^{2-} and elemental sulfur measurements (correlation slope of 0.986), indicating no biogenic sulfur during this time period. The discrepancy between these two studies may indicate that biogenic sulfur is only emitted during the summer, or be the result of the larger error associated with the 24 hour filter samples analyzed with XRF as part of the work done by Shakya and Peltier (2013).

1.5 Transport

Emissions from sources outside of the non-attainment area contribute negligibly to $PM_{2.5}$ during the winter (Alaska Department of Environmental Conservation, 2015). At most 1 $\mu g\ m^{-3}$ of ambient $PM_{2.5}$ in Fairbanks is due to transport from Asia (Zhang, 2010) and (Cahill, 2003).

1.6 Source Profiles

Source profiles are measured by sampling pure exhaust from a specified source. The sampled material is diluted, cooled, separated by particle size, and collected either by filtration or another method. The method of cooling the exhaust varies between source profiles and may alter source profile measurements, particularly of semi-volatile compounds. After cooling, particulates are often collected and analyzed using similar methodology as the ambient filters (described in Chapter 2), though not always. For example, the source for the gasoline exhaust profiles used in this work, Zielinska et al., (1998) used a flow rate of 113 L min^{-1}, essentially the same flow as the URG sampler used to collect ambient data in Fairbanks, and similar analysis methods. Source profiles are utilized in CMB analysis (Section 1.7.3).

1.7 Prior Modeling Results

1.7.1 SANDWICH Mass Balance Modeling

During transport and storage of the filters the particulate composition changes due to volatilization and deposition. The ADEC uses the SANDWICH (Sulfate, Adjusted Nitrate, Derived Water, Inferred Carbonaceous Material Mass Balance Approach) method to adjust measured mass concentrations to represent the actual composition of the particles collected on the filter (Frank, 2006). This method estimates the amount of volatized nitrate (based on temperature), adjusts the ammonium concentration to achieve charge balance, and uses the extended aerosol inorganic model (Clegg and Wexler, n.d.) to estimate PBW. SANDWICH addresses mineral oxides by calculating the "crustal material" utilizing Equation 1-1 (Frank, 2006). Crustal material is also referred to as other primary particulate material (OPP).

Thermal optical methods were used to measure the organic carbon (OC) and elemental carbon (EC) mass in the particulates collected on the filters. In this method, the carbon collected on the filters is combusted completely to CO_2, which is then measured using a flame ionization detector (FID). This measurement does not take into account oxygen and hydrogen which are present on most organic carbon molecules. The organic carbon mass (OCM) is estimated based on mass closure (Equation 1-2) in SANDWICH (Frank, 2006). Composition measurements other than OCM are subtracted from the gravimetric $PM_{2.5}$ mass, and the result is the estimated OCM. Results from using the SANDWICH mass balance approach to estimate the Fairbanks $PM_{2.5}$ composition are shown in Figure 1.4.

$$OPP = 3.73 \times Si + 1.63 \times Ca + 2.42 \times Fe + 1.94 \times Ti \qquad \text{[Equation 1-1]}$$

$$OCM = PM_{2.5}\,\text{mass} - (SO_4^{2-} + NO_3^{-} + PBW + NH_4^{+} + EC + OPP + 0.5) \qquad \text{[Equation 1-2]}$$

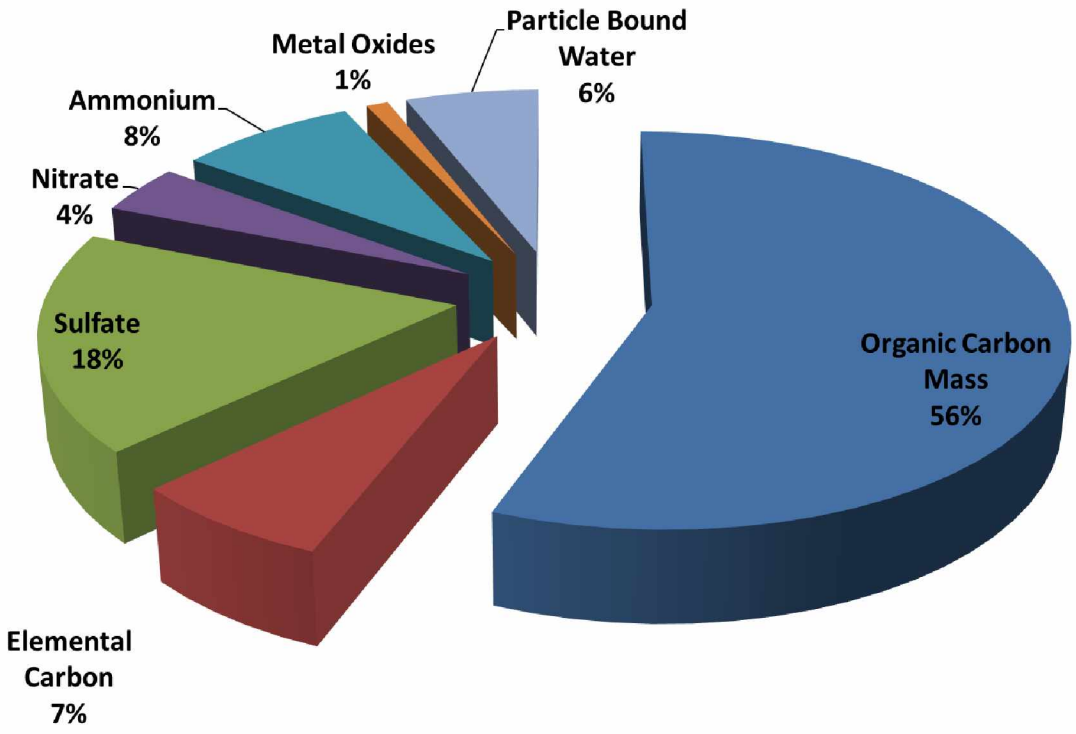

Figure 1.4: SANDWICH model results showing the estimated average 2006-2010 $PM_{2.5}$ composition from the Fairbanks State Office Building for winter days whose $PM_{2.5}$ levels were in the top 25% of polluted days (Huff, 2014).

1.7.2 Organic Carbon Mass Estimations

The SANDWICH method provides one approach to estimating the OCM. Another approach is to multiply the measured OC by a literature based multiplier, as shown in Equation 1- 3. Figure 1.5 shows the results of using this approach to calculate the composition of the Fairbanks $PM_{2.5}$. The results of this approach are very similar to the results obtained from using the SANDWICH approach.

Equation 1-3 uses the 1.4 multiplier that is for "fresh" particles. For "aged" particles, some sources replace the 1.4 multiplier with 1.8 (Chow et al., 2010). The terms "fresh" and "aged" are

not clearly defined, but refer to relative amounts of oxidation and other atmospheric processing. The ADEC assumes Fairbanks particles have experienced negligible processing, and thus uses the 1.4 multiplier. The 1.4 multiplier is also used in this thesis.

$$OCM\ (\mu g\ OCM/m^3) = [1.4\ \mu g\ OCM/\mu g\ OC] * [measured\ OC\ (\mu g\ OC/m^3)] \qquad [Equation\ 1\text{-}3]$$

While use of a multiplier between 1.4 and 1.8 allows for mass closure, and is used almost exclusively in particulate literature and regulatory work, there is evidence that these multipliers are too low. Turpin and Lim (2001) report that use of a multiplier greater than 1.6 (urban) up to 2.1 (rural) would be more appropriate. These results are based on gas chromatograph mass-spectrometer (GCMS) identification of the organic compounds in ambient $PM_{2.5}$. Using this method, highly polar multifunctional compounds are not eluted through the GC and are not included in the results of this analysis. These compounds make up 80-95% of the OC in $PM_{2.5}$, and thus (Turpin and Lim, 2001) were only able to identify 7-15% of the total OCM, limiting the accuracy of the multipliers obtained from GCMS measurements. The nature of this analytical issue indicates that the correct multiplier is likely even higher than 1.6 to 2.1, since the polar organic molecules that are omitted have a larger molecular mass to carbon mass ratio than the less polar molecules that were able to be measured.

1.7.3 Source Apportionment Modeling

Previous research has attempted to identify the sources of the Fairbanks ambient $PM_{2.5}$ by inputting speciation data into algorithm based models. Two of the models that have been used to interpret the Fairbanks data include chemical mass balance (CMB) and positive matrix factorization (PMF) modeling, which utilize different strategies to identify particulate sources.

CMB combines different source profiles to best represent the measured ambient $PM_{2.5}$ emissions. The advantage of this approach is that the source profiles truly represent the primary emissions of actual emitters. However, emissions within a single source vary from one emitter to another. For example, a woodstove will produce different emissions based on its age and type of fuel used in the appliance. These differences are not accounted for with CMB modeling. CMB modeling also does not account for secondary aerosol formation or transformation.

PMF modeling does not utilize source profiles. Rather, this method uses correlations within the $PM_{2.5}$ composition data to generate mathematical constructs referred to as source groups or factors that are representative of one or more actual sources. The model interprets correlation between different compositional measurements as an indicator that these components are from the same source. How well these factors distinguish the actual sources from one another depends on both environmental variables and data quality. False correlations may be produced by an environmental factor (such as cold temperatures) simultaneously increasing the contribution from multiple sources (wood and oil stoves). These factors are named based on how closely they represent a source profile. PMF modeling accounts for secondary aerosol formation since it is based on ambient measurements, not source profiles.

Table 1.3 shows the results of both CMB and PMF modeling that was used to analyze particulate data from Fairbanks. Both models found that wood smoke was the largest single source of particulate mass. Ward (2013) performed CMB analysis on the Fairbanks data set using two separate groups of source profiles. The first utilized ninety-one EPA source profiles (EPA, 2014b) or profiles taken by the University of Montana (Ward, 2013), and the second relied on nine source profiles that were taken with fuel types and combustion units specific to the Fairbanks area (Ward, 2013). Both analyses determined wood smoke to be the largest single contributor to $PM_{2.5}$ in

Fairbanks, however there is a larger range in the results from the Fairbanks profiles (Table 1.3). The difference between CMB analyses is considered a "good fit," indicating that the choice of profiles is not affecting the analysis results (Ward, 2013). Wang and Hopke (2014) utilized PMF modeling to address the same question using the same data, but from a slightly different period of time. This model attributed 40% of $PM_{2.5}$ to a wood smoke factor. This means that the model found 40% of the ambient particulate mass concentration was attributed to a profile that appears to fit the emission profile of wood smoke, but could include mass lost or gained from other emission sources.

Source apportionment modeling (Table 1.3) shows inconsistency with the emission factor based modeling results (Table 1.2). However, both approaches determined wood smoke to be the largest single contributor to breathing level particulates.

Table 1.3: Contribution of wood smoke to $PM_{2.5}$. Model output using Fairbanks SOB data (Ward, 2012) and (Wang and Hopke, 2014).

Reference	Model, Profiles	Wood Smoke
(Ward, 2012)	CMB, EPA	60-80%
(Ward, 2012)	CMB, Fairbanks	30-77%
(Wang & Hopke, 2014)	PMF	40%

1.8 Hypotheses

1.8.1 Hypothesis 1: Significant differences in $PM_{2.5}$ composition and mass concentration will exist between North Pole and Fairbanks sampling sites.

We hypothesize that the component/$PM_{2.5}$ mass ratios of major components (OC, EC, SO_4^{2-}) and minor components (K^+ and Zn) will differ spatially between sampling sites in North Pole and Fairbanks due to different particulate sources in these cities. The Fairbanks Home

Heating Survey (Table 1.4) found that more people use wood to heat their homes in North Pole than Fairbanks. Based on the composition of wood and oil source profiles (Section 3.5) we[1] hypothesize that there is a greater $OC/PM_{2.5}$ ratio in North Pole, and a greater $SO_4^{2-}/PM_{2.5}$ ratio in Fairbanks.

Table 1.4: Prevalence of wood and oil in home heating. 2013, 2014, 2015 home heating survey results. The percentage of time that various heating devices are used to heat homes in the FNSB was estimated by respondents to the Fairbanks Home Heating Survey, and normalized to account for concurrent use of multiple heating devices (Carlson and Zhang, 2015).

Location	Wood Contribution	Oil Contribution
Downtown Fairbanks	12.1%	83.1%
North Pole	28.3%	68.4%

1.8.2 Hypothesis 2: A reduction in the $OC/PM_{2.5}$ ratio will be observed after 2010.

The Wood Stove Changeout Program (WSCP) which began in 2010 provided a financial incentive for homeowners to replace polluting hydronic heaters and older wood stoves with EPA certified devices. Hydronic heaters, also known as outdoor boilers, can burn a wide range of fuel types and quality, and modeling results indicate that hydronic heaters are responsible for the vast majority of the particulate pollution in the Fairbanks area (Davies et al., 2009). Replacing a non-certified stove with a certified stove is known to reduce the emissions per heat produced (Davies et al., 2009), thus the 1187 wood stoves and hydronic heaters exchanged as of the 2013-2014 winter will have certainly reduced the emissions from these homes. The Burn Wise Education Program which began in the summer of 2010 with the hiring of the programs first full time education and outreach employee (Thompson, T.: Personal Communication, email, ADEC, 2016)

[1] "We" is defined in this thesis as the author and co-authors of the research that lead to this thesis. This includes Kristian Nattinger, William Simpson, and Deanna Huff.

may also have reduced the wood smoke emissions during this time period. However, it is not certain if the total emissions from wood smoke will have decreased significantly during this time period. We hypothesize that a decrease in wood stove based emissions has occurred and will result in a decrease in the ambient $OC/PM_{2.5}$ ratio, and subsequent increase in all other $PM_{2.5}$ components. This increase will be most noticeable in the next largest component, the $SO_4^{2-}/PM_{2.5}$ ratio. This hypothesis is based on fuel content estimates from Appendix III.4.7 of the State Implementation Plan (SIP) (Alaska Department of Environmental Conservation, 2015), and source profile data (Section 3.5). Table 1.5 shows the total number of stoves replaced as of the end of 2013 (essentially the end of the data set used in this thesis). Due to the increase in number of stoves replaced we anticipate finding a decrease in the $OC/PM_{2.5}$ ratios and an increase in the $SO_4^{2-}/PM_{2.5}$ from 2011 to 2013.

Table 1.5: Number of stoves replaced by the WSCP (Huff, 2014). For a more detailed list of changeouts Figure 5.1.

Time Period	Number of Stoves Replaced
End of 2011	325
End of 2013	1187

If the sulfur content of the fuel oil used in the Fairbanks area has changed during the study period, this change would confound the attempt to use composition to assess the effect of the WSCP. Table 1.6 shows fuels used in electrical generation. Note that the sulfur content of #2 fuel oil is not the measured concentration in the fuel oil refined in the Fairbanks area, but rather the maximum allowed under ASTM specifications. The Naphtha fueled North Pole Expansion Plant that went online in 2006 (GVEA, 2015) would reduce the amount of atmospheric sulfur emitted

from electrical generation in North Pole, however it is unknown if this change could have affected breathing level particulates (Section 1.3.1).

Table 1.6: Sulfur content and SO_2 emissions of different fuel types (Alaska Department of Environmental Conservation, 2014). The sulfur content for #2 fuel oil is based on the maximum specified sulfur for S5000 rated #2 fuel oil (ASTM International, 2010).

	HAGO	**#2 Fuel Oil**	**Naptha**	**ULSD**
Sulfur (wt%)	1	0.5	0.05	0.0015
SO_2 emissions (lb $MMBtu^{-1}$)	1.01	0.51	0.06	0

1.8.3 Hypothesis 3: Secondary sulfur oxidation is taking place during the Fairbanks winter.

Exploratory investigations into the possible secondary oxidation of atmospheric gaseous SO_2 to particulate SO_4^{2-} were completed. The sulfur oxidation ratio (SOR) (Section 2.8) was used as an indicator of the amount of oxidation (both primary and secondary) taking place in the airshed. We assumed that the SOR of directly emitted #2 fuel oil exhaust is entirely due to primary oxidation, and compared the primary SOR to the ambient SOR to determine the presence of secondary sulfur oxidation. Based on the inability of the CMAQ atmospheric chemistry model to account for the measured SO_4^{2-} without secondary oxidation (Huff, 2014), we hypothesized that measureable secondary oxidation is taking place.

The relationship of the SOR with Zn as a tracer for other transition metals was investigated to assess if metal catalyzed oxidation is occurring (Section 1.4.3). One possible source for these metals is the combustion of waste motor oil, whose source profile contains large amounts of metals (Ward, 2013). Transition metals such as iron (Fe) and/or manganese (Mn) which have been observed to catalyze this reaction are measured in Fairbanks ambient $PM_{2.5}$ very close to or below the MDL of x-ray fluorescence analysis (Section 2.1.2) and thus cannot be used in this analysis. Zinc (Zn) is a known additive to motor oil (Wang and Hopke, 2014), is observed in the ambient

Fairbanks particulate material at concentrations above the MDL, and is observed in the source profile for waste oil two orders of magnitude above the level found in other local Fairbanks source profiles (Ward, 2012). Table 1.7 summarizes the reasons that Zn was chosen as the best tracer for other transition metals sourced from the burning of waste motor oil. As further justification for the use of Zn as a tracer for waste oil combustion, PMF modeling found an unknown factor that they named the "unknown Zn profile" due to the high concentration of Zn in this factor. This factor was the third most prevalent winter $PM_{2.5}$ source from this analysis (Alaska Department of Environmental Conservation, 2014). The modelers attributed it to waste oil burning, vehicle oil burning, or another unknown source. Thus, investigating Zn may allow a more complete understanding of the sources of Fairbanks $PM_{2.5}$ as well as provide a tracer for waste oil and co-emitted transition metals. Higher concentrations of Zn will be assumed to represent higher concentrations of all metals including Fe and Mn. Zn and other metal particulates are released as a result of vehicle oil burning and brake ablation (Sanders et al., 2003) and thus increased traffic will confound the use of zinc as a tracer for waste oil combustion. In particular, increased heavy truck traffic is known to increase particulate Zn. Large amounts of Zn are found in the PMF factor for diesel, and both truck traffic and the burning of waste oil for heat increase in the winter (Wang and Hopke, 2014).

Spatial comparison (Section 1.8.1) of Zn concentrations was also completed to investigate differences between Fairbanks and North Pole concentrations, but no hypothesis regarding waste oil combustion can be made since quantitative data does not exist on the amount of waste oil burnt in Fairbanks or North Pole. However, greater vehicle traffic may introduce more Zn into the air through brake ablation in Fairbanks than in North Pole.

Table 1.7: MDL, ambient concentrations, and Fairbanks source profile concentration of Zn. MDL is from (EPA, 2014a), mean ambient concentration is from (EPA, 2014b), and the waste oil profile is from (Ward, 2013).

Zn XRF MDL	Mean [Zn] in Ambient Fairbanks Air	[Zn] in Waste Oil Source Profile
0.00058 $\mu g/m^3$	0.062 $\mu g/m^3$	0.161 $\mu g/m^3$

Chapter 2: Methods, Sampling Sites and Data Sources

2.1 Sampling and Analysis Methods

No new data were collected as part of this work. $PM_{2.5}$ mass concentration and composition data were collected at a variety of stationary and mobile sites in the Fairbanks non-attainment zone as part of the FNSB's long term air quality monitoring effort, and these data were analyzed for this thesis. This data set includes four sampling sites and spans 2006-2014 at the Fairbanks SOB site. Other sampling locations have shorter periods of available data.

2.1.1 Sampling Methods

2.1.1.1 Sampling Methods Overview

Ambient air was sampled with one of two ambient air samplers, either the MetOne Super Speciation Air Sampler System (SASS) or the URG-3000N (URG). Both samplers sort ambient particles by size to ensure only particles with an aerodynamic diameter less than 2.5 microns are collected on the filters. The SASS sampler uses a Sharp Cut Cyclone (Met One Instruments Inc, 2016), and the URG sampler uses the URG-3N-MC-CA cyclone built exclusively for the URG sampler (URG Corporation, 2016). Different sampling methods may impact the results of organic carbon analysis due to adsorption and desorption of VOCs. The size sorted $PM_{2.5}$ particles are collected on quartz filters for thermal optical carbon analysis, Teflon filters for gravimetric mass concentration or x-ray fluorescence (XRF) analysis, and nylon filters for ion chromatography (IC) analysis. Samples were collected every third day by drawing ambient, size sorted air for 24 hours through the respective filters starting at exactly midnight Fairbanks time. It is unknown if daylights

savings time is accounted for, but either way there would be negligible impact on the data since at most two data points would be affected by this change.

Site selection was accomplished by choosing the sampling locations that would provide the longest term representative measurements of the two airsheds. Two stationary sites from North Pole and two from Fairbanks were selected for this study (Figure 2.1).

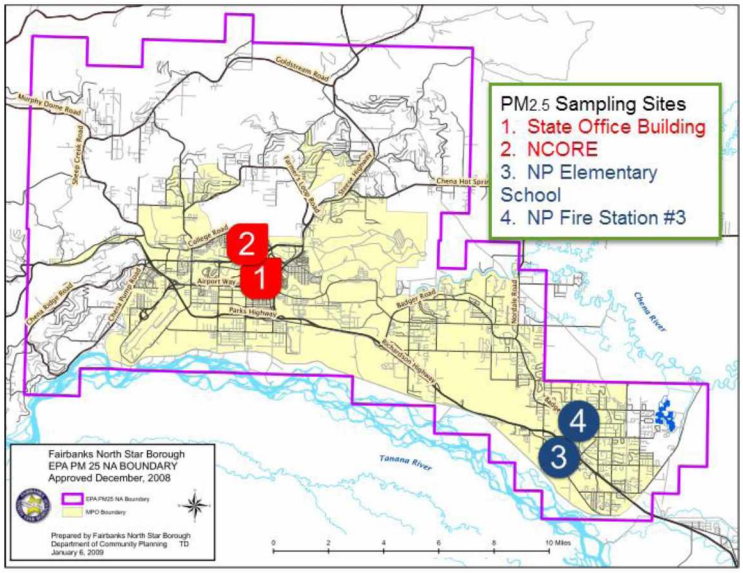

Figure 2.1: Fairbanks $PM_{2.5}$ nonattainment boundary. Selected sampling locations are depicted within the boundary established by EPA December 2009. The distance between sampling locations is: Fairbanks State Office Building to Fairbanks NCORE = 0.48 km. North Pole Elementary School to North Pole Fire Station#3 = 2.1 km. Fairbanks sites to North Pole sites about 21 km.

2.1.1.2 Carbon Sampling Method Discrepancies

The URG sampler has a higher face velocity than the SASS sampler, and thus from the same air mass should measure less OC due to higher volatilization and lower adsorption of VOCs from the filter (Solomon et al., 2000). Elemental carbon does not adsorb or volatize on filters the way OC does, and thus the switch of sampling methods should not impact the EC measurement.

Carbon sampling methods also utilize filters which have a different affinity for VOCs and rate for the particulate OC to reach saturation/equilibrium with VOCs. IMPROVE uses the Pallflex Tissuquartz brand quartz fiber filter, and STN uses the QMA brand filters prior to 2007 (Chow et al., 2010).

2.1.2 Analysis Methods

Filters were cold transported to an EPA designated lab for analysis of $PM_{2.5}$ speciation and gravimetric mass concentration.

2.1.2.1 Inorganic Analysis

Water soluble inorganic ions including sulfate (SO_4^{2-}), nitrate (NO_3^-), ammonium (NH_4^+), potassium (K^+), chlorine (Cl^-) and others not used in this thesis were measured with ion chromatorgraphy (IC). The particulates caught on the nylon filters were dissolved in de-ionized water (DI), separated by IC and detected by changes in conductivity (Harris, 2003). Individual elements (above atomic number 11) were measured with XRF which exposes the sample to X-rays that eject inner shell electrons from the sample. The dropping of outer shell electrons to fill these vacancies results in element specific emission spectra (Yatkin, 2014). Elements measured include zinc (Zn), sulfur (S), potassium (K), and others not used in this thesis. Particulate composition was analyzed at the Research Triangle Institute (RTI) laboratory (Ward, 2013), and this lab utilizes a QC metric. Prior to posting particulate data on the AQS database, the EPA also rejects any composition values below the MDL (EPA, 2014b).

2.1.2.2 Carbon Analysis

Thermal optical analysis (Chow et al., 1993) was used to measure OC and was completed at the Desert Research Institute (DRI) lab (Ward, 2013). Two analysis methods were used, either the speciated trend network (STN) or the interagency monitoring of protected visual environments (IMPROVE) method. Both protocols specify detailed parameters involved with the analysis such as the gas flow rate at each temperature step. Thermal optical analyzers (Figure 2.2) determine the total carbon (TC) in the particulate material and then split this measurement into OC and EC based on an optical correction. The STN method is a modification of the National Institute of Occupation Safety and Health (NIOSH) general guideline for thermal optical analysis, and this method will be referred to as NIOSH in this thesis. Many specific protocols exist as a result of modification of NIOSH principles. Different forms of NIOSH produce different EC and OC values, even when using the same optical correction (Chow et al., 2005). Two forms of IMPROVE protocols exist, IMPROVE and IMPROVE-A. IMPROVE-A is the newer version of IMPROVE that utilizes different temperatures and is used with all measured IMPROVE data in the Fairbanks data set. Both IMPROVE methods provide comparable measurements, and conversions developed to convert to IMPROVE are valid to convert to IMPROVE-A (Wu et al., 2012).

In order to analyze a particulate filter sample using a thermal optical analyzer (Figure2.2), a small punch is taken from the quartz fiber filter, and heated in a stream of pure helium, which volatizes the carbon in the particulate material. The gas mixture passes through an oxidizer which fully converts it to CO_2, and the methanator reduces it to methane which is measured by a flame ionization detector (FID). The temperature is ramped up, and at a specified time oxygen is added to the helium stream. Theoretically, OC combusts entirely in the pure He stream and EC combusts entirely after the addition of oxygen.

This simplifying assumption is not entirely true. As the instrument heats the sample, OC chars, forming EC like substances that do not volatize with the OC fraction, and absorb more light than the OC fraction. To account for this issue, laser light is applied to the sample and the transmittance (TOT) and/or reflectance (TOR) of this light is measured. The division between OC and EC occurs when the transmittance or reflectance of the sample returns to its initial value (Han et al., 2013). Thus, the OC/EC split is method defined (Figure 2.3) and occurs either before or after the addition of O_2 (Peterson & Richards, 2002), (Karanasiou et al., 2011).

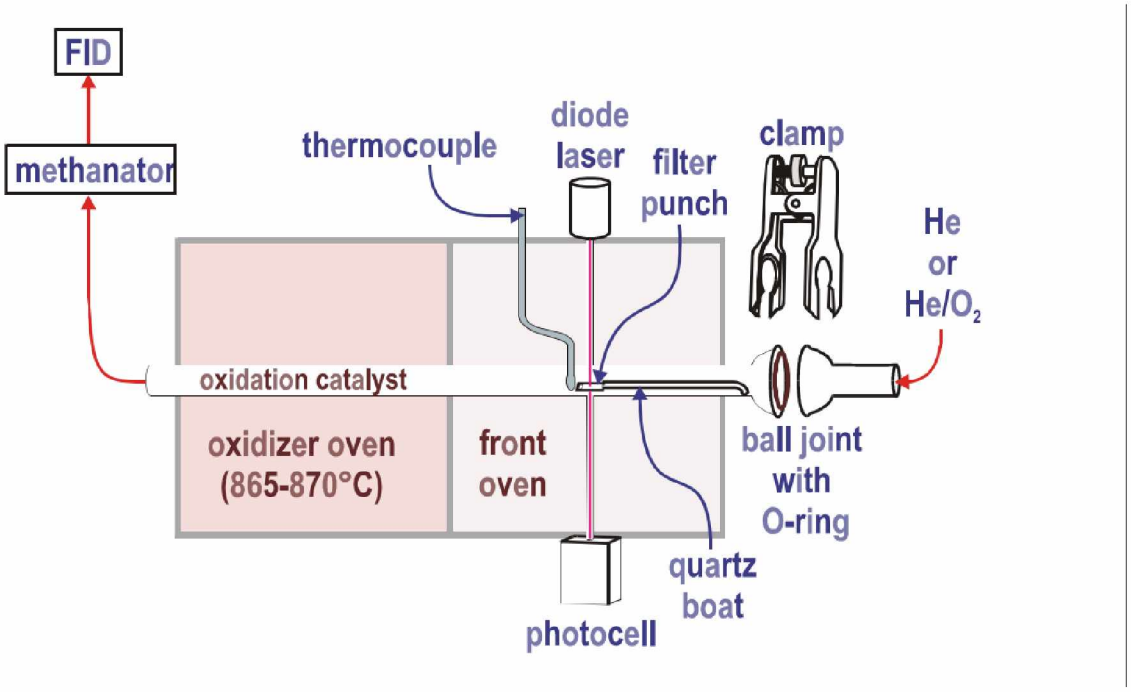

Figure 2.2: Schematic of the thermal optical analyzer, DRI model 2001 (Chow et al., 2004).

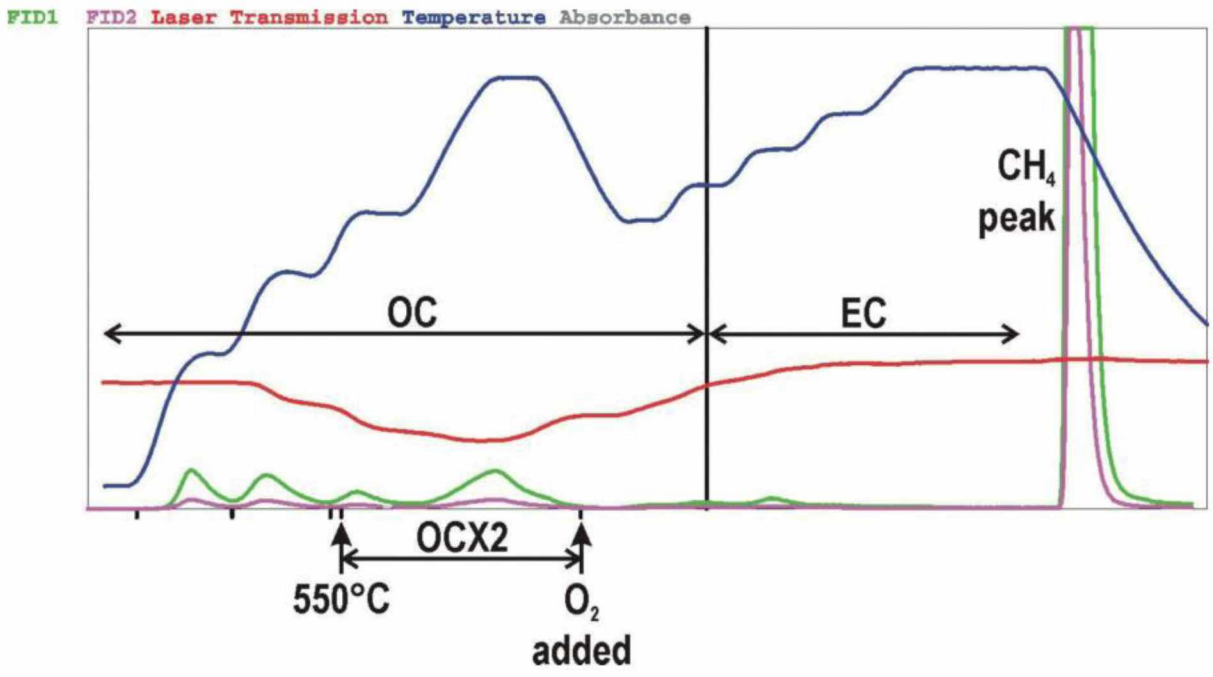

Figure 2.3: Example thermogram from thermal optical analysis. The y-axis is a relative axis, showing the flame ionization detector signals measuring the CO_2 signal (FID1 and FID2, green and purple lines), the amount of light that passes through the sample (Laser Transmission), and the sample temperature (Temperature, blue). The x-axis represents the time that the instrument is running (Peterson and Richards, 2002). Axis are not labeled as these are relative values with units not specified in the source for this image.

2.1.2.3 Carbon Analysis Method Discrepancies

In general, IMPROVE and NIOSH TC measurements agree within 10% (Chow et al., 2005). This is considered to be good agreement, especially considering that the measurements used in this study were made at different labs and on different instruments.

This level of agreement is not observed after the OC/EC split. IMPROVE EC values tend to be twice those measured with NIOSH. The key difference between the analysis methods lies in the heating/cooling cycles. Specifically, the temperature when oxygen is added during analysis, referred to as the peak inert mode temperature, is different for the two methods. The maximum

analysis temperature is also different (Table 2.5). The IMPROVE method also switches to an oxidizing atmosphere without the cool down step used by NIOSH (Peterson and Richards, 2002).

The lower peak inert mode temperature used in IMPROVE methods results in IMPROVE EC measurements 1.2-1.5 times larger than the NIOSH EC (Cheng et al., 2011), thus decreasing the OC measurement as was observed in the Fairbanks data (Figure 3.1). The discrepancy between EC measured with NIOSH vs IMPROVE is attributed to the allocation of carbon evolved without oxygen up to 850°C to OC (NIOSH) rather than EC (IMPROVE) (Peterson and Richards, 2002), (Chow et al., 2001). Chow et al. (2001) contend that the carbon evolved during heating to 850°C is EC due to the increased light transmittance, and argue that the oxidation removing the carbon during the heating to 850°C is sourced from adjacent mineral oxides. This explanation is supported with studies that utilize manganese oxide as the oxygen source in thermal optical analysis, rather than adding O_2 to the helium gas stream. During this method, graphite reacts negligibly with MnO_2 at 525°C, and completely combusts at 850°C. Assuming that MnO_2 releases O_2 at a similar temperature as the environmentally derived carbonates, sulfates, and nitrates found on the filters, this would indicate that above 850°C carbon oxidized in the pure helium environment could be from EC, and the IMPROVE method more accurately assesses the OC:EC ratio. Peterson & Richards (2002) argue that the increase in transmittance could be due to removal of light-absorbing OC, or the reaction of OC with mineral oxides. They note that the increase in transmittance is not related to mineral oxide (sulfate or nitrate) loadings. Table 2.1 summarizes the differences between the results of using either method, and the difference between using TOT vs TOR optical corrections.

Soil-derived carbonates could evolve as OC or EC in thermal optical methods (Karanasiou et al., 2011). Since the IMPROVE maximum analysis temperature is 120°C below that used in

NIOSH protocols, and below the melting point (about 850°C) of soil-derived $CaCO_3$, the IMPROVE method may not experience the same carbonate influence that affect NIOSH methods. It is assumed in this thesis that Fairbanks winter particulates do not contain significant amounts of soil derived $CaCO_3$ due to the lack of wind-blown dust during the winter.

Table 2.1: Literature summary of differences between the data produced by using different thermal optical analysis protocols on the same filter samples.

Source	NIOSH vs IMPROVE	TOR vs TOT
Cheng et al. (2011)	$EC_{IMPROVE\ TOT} > EC_{NIOSH\ TOT}$	$EC_{IMPROVE\ TOR} > EC_{IMPROVE\ TOT}$
J. C. Chow et al. (2010)	$EC_{IMPROVE} > EC_{NIOSH}$ $OC_{IMPROVE} < OC_{NIOSH}$	
Peterson & Richards (2002)	$EC_{IMPROVE} > EC_{NIOSH}$	
Judith C. Chow et al. (2009)	$EC_{(IMPROVE/TOR)}\ 10\% > EC_{(STN-NIOSH)}$	$EC_{(TOT)} < EC_{(TOR)}$
Judith C Chow et al. (2004)		$EC_{TOR} > EC_{TOT}$

2.2 Associated Error

2.2.1 Sampling Error

Filter samples are analyzed using standard methods. The largest source of error in $PM_{2.5}$ composition measurements is from inhomogeneous loading of particulates on the sample filters (Desert Research Institute, 2005). Filter loading inhomogeneity produces 10-30% error in the total carbon (TC) mass concentration, the sum of the EC and OC, but has negligible impact on the IC and XRF measurements. IC analysis is performed by dissolving particles from the entire Teflon filter in deionized water, and XRF uses a "sample spinner" that allows measurement of all parts of the filter throughout the analysis. Thermal optical analysis, on the other hand, measures carbon on only a small punch from the filter. In order to ensure inhomogeneous filter loading does not create large errors in carbon measurements, DRI analyzes duplicate punches every 10^{th} filter, and

if punches from the same filter have >10% discrepancy between carbon analysis, the data from that filter is rejected and additional filters surrounding the rejected filter are tested using the same method. This 10% cutoff corresponds to a maximum error about ten times the method detection limit (MDL) of TC for samples with a TC mass concentration greater than 5 μg m^{-3} (Desert Research Institute, 2005).

2.2.2 Analytical Error

Analytical errors that result from the inherent error in any method/instrument/operator may affect carbon analysis more than IC and XRF analyses. However, the analytical error is less than the sampling error in the carbon measurements and thus the potential error is limited to the sampling error of less than 10%. Measurements with greater $PM_{2.5}$ mass concentration have improved accuracy (Chow et al., 1993). The $PM_{2.5}$ components chosen for this work were measured at values above their method specific MDL for most of the sampling days (Table 2.2).

Table 2.2: Federal method detection limits (MDL). Parameter codes, method codes, and MDL values were obtained for the data used in this work from (EPA, 2014a).
* Parameter code not found in the AQS parameter code list, and thus the AQS method code was used instead to find the MDL.
**Method code 831 was not found in AQS parameter code list, and thus the MDL is based on parameter code 88321 (method # 829).

Analyte	Parameter Code	Method Code	Federal MDL ($\mu g\ m^{-3}$)
SO_4^{2-}	88403	812	0.012
K^+	88303	812	0.014
NO_3^-	88306	812	0.008
NH_4^+	88301	812	0.017
Zn	88167	105	0.00058
OC SASS/NIOSH/TOT	88305	813	0.245
OC URG/IMPROVE/TOR	88370*	838	0.002
EC SASS/NIOSH/TOT	88307	105	0.245
EC URG/IMPROVE/TOR	88380*	831**	0.002

2.3 Data Acquisition and Processing Overview

All data were extracted from the US EPA web site, located in the Air Quality System (AQS) database (EPA, 2014b), through the use of python scripts written by William R. Simpson, and this extraction was checked manually by Kristian Nattinger who directly downloaded and checked the excel files.

Fairbanks State Office Building (SOB) data were available for the entire study period on the AQS database. Fairbanks National Core (NCORE), North Pole Fire Stations #3 (NPFS3) and North Pole Elementary School (NPE) data were partly available on AQS. Some data for November 2011 - March 2013 were obtained directly from Deanna Huff (DEC) as they were not available on

the AQS database. Table 2.3 shows the samplers and analysis methods changed during the time period analyzed in this work.

In order to determine the best way to analyze the data set, a number of different analysis techniques were attempted, and the approaches that best answered the guiding hypotheses were chosen. The final version of the data was processed with a python script written by William R. Simpson. This script produced quality controlled and blank subtracted data from November 1 - end of February, and created a data set with consistent OC and EC measurement values. The script also calculated the SO_2 to SO_4^{2-} equivalent, OPM, reconstructed mass concentration (RCM concentration, Section 2.4.2), component/$PM_{2.5}$ mass ratios, and the NH_4^+ needed to neutralize SO_4^{2-} and NO_3^-. The data file produced with this script was then loaded into IGOR version 6.3.7.2 graphing and analysis software, Wavemetrics Inc. (Portland OR), and analyzed using macros written by William R. Simpson. Minor modifications to the macros were made by Kristian Nattinger to include Zn in relevant calculations, and the SOR for individual days was calculated at the command line and saved as a wave. All scripts and data files used in this work are available in the data archived with this thesis. See the Appendix for a full description of the scripts.

Table 2.3: Sampler and Analysis method for each analyte of interest for each location used in this work.
*Sampler unknown for NPE data since the files from Deanna Huff, ADEC did not contain this information, and these data are not available on AQS.
**Both types of samplers/analysis methods exist at the Fairbanks SOB during the 2011-12 and 2012-13 seasons. SASS-NIOSH data are used preferentially over the URG-IMPROVE data in our analysis when both types of data exist.

Site	Sampler (Analyte) – Method	Start Date (M/D/Y)	End Date (M/D/Y)
SOB	SASS (Ions, metals) – IC and XRF	1/2/2006	12/31/2014
	SASS (Carbon) – NIOSH	1/2/2006	10/7/2009
	URG (Carbon) – IMPROVE	10/1/2009	12/28/2014
	SASS (Carbon) –NIOSH Colocated Data**	11/2/2011	3/29/2013
	SASS (non-FRM mass conc.) – Gravimetric	1/2/2006	9/29/2014
NCORE	SASS (Ions, metals) – IC and XRF	11/2/2011	7/31/2014
	SASS (Carbon) – NIOSH	11/2/2011	3/29/2013
	SASS (Carbon) – IMPROVE	11/3/2013	8/10/2015
	SASS (non-FRM mass conc.) – Gravimetric	11/2/2011	7/31/2014
NPFS3	SASS (Ions, metals) – IC and XRF	3/1/2012	3/30/2014
	SASS (Carbon) – NIOSH	3/1/2012	3/29/2013
	SASS (Carbon) – IMPROVE	11/3/2013	3/30/2014
	SASS (non-FRM mass conc.) – Gravimetric	3/1/2012	3/29/2013
NPE	SASS* (Ions, metals) – IC and XRF	11/2/2011	3/29/2013
	SASS* (Carbon) – NIOSH	11/2/2011	3/29/2013
	SASS* (non-FRM mass conc.) – Gravimetric	11/2/2011	3/29/2013

In addition to the data used to search for trends, a collocated data set was obtained to allow creation of a OC/EC conversion factor (Section 2.4.3). The EPA mandated a change in the carbon sampling and analysis methods across the network in the late 2000's, and this change was implemented at the Fairbanks SOB site in October 2009. To assure the ability to compare data from before and after the sampler/method change, the ADEC funded a study that compares the new sampling/analysis methods to the old methods. In this study, SAAS and URG samplers, both located on the roof of the Fairbanks SOB, concurrently collected 24-hour quartz fiber filter

measurements. SASS filters were analyzed with NIOSH and URG filters were analyzed with IMPROVE thermal optical methods. Data from this study was obtained directly from the ADEC. Data were also obtained directly from the ADEC for a similar study of collocated instruments in Fresno, CA.

2.4 Initial Data Processing

2.4.1 Data Processing- Blank Correction

Sampling artifacts from adsorption of semi-volatile organic gases or contamination from handling of the filters were accounted for by subtracting the average of field and trip blank filters that were collected as part of the analytical program. Field blank filters are passively exposed to ambient air for a set period of time based on the analysis method. They are then packed and shipped to the same lab and analyzed on the same instrument as the measurement filters. This treatment is used to account for passive deposition and loss of particulate components that may occur on the sampling filters. Table 2.4 shows the average for all blanks taken during the time period used in this work.

Table 2.4: Mean blank values for the FNSB. Data from 2006-2014, or a subset of that time period depending on site (EPA, 2014b). Mean values and number of filters represent both trip and field blanks. SAAS/IMPROVE data from NCORE and NPFS3, all other data from Fairbanks SOB.

Parameter	# Filters	Mean Blank Value (ug/m^3)
$OC_{SAAS/NIOSH}$	n=46	1.212
$EC_{SAAS/NIOSH}$	n=46	0.025
$OC_{URG/IMPROVE}$	n=10	0.137
$EC_{URG/IMPROVE}$	n=10	0.000
Gravimetric $PM_{2.5}$	n=72	0.759
$OC_{SAAS/IMPROVE}$	n=4	0.687
$EC_{SAAS/IMPROVE}$	n=4	0.000
SO_4^{2-}	n=73	0.051
NO_3^-	n=73	0.027
NH_4^+	n=73	0.006

Literature sourced field blank values are 1.05 ± 0.47 μg m^{-3} TC for SASS samplers, and 0.26 ± 0.05 μg m^{-3} for IMPROVE Module C Sampler (Chow et al., 2010), showing good agreement with the mean values calculated as part of this work. Table 2.5 depicts the reasons for this discrepancy which is the result of two competing factors: amount of time the blank filter is exposed to ambient air (1-15 minutes for NIOSH filters, and 7 days with IMPROVE filters) and flow rate of the sampler. The shorter exposure time for NIOSH filters does not adequately represent the adsorption of VOCs, and results in 20-30% lower TC areal density on blank filters. However, this effect is overshadowed by the higher flow rate and smaller exposed filter area with the URG samplers often used with the IMPROVE method, which corresponds to a 4 times lower field blank ambient TC equivalent due to increased desorption with the URG samplers (Chow et al., 2010). Passive deposition of EC is considered negligible (Chow et al., 2010), and only negligible EC blank values are observed in the Fairbanks SOB data.

Table 2.5: Carbon sampler and analysis operating parameters. Note that the NIOSH method used with these samples is the Speciated Trend Network (STN) method.

Sampler Parameters	**Met One SAAS**	**URG 3000N**
Filter area	11.76 cm^2	3.53 cm^2
Flow Rate	6.7 L/min	22.8 L/min

Analysis Parameters	**NIOSH**	**IMPROVE-A**
Filter Type	QMA quartz fiber (pre-2007)	Pallflex Tissuequartz
Max Analysis Temp	920 °C	800 °C
Peak Inert Mode Temperature	850 °C	580 °C
Field Blank Bias	NIOSH 20-30% < IMPROVE	

2.4.2 Calculation of the Reconstructed Mass Concentration

The reconstructed mass (RCM) concentration is a way of calculating the particulate mass concentration from only composition measurements. The RCM concentration utilizes a different sampler and different analytical technique than the gravimetric mass concentration, and thus comparison of RCM concentration with the gravimetric mass concentration is a way to ensure the accuracy of the composition measurements. The RCM concentration was calculated with Equations 2-1, 2-2 and 2-3. Units on the concentrations are $\mu g\ m^{-3}$.

The RCM takes into account the mineral oxides commonly found in particulates through calculation of the other primary material (OPM) as described in Section 1.7.1. Equation 2-2 was utilized to calculate OPM in PMF modeling (Wang and Hopke, 2014) as well as this thesis. This

equation uses a slightly different multiplier to account for silicon oxides than the multiplier used in SANDWICH modeling (Equation 1-1).

$$OCM = OC \times 1.4 \quad \text{[Equation 2-1]}$$

$$OPM = 2.49 \times Si + 1.94 \times Ti + 1.63 \times Ca + 2.42 \times Fe + 1.8 \times Cl \quad \text{[Equation 2-2]}$$

$$\text{RCM concentration} = OCM + OPM + EC + SO_4^{2-} + NO_3^- + NH_4^+ \quad \text{[Equation 2-3]}$$

2.4.3 Data Processing: OC/EC Correction Methods

2.4.3.1 Motivation

Analysis of the uncorrected 2006-2014 time series of the $OC/PM_{2.5}$ ratio at the Fairbanks SOB sampling site revealed a noticeable drop on 10/1/2009 (Figure 3.1). This apparent change in particulate composition is attributed to the EPA mandated change in the carbon sampling and analysis methods in 2009 (Alaska Department of Environmental Conservation, 2014). The methods switched from SAAS/NIOSH to URG/IMPROVE at the Fairbanks SOB site (Table 2.3), and these techniques have different operating parameters (Table 2.5) that lead to different measurement values. Other sampling sites used different combinations of these samplers and analysis methods (Table 2.3). All measurements must be converted to a consistent basis prior to analysis of temporal trends or spatial differences.

2.4.3.2 Fresno OC/EC Correction

The current method utilized by the ADEC for creating a consistent data set involves correlating collocated URG/IMPROVE and SAAS/NIOSH data from Fresno, CA. The line of best fit from these correlations is used to convert the URG/IMPROVE data to a SASS/NIOSH like

format, as part of the SANDWICH method (Section 1.7.1). In this thesis, a similar correction based on the Fresno data was created. We obtained the Fresno data directly from ADEC and correlated the OC and EC values (Figure 2.4), then used this correlation to convert the post 2009 data set to a SASS/NIOSH like format, blank subtracted these values, and calculated TC as the sum of OC and EC. This method uses a slightly different approach than the ADEC used in the SANDWICH method. Table 2.7 lists the corrections used in this thesis.

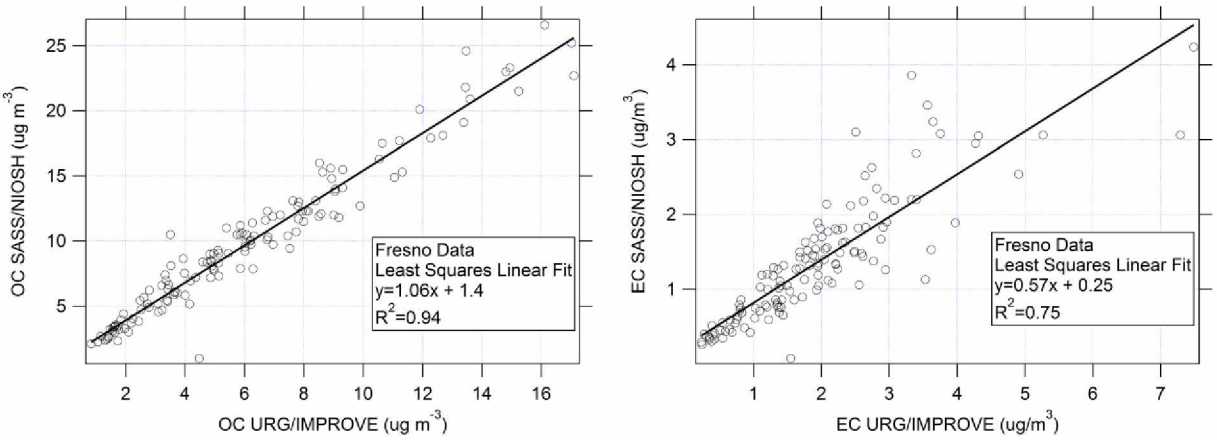

Figure 2.4: Fresno OC/EC correlation slopes. These figures were developed using data from the Fresno co-location study. Note that these data are not blank subtracted prior to correlation, and thus these plots have a non-zero intercept.

OC/EC correction factors are affected by particulate concentration, composition and source (Chow et al., 2009). Thus, we chose not to use the Fresno correction to correct Fairbanks data. Possible causes of composition (and subsequently location) based discrepancies include higher TC filter loadings leading to less accurate EC measurements (Chiappini et al., 2014) or catalytic removal of EC at lower temperatures by metals such as potassium (K). Fresno $PM_{2.5}$ has an 8% lower OC/TC ratio than Fairbanks $PM_{2.5}$, possibly due to lower wood smoke and higher diesel contributions (Section 3.5). Table 2.6 lists the IMPROVE parameter codes used in the Fresno data set and the Fairbanks data set, and since these codes are different there are (probably small) differences in the analysis and sampling methods as well (EPA, 2014b).

Table 2.6: Parameter codes for carbon measurements from Fairbanks and Fresno. Note that the OC/EC parameter codes are different for IMPROVE data (EPA, 2014b).

Parameter Codes from AQS				
Study Location	**$OC_{(NIOSH/TOT)}$**	**$EC_{(NIOSH/TOT)}$**	**$OC_{(IMPROVE/TOR)}$**	**$EC_{(IMPROVE/TOR)}$**
Fairbanks	88305	88307	88370	88380
Fresno	88305	88307	88320	88321

Table 2.7: OC/EC correction equations. These forced zero linear regressions are from collocated SAAS and URG samplers, analyzed with NIOSH and IMPROVE thermal optical carbon methods respectively. Input values are the ambient mass concentration, $\mu g\ m^{-3}$. "Corrected" values are the values used in this work, and are on a blank subtracted SASS/NIOSH-TOT basis.

Correction (Data Source) n=# Samples	**Correction type**	**Conversion Equation**
Correction used in this work (Fairbanks) n=89	URG/IMPROVE to SASS/NIOSH-like	$TC_{corrected} = 1.268 \times (OC_{URG/IMPROVE\text{-}TOR} - 0.137 + EC_{URG/IMPROVE\text{-}TOR})$
	SASS/IMPROVE to SASS/NIOSH-like	$TC_{corrected} = 1.000 \times (OC_{SASS/IMPROVE\text{-}TOR} - 0.687 + EC_{SASS/IMPROVE\text{-}TOR})$
	SASS/NIOSH blank subtraction	$TC_{corrected} = (OC_{SASS/NIOSH\text{-}TOT} - 1.212 + EC_{SASS/NIOSH\text{-}TOT})$
	URG/IMPROVE to SASS/NIOSH-like	$EC_{corrected} = 0.8 \times (EC_{URG/IMPROVE\text{-}TOR})$
	SASS/IMPROVE to SASS/NIOSH-like	$EC_{corrected} = 0.8 \times (EC_{SASS/IMPROVE\text{-}TOR})$
	SASS/NIOSH blank subtraction	$EC_{corrected} = EC_{SASS/NIOSH\text{-}TOT} - 0.025$
	any form to SASS/NIOSH-like	$OC = TC - EC$
Correction developed in this work (Fresno) n=133	URG/IMPROVE to SASS/NIOSH-like	$OC_{SASS/NIOSH} = 1.4352 \times OC_{URG/IMPROVE} + 1.10557 - 1.212$
	URG/IMPROVE to SASS/NIOSH-like	$EC_{SASS/NIOSH} = 0.5722 \times EC_{URG/IMPROVE} + 0.2509 - 0.025$
	any form to SASS/NIOSH-like	$TC = OC + EC$
Correction in use by the ADEC (Fresno) n=133	URG/IMPROVE to SASS/NIOSH-like	$OC_{SASS/NIOSH} = (OC_{URG/IMPROVE} + 0.3593) / 0.6581$
	URG/IMPROVE to SASS/NIOSH-like	$EC_{SASS/NIOSH} = 0.5722 \times EC_{URG/IMPROVE} + 0.2509$

2.4.3.3 Fairbanks OC/EC Correction

An OC/EC correction factor was developed to convert URG-IMPROVE data to a SASS-NIOSH-like format by correlating collocated data from a study in Fairbanks. This data is described in Section 2.3. The Fairbanks data set was chosen rather than the Fresno data set because a conversion based on Fairbanks data will more accurately represent the concentration, composition and sources of the particulates from the Fairbanks area.

Figure 2.5 shows the correlation of blank subtracted TC and EC values measured on collocated samples from the Fairbanks SOB site during the 2011–2012 and 2012–2013 violation seasons sampled and analyzed by SASS/NIOSH and URG/IMPROVE respectively. Despite the exclusion of March from all analyses in this thesis, March was included in conversion development in order to increase the total number of data points available. OC was calculated as the different between TC and EC. The use of forced zero intercept correlation is based on the assumption that blank subtraction removes all particulate mass concentration that is not due to deposition on the filter. The resulting correlation slopes were used for converting URG-IMPROVE data to a SASS-NIOSH-like format. North Pole and NCORE sampling sites continued to use the SASS sampled filters after 2009, and in order to convert from SASS-IMPROVE to SASS-NIOSH, it was assumed that TC was conserved between thermal optical analysis methods (Section 2.4.2), and thus only the EC measurements were corrected, and OC was calculated as the difference between TC and EC. This correlation is the basis for the OC/EC correction factor developed and used in this thesis.

The use of different optical corrections might raise concern as to the validity of this method since different optical corrections may result in different OC/EC splits. Reflectance based optical corrections are affected more by near surface OC charring than transmittance based correction. Transmittance corrections are more affected by charring within the filter (Chow et al., 2004). Since

this correction is based on collocated measurements that have similar particulate composition, this bias should not affect the conversion factor.

The correlation slope of 1.267 observed in the TC collocated data is due to the difference in samplers rather than in analysis methods, since TC does not depend on the analysis method (Chow et al., 2005), and thus we ascribe the difference in OC measurements to the change in sampler rather than analysis method. This discrepancy is expected based on the differences in the sampling methods (Section 2.1.1).

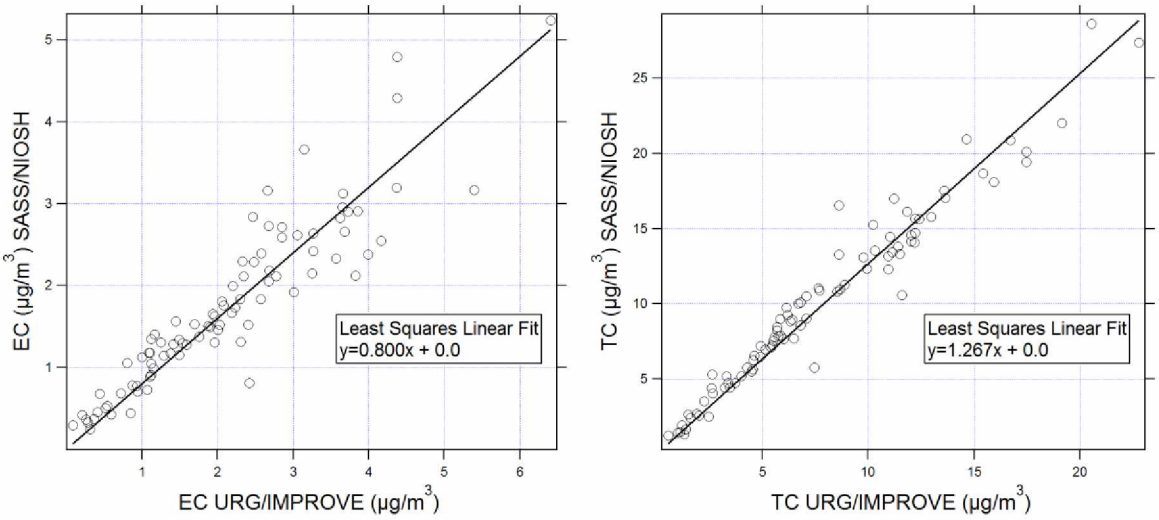

Figure 2.5: TC and EC correlation for Fairbanks SOB November – March, 2011-2012 through 2012-2013 collocated data. These correlations are used to correct OC and TC data in this work.

2.4.3.4 OC/EC Correction Checks

To confirm that the OC/EC correction developed here is valid four separate assessments of the correction were performed. First, the OC/$PM_{2.5}$ time series was inspected to determine if the visually apparent drop in 2009 due to the method change had been removed. Next, the RCM concentration based on the corrected carbon measurements was compared with the gravimetric mass concentration. This check compares two entirely separate methods for measuring (and filters

for collecting) the ambient $PM_{2.5}$ mass concentration and thus good agreement is an indicator of both the effectiveness of the correction factor and the quality of the analytical work. Next, the URG-IMPROVE data was converted to a SASS-NIOSH-like format and correlated with a forced zero intercept with the collocated measured SASS-NIOSH data. Since the correlation was developed using least squares regression, which minimizes only the variation from the line of best fit in the y-direction, and this assumes no error on the x-axis. Correlation plots such as this were always done with the SASS/NIOSH data on the y-axis, and corrected URG-IMPROVE data on the x-axis. The seasonal mean ambient OC concentrations were compared using the t-test to ensure that use of the OC/EC correction does not bias the mean values.

2.5 Data Processing– Sample Variability

Initial analysis of the full data set showed large day to day variability in the ambient concentration of all $PM_{2.5}$ components, due to large fluctuations in the ambient $PM_{2.5}$ mass concentration. This is likely attributable to changes in overall emissions and meteorology. Inversions trap pollutants, wind disperses polluted air, and cold temperatures can change burning behavior. It is unknown if colder temperatures result in greater wood or greater oil use.

To remove the effects of trapping and investigate the composition of the particles, the ambient concentration of each component ($\mu g\ m^{-3}$) was divided by the total particle mass concentration ($\mu g\ m^{-3}$), to yield the mass based component/$PM_{2.5}$ ratio (unitless). Calculation of violation season mean and standard deviation was used to assess the average concentration during a specific winter and eliminate day to day fluctuations in the $PM_{2.5}$ mass concentration. Figure 2.6 shows that the mean and median $PM_{2.5}$ mass concentration represent trends in these seasonal averages similarly, and thus the mean was chosen as the form of averaging used in this thesis. This also indicates that the component/$PM_{2.5}$ ratios are symmetrically distributed around their average.

In order to quantify the error associated with the calculation of mean values, the standard deviation was calculated. It was assumed that the standard deviation also accounts for errors associated with sampling and analysis (Section 2.2).

The full $PM_{2.5}$ gravimetric mass concentration data set showed large seasonal variability, due to seasonal changes in sources. Figure 2.7 depicts the average number of measurement days in violation of the EPA standard per month, and the seasonal variability was addressed by choosing the subset of data when the majority of violations occur each year: November 1 - end of February, referred to in this work as the "violation season" and marked in purple in Figure 2.7. The ADEC includes March in their violation season, however in this thesis March was omitted to focus our analysis on the winter months when the majority of violations occur.

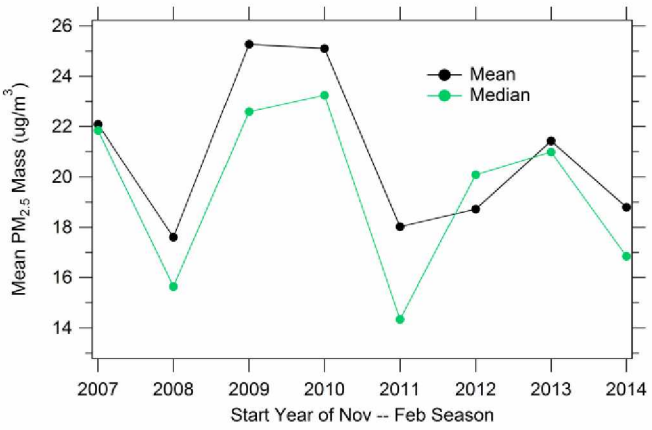

Figure 2.6: Trends in mean and median $PM_{2.5}$ mass concentration. Violation season Fairbanks SOB data. Original data from (EPA, 2014b).

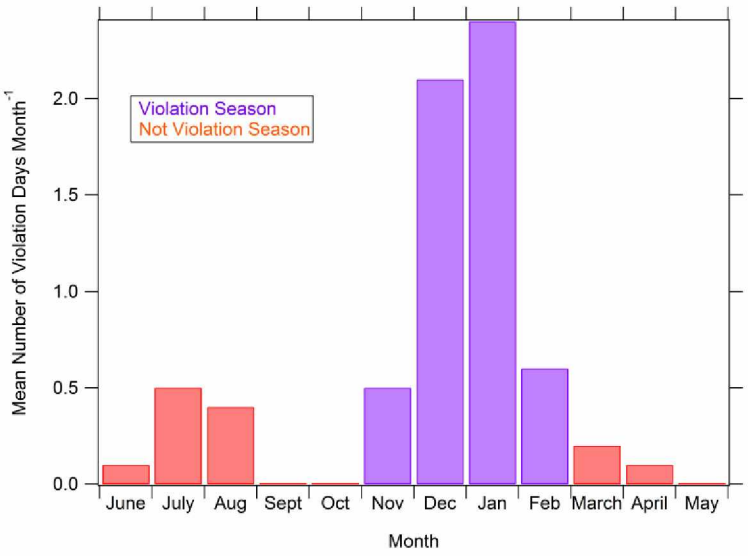

Figure 2.7: Mean number of measurement days in violation of the NAAQS per month for the study period. 2006-2014 (EPA, 2014b). Measurement days occur once every three days, thus one violation day per month indicates there may be three actual days in violation of this standard. Months marked in purple were chosen as the violation season in this thesis.

2.6 Data Processing- Quality Control (QC)

In addition to the QC metrics employed by the analytical labs and EPA (Section 2.2) we developed an additional QC metric. This method is based on agreement between the RCM

concentration (Section 2.4.5) and gravimetric mass concentration. Data were rejected if the difference between the gravimetric mass concentration and the reconstructed mass concentration was more than 3.5 $\mu g\ m^{-3} \pm 10\%$ of the average of the reconstructed and gravimetric mass concentration (Figure 2.8). The value 3.5 $\mu g\ m^{-3}$ is 10% of the current EPA NAAQS limit (EPA, 2014b). This QC ensures that large measurements that are clear outliers are rejected, but does not remove small measurements that may introduce error in component/$PM_{2.5}$ calculations. The method removed 31 of 312 data points from the SOB data, 14 of 118 from the NCORE data, 19 of 80 for NPE data, and 4 of 75 from the NPFS3 data. The large portion of points removed by the QC from the NPE data set indicates that a large portion of the composition data does not match the gravimetric data, possibly due to this sampling site being newer than the other sites and short lived. Additionally, filters from the NPE location were never analyzed for OC/EC using IMPROVE methods, which may have introduced error, though details of how these analyses were completed were not known at the time of writing this thesis. Outlier removal was accomplished with a python script (see Appendix B).

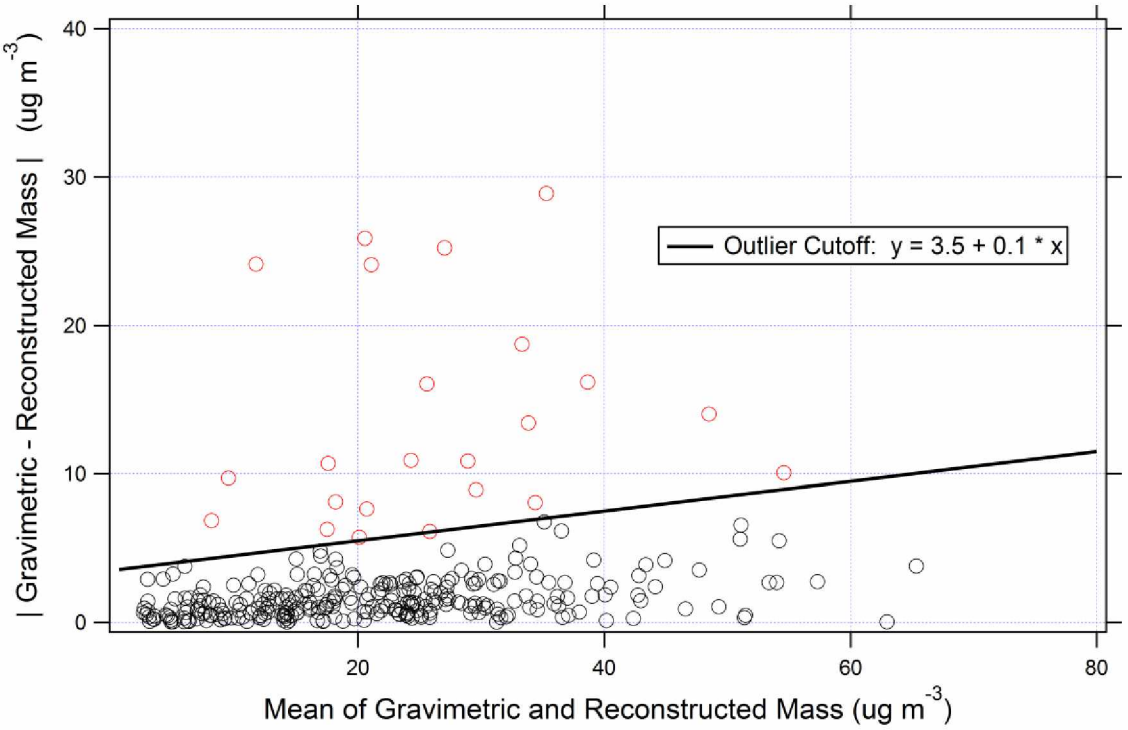

Figure 2.8: Criteria for removing outliers. The red points have been removed from the 2006-2014 SOB data set that is used in this work. Original data from (EPA, 2014b).

Since about 70% of the particulate mass is OCM and SO_4^{2-}, the majority of outliers removed by this metric are due to errors in these two measurements. Errors in the low concentration components such as metals are probably seldom removed. Extreme outliers in the potassium ion (K^+) and elemental potassium (K) data were observed on January 1 and December 31 in many of the data sets. Peltier, (2012) observed spikes in cadmium and other elements in hourly $PM_{2.5}$ data shortly after midnight on January 1, 2012, and attributed these spikes to the local fireworks display. Similar outlier values were observed on January 1 and December 31 in the data set used in this thesis, and potassium measured with both XRF and IC was removed using an IGOR script.

2.7 Data Processing- Statistical Methods

The t-test (at 95% confidence) was used to determine statistically significant differences in temporal trends by assessing the statistical different between each violation season and the mean for all violation seasons. This test was completed for all major and some minor components. The t-test compares the mean and standard deviation values for the two distributions to determine if the normally distributed populations are significantly different, and is depicted in Equation 2-1.

$$t = \frac{\overline{x_1} - \overline{x_2}}{\sqrt{\frac{s_1^2}{n_1}} + \sqrt{\frac{s_2^2}{n_2}}} \qquad \text{[Equation 2-1]}$$

Where $\overline{x_1}$ and $\overline{x_2}$ are the mean for the parameter of interest in population 1 and 2 respectively, s_1 and s_2 are the standard deviations of population 1 and 2 respectively, n is the number of points in either population, and t is the t-score that is compared to the t-critical to determine significance. The paired t-test (at 95% confidence) was used to determine statistically significant differences between sampling sites. This test calculates the sum of the difference in each paired measurement (taken on the same day) as opposed to calculating the difference between the mean values as is done in a non-paired t-test. Equation 2-2 shows the formula for calculating the t-score for one paired data point to compare site 1 and site 2. The t-score is calculated for all data pairs, and the mean t-score is determined for the time period of interest.

$$t = \frac{x_1 - x_2}{\sqrt{\frac{s^2}{n}}} \qquad \text{[Equation 2-2]}$$

Use of the t-test is not valid for testing the difference in ambient mass concentrations, since these concentrations are not normally distributed (Figure 2.9, right plot). Component/$PM_{2.5}$ ratios are approximately normally distributed based on visual inspection of the histograms. Histograms were made for all component/$PM_{2.5}$ ratio data sets used in this thesis to ensure that the data

appeared normally distributed. An example histogram is shown with red bars in Figure 2.9 (left plot). The black line represents the normal probability distribution that was created by IGOR to best fit the histogram.

In order to determine if a line of best fit represents a significant trend, the slope of the line was compared to a slope of zero using the t-test (not paired, 95% conf.). The standard deviation of the slope of the line of best fit from each plot was obtained from IGOR. The slope of the line was treated as the mean value in the t-test equation.

Figure 2.10 (left plot) shows that $PM_{2.5}$ gravimetric mass concentrations were not normally distributed, and thus use of the t-test was not valid with this data set. The left tail of this distribution encompasses data that is below zero concentration, further decreasing the validity of this test. Figure 2.10 (right plot) shows how a $\log_{10}$ transformation of the data made it more normally distributed. This transformation is sufficient we feel to validate use of the paired t-test with the understanding that the $\log_{10}$ transformed data set is only roughly normal. These tests were performed in IGOR, and all reference to "significance" in this thesis with regards to spatial differences is to the paired t-test at the 95% confidence interval on either the component/$PM_{2.5}$ ratios or log normalized gravimetric mass concentration. All reference to "significance" with regards to temporal change is to the (not paired) t-test at 95% confidence interval.

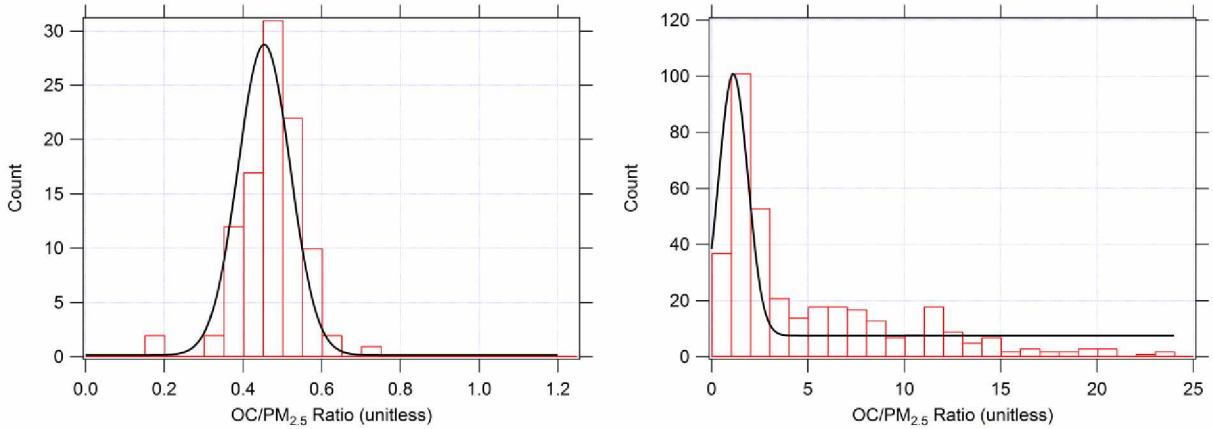

Figure 2.9: Histograms of SOB OC mass concentration and $OC/PM_{2.5}$ ratios for 2009-2010 through 2013-2014 violation seasons. Curves represent the normal distribution curve that best fits the data. Original data from (EPA, 2014b).

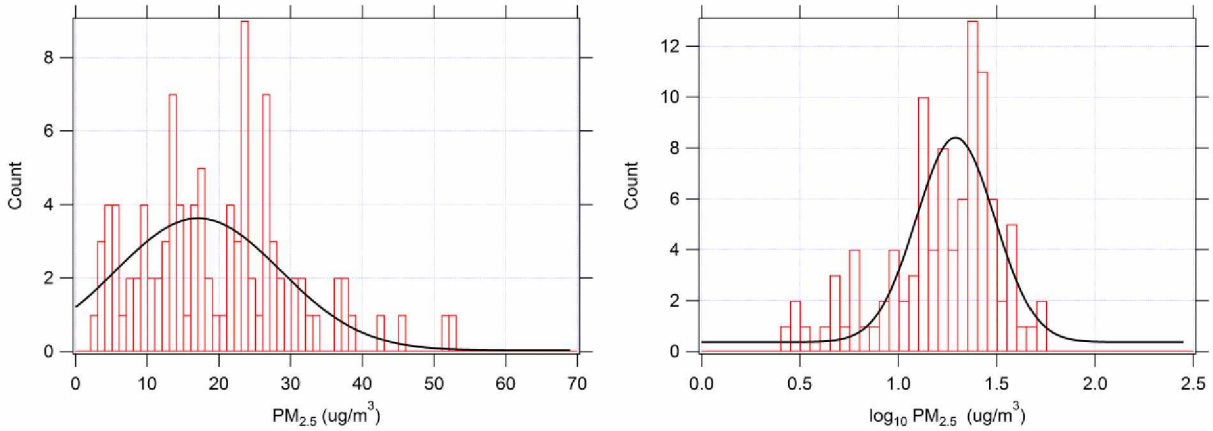

Figure 2.10: Histograms of gravimetric $PM_{2.5}$ and log_{10} normalized $PM_{2.5}$ SOB 2006-2007 through 2013-2014 violation season data. Lines of best fit are the normal probability distribution curve that best fits the data. Original data from (EPA, 2014b).

2.8 Data Processing– Sulfur Oxidation

2.8.1 Sulfur Oxidation Ratio (SOR) Calculation

As one approach to assess the amount of secondary oxidation taking place in the atmosphere, the SOR was calculated (Equation 2-3) for the entire time period that SO_4^{2-} and SO_2 data were available from the Fairbanks NCORE site, the only location where SO_2 was measured. The SOR is the ratio of SO_4^{2-} in the ambient $PM_{2.5}$ to the SO_4^{2-} that could be produced if all of the

ambient SO_2 was oxidized to SO_4^2, which is referred to as the total potential SO_4^{2-}. The SOR is always between zero and one, and can be equivalently calculated on a SO_2, S, or SO_4^{2-} basis. In this thesis the SOR was calculated on a SO_4^{2-} basis. The SOR generally is not affected by air mass dilution or by emission changes in other particulate components, with some exceptions. Assuming that secondary oxidation is taking place through manganese (Mn) and iron (Fe) catalyzed oxidation, the SOR could be affected by emission changes in these catalysts. Possibly, changes in the removal rates of SO_2 and SO_4^{2-} could impact the SOR as well.

$$SOR = SO_4^{2-} / (SO_4^{2-} + SO_2 \text{ converted to equivalent } SO_4^{2-}) \quad \text{[Equation 2-3]}$$

2.8.2 Determination of Secondary Oxidation

The analysis approach used by Shakya and Peltier (2013) was replicated to determine if secondary oxidation is indicated by the observed ambient SOR. Shakya and Peltier (2013) based their approach on Ohta (1990) who compared the ambient SOR to the primary SOR of a #2 fuel oil source profile from the EPA, and determined the maximum primary SOR of heating oil to be 10%. Ambient SOR values above this cutoff were considered to be the result of secondary oxidation.

The combustion of #2 fuel oil is also the most likely source for sulfur in the Fairbanks airshed. It was not possible to determine the primary SOR for #2 fuel oil with Fairbanks specific or EPA source profiles since SO_2 measurements were not taken as part of these profiles (Section 2.13). The ADEC uses a combination of emission factors and source profiles to calculate the SO_2 and SO_4^{2-} emission factors, and the same sources were used to calculate the SOR in this thesis. The SO_2 emission factor was calculated from the EPA emission factor for #2 fuel oil, given in Equation 2-4. The SO_4^{2-} emission factor was calculated from the Fairbanks specific #2 fuel oil

source profile. This profile provides a filterable PM emission factor of 0.457 lbs. PM (1000 gallons)$^{-1}$, and the PM is 33% SO_4^{2-} (Huff, D.: Personal Communication, email, ADEC, 2016), which differs slightly from the original profiles (Ward, 2013) due to renormalizing the measured mass percent SO_4^{2-} to the total mass of all particulate components in the source profile (to the best of our knowledge). Equation 2-5 shows how the SO_4^{2-} emission factor was calculated. Equation 2-6 combines these formulas to calculate the primary SOR for #2 fuel oil.

$$\text{Sulfur Dioxide EF} = \frac{142lbs\ x\ Sulfur\ content\ of\ fuel}{1000\ gallons} \quad \text{[Equation 2-4]}$$

$$\text{Sulfate EF} = \frac{0.457lbs\ PM*Sulfur\ content\ of\ fuel}{1000\ gallons}\ x\ \frac{0.33\ lbs\ Sulfate}{lb\ PM} \quad \text{[Equation 2-5]}$$

$$\text{Primary SOR for \#2 Fuel Oil} = \frac{Sulfate\ EF}{Suflate\ EF + Sulfur\ Dioxide\ EF} \quad \text{[Equation 2-6]}$$

Due to the concern that the combination of source profiles from OMNI and the EPA emission factor could lead to errors in the above calculation, an alternative approach was also used based on the primary SOR values obtained directly from the EPA #2 fuel oil emission factor document. Office of Air Quality Planning and Standards, (1995) states that 95% of sulfur in fuel oil is oxidized to SO_2, 1-5% to SO_3 (which readily forms SO_4^{2-}), and 1-3% to SO_4^{2-}, and by combining these values a primary SOR was calculated.

2.8.3 Metal Catalyst Investigation

To assess whether transition metals may be involved in catalyzing the oxidation of SO_2, trends in the ambient SOR were compared with concentrations of Fe and Mn. In addition, trends and spatial variability in the Zn/$PM_{2.5}$ ratio were assessed as a possible indicator of waste oil combustion, and subsequent source for transition metals (Section 1.8.3).

2.9 Data Processing - Non-Sulfate Sulfur (NSS)

To assess if forms of sulfur exists within the particles other than SO_4^{2-}, the sulfur content measured with XRF was correlated with the sulfur content of the SO_4^{2-} measured with IC. This required conversion of the SO_4^{2-} to sulfur, using the conversion factor 0.334 μg sulfur/μg SO_4^{2-}. A linear least squares regression was fit to the data and the slope was used to determine the average discrepancy between the two measurements.

2.10 Data Processing– Spatial Analysis

Comparison of long term averages at the different sampling sites was made difficult by the fact that there is no time period greater than one violation season that includes data from all four sampling sites. In order to compare the four sites, the 2011-2012, 2012-2013, and 2013-2014 violation seasons were selected from all sampling sites (acknowledging that some sites do not have data for one or more of these seasons). Use of the paired t-test (section 2.7) ensured that only same day measurements were included in the statistical tests.

2.11 Data Processing – Temporal Analysis

Since the SOB site has the longest continuous period of data collection, this site was used to assess changes in particulate composition with time. An IGOR macro was used to calculate the mean and standard deviation for the $OC/PM_{2.5}$, $SO_4^{2-}/PM_{2.5}$, $EC/PM_{2.5}$, $NH_4^+/PM_{2.5}$ and $NO_3^-/PM_{2.5}$ ratios for each violation season. The t-test was used to compare the mean violation season component/$PM_{2.5}$ ratio from each season with the mean of the full 2006-2007 through 2013-2014 violation seasons, allowing assessment of temporal change. The decision to use the statistical tests to look for years with significantly different values from the mean of the full data set allowed assessment of changes that occur due to a specific incident. Some possible causes for such a

change include an increase in the sulfur content or price of #2 fuel oil. We anticipate that these step-like changes will be more likely than linear trends.

To investigate the possibility of linear temporal trends in particulate composition, the mean component/$PM_{2.5}$ ratios from the 2006-2007 through 20013-2014 violation seasons were plotted and fit with a least squares linear regression in IGOR. The slope of the linear fit was compared with a slope of zero using the t-test (95% conf.) by treating the slope like the mean in the t-test equation (Equation 2-2), the standard deviation of the slope as the standard deviation, and the number of points being eight. Eight is the number of violation season mean values used in determining the trend line. Trends with a slope that is not significantly different from zero will be considered to have no linear trend.

2.12 Source Profile Selection Methods

Selection of source profiles was done in a systematic way to allow careful assessment of potential sources of the measured ambient $PM_{2.5}$ based on emission composition. The four most likely sources for breathing level $PM_{2.5}$ in this airshed are: wood smoke, #2 fuel oil exhaust, gasoline exhaust, and diesel exhaust. Coal was not chosen as a likely contributor to breathing level $PM_{2.5}$ since only 0.5% (multi-year average) of home heating is done with coal (Alaska Department of Environmental Conservation, 2015), and evidence is inconclusive if transport of coal based point source $PM_{2.5}$ from above the inversion is sufficient to impact the breathing level $PM_{2.5}$ composition (Section 1.3.1).

EPA SPECIATE profiles were selected for wood smoke, gasoline exhaust, and diesel exhaust since the large numbers of profiles available allowed reasonable averaging.

The nine Fairbanks specific profiles are available in Ward (2013), and some (but not all) of the EPA SPECIATE profiles used by Ward (2013) are available on the EPA SPECIATE

database. A large number of other profiles are available from EPA SPECIATE as well (EPA, 2014b).

Profiles from the EPA database were selected if they were for $PM_{2.5}$ or smaller particles, had obtainable references for methods, the methods included analytical and normalization methodology, and the methodology was reasonably similar to the methods used in the ambient Fairbanks data. An adequate number of profiles that fit the above criteria were available for wood smoke, diesel exhaust and gasoline exhaust, but not #2 fuel oil combustion. None of EPA profiles that could be found on the website for #2 fuel oil exhaust specified the sulfur content of the fuel oil being tested. Since the sulfur content of #2 fuel oil is much higher in Fairbanks than in other parts of the US, these profiles could not be used. The EPA profiles used by (Ward, 2013) were not averaged in this thesis since the original measurements that these profiles were based on were from an industrial boiler, and were not recommended by the EPA who cite "bad data quality" in the description of the profile. Thus the one available Fairbanks specific profile for #2 fuel oil exhaust was used instead of averaging a larger number of non-representative profiles. Use of just one profile of course does not allow for a representative assessment of the average emissions from an oil burner in Fairbanks, as there is large variability between source profiles for oil burners from other locations (EPA, 2014b), and Fairbanks likely has similar variability in stove type, age, maintenance and other factors that affect emissions. Future source profile work should focus on increasing the number of profiles for #2 fuel oil exhaust that are representative of Fairbanks conditions.

EPA source profiles available on the EPA SPECIATE website are sourced from primary literature. Wood smoke and gasoline exhaust profiles used in this thesis were from Houk et al. 1989 and Watson and Chow (1988). Diesel exhaust profiles were from Zielinska et al. (1998).

2.13 Source Profile Processing Methods

Source profile measurements in the SPECIATE database were given in one of three formats: normalized to gravimetric mass concentration, RCM concentration, or sum of species (Table 2.8) (Hsu et al., 2014). All profiles used in this thesis were normalized to RCM concentration after being obtained from the database. When calculating the RCM only the three major species were used: OCM, EC, SO_4^{2-}. This included profiles that were already normalized to RCM concentration (gasoline exhaust), as well as profiles not already normalized to RCM (all others), which allowed all profiles to be compared on the same basis. This approach differs from the ambient RCM concentration calculation (Section 2.4.2), since mineral oxides, which are accounted for by calculating the other primary material (OPM), were not included as these were not measured in all profiles and represent less than 2% of the mass in the ambient Fairbanks data.

Table 2.8: Normalization options for profiles in the EPA SPECIATE database.

Normalization	Description
Reconstructed Mass (RCM)	Sum of major components including OCM
Sum of species	Sum of major components, but using OC instead of OCM
Gravimetric	Measured mass of particulate material on filter

Chapter 3: Results of $PM_{2.5}$ Analysis

3.1 OC/EC Correction

3.1.1 Method Performance

Figure 3.1 (left panel) shows the effect that the change in carbon sampling and analysis methods in 2009 had on the $OC/PM_{2.5}$ ratio. The reasons for the lower OC measurement values obtained with URG/IMPROVE methods is explained in Section 2.4.3. Figure 3.1 (right panel) shows the effect of the Fairbanks specific OC/EC conversion factor when it was used to correct URG/IMPROVE data to a SASS/NIOSH format, and how the other initial corrections (Sections 2.4.1 and 2.4.2) removed seasonal variability and gross outliers. Figure 3.2 shows a correlation of the RCM concentration (reconstructed with the corrected OC/EC data) and the collocated gravimetric mass concentration. Points that are removed by the QC metric (shown in red) all fall far from the expected line with a slope of one, illustrating how agreement between reconstructed and gravimetric mass concentration is the basis for the QC metric. Figure 3.3 shows URG/IMPROVE OC and EC data corrected to a SASS/NIOSH format correlated with the collocated SASS/NIOSH data. The slope is very close to 1 and the fit has an R^2 value close to one.

The correction developed as part of this work to convert SASS/IMPROVE data to SASS/NIOSH allows comparison of the NCORE and NPFS3 sites to other sites. While the Fresno URG/IMPROVE to SASS/NIOSH correction has been used by the ADEC to convert the SASS/IMPROVE data, it does not account for no change in sampler. Use of different samplers are known to affect the OC/EC data. However, we were not able to test the SASS/IMPROVE to SASS/NIOSH correction by directly comparing corrected and measured data as we did with the

URG/IMPROVE to SASS/NIOSH data since the SASS/IMPROVE to SASS/NIOSH correction is not based directly on collocated measurements, but rather on the correlation of SASS/NIOSH vs. URG/IMPROVE collocated measurements and literature derived assumptions (Section 2.1.2.2). While this correction method appears sound, we cannot guarantee it to the level of accuracy that we can guarantee the URG/IMPROVE to SASS/NIOSH method.

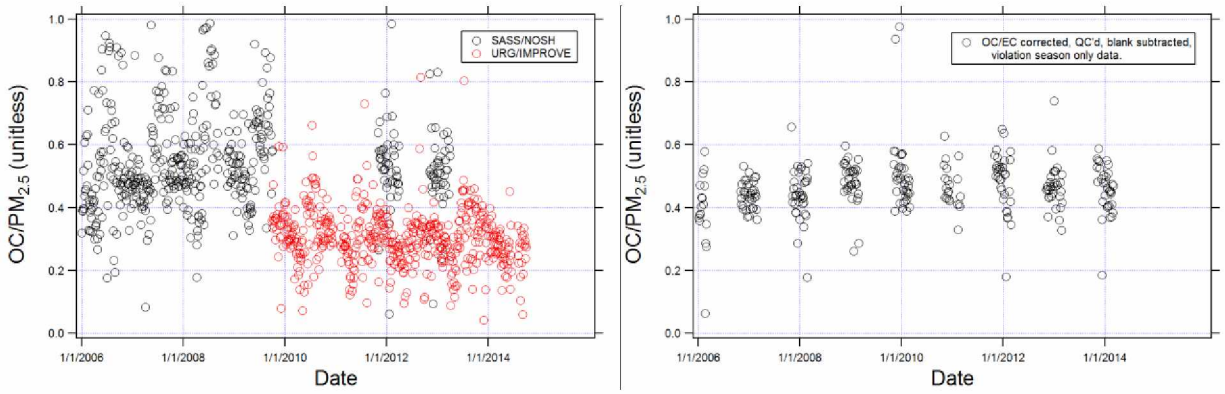

Figure 3.1: Effect of the pre-analysis data corrections on the $OC/PM_{2.5}$ ratio. Left: Raw $OC/PM_{2.5}$ ratios calculated from the raw ambient mass concentration data from the AQS database and from the ADEC. Right: Same data, corrected with the OC/EC correction developed in this thesis, filtered to include only violation season data, blank subtracted and quality controlled. Fairbanks SOB 2009-2010 through 2013-2014 violation season data. Unmodified data from (EPA, 2014b).

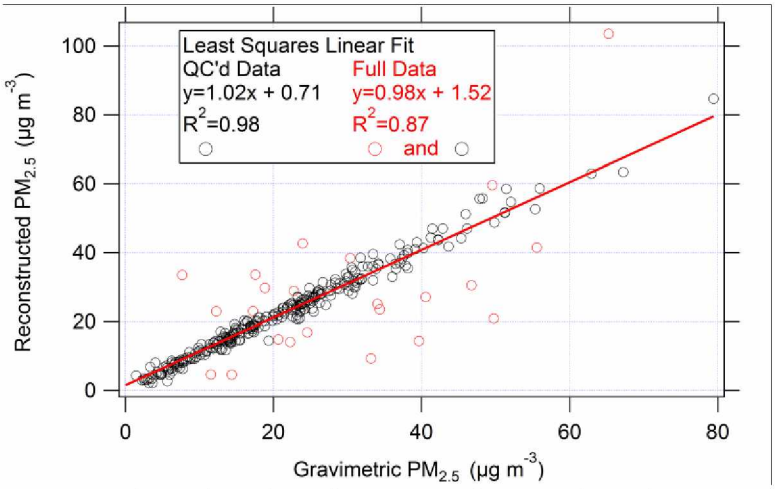

Figure 3.2: RCM concentration plotted against same day gravimetric mass concentration. The RCM concentration was calculated from data corrected with the Fairbanks OC/EC correction developed in this work. Red data points are data that were removed by the QC metric (Section 2.6). Fairbanks SOB 2009-2010 through 2013-2014 violation season data. Statistics provided for the full data include data that were removed and data that were not removed by the QC metric (the full data set).

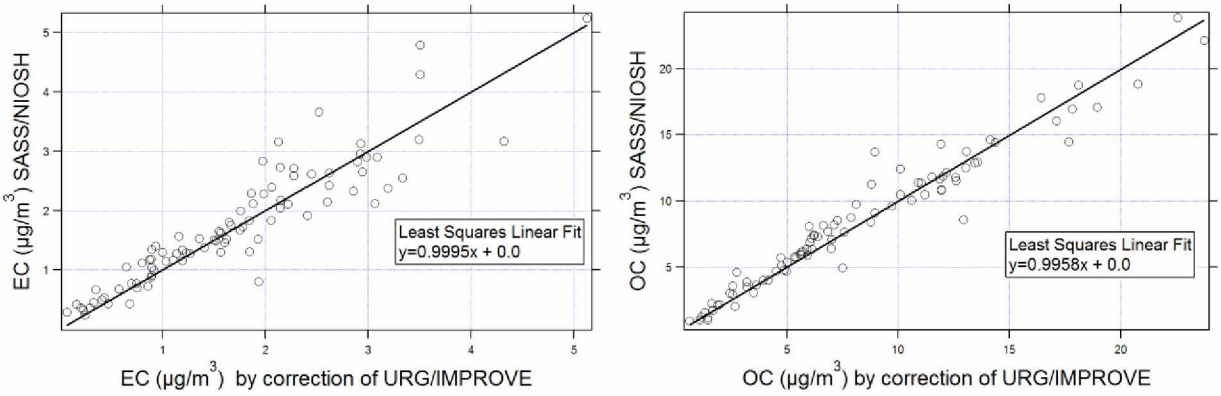

Figure 3.3: Correlation of collocated measured SASS/NIOSH data and URG/IMPROVE data converted to a SASS/NIOSH like format using the Fairbanks correction. All data are blank subtracted, and the fit line is given a forced zero y-intercept, thus R^2 values are not valid. Fairbanks SOB 2009-2010 through 2013-2014 violation season data.

3.1.2 Comparison to Fresno Based Method

The ADEC uses a correction factor based on collocated data from Fresno (Section 2.4.3.2). As part of this thesis, this same collocated data from Fresno was used to develop a similar correction factor, and was compared to the OC/EC correction based on Fairbanks data that was

also developed and used in this work (Section 2.4.3.3). The 2009-2010 through 2013-2014 violation season SOB OC/EC data was corrected with both methods, and Figure 3.4 shows that there are visible (but non-significant) differences in the violation season mean $OC/PM_{2.5}$ ratios after correction depending on which correction method was used. Table 3.2 shows that the differences in both $OC/PM_{2.5}$ and $EC/PM_{2.5}$ ratios are not significant. The $OC/PM_{2.5}$ ratio is not close to significant, however the EC measurements are very close to being significantly different.

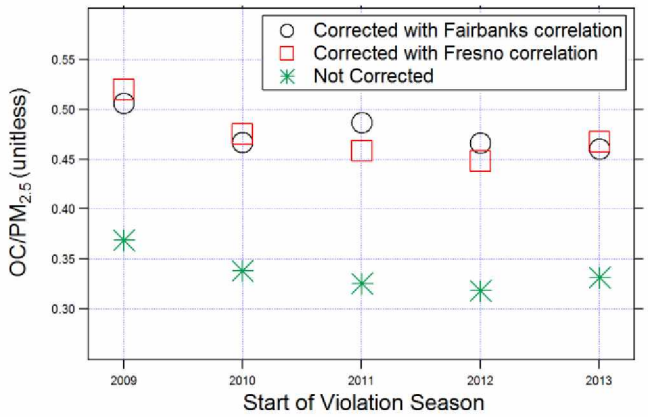

Figure 3.4: Comparison of Fairbanks and Fresno based corrections. Mean $OC/PM_{2.5}$ ratios from the Fairbanks SOB 2009-2010 through 2013-2014 violation seasons.

Table 3.1: T-test (95% conf.) results comparing Fresno and Fairbanks correction methods on $OC/PM_{2.5}$, $EC/PM_{2.5}$ and $TC/PM_{2.5}$ ratios. Data from Fairbanks SOB 2009-2010 through 2013-2014 violation seasons. T-critical is about 2.

	$OC/PM_{2.5}$	**$EC/PM_{2.5}$**	**$TC/PM_{2.5}$**
t-score	0.7	1.9	0.21

Figure 3.5 shows a correlation of the Fresno vs Fairbanks methods applied to the full corrected OC and EC data set. The OC correlation has a slope greater than one, indicating that the Fairbanks correction creates a higher corrected OC value then the Fresno correction. The EC correlation has a slope less than one, indicating that the Fairbanks correction creates a lower corrected EC value than the Fresno correction. EC has the correlation slope furthest from one.

Since both corrections are based on linear fits, all corrected points fall exactly on the line of best fit. Figure 3.6 shows a correlation of the TC measurements corrected with both methods, and the very good correlation indicates that the low EC discrepancy seems to be balanced by the high OC discrepancy, resulting in a very good TC correlation. There are some scattered points in Figures 3.5 and 3.6 that are the result of the Fairbanks method preferentially picking the measured SASS/NIOSH data during the period of where collocated measurements were available, and the Fresno method continuing to use the converted URG/IMPROVE data.

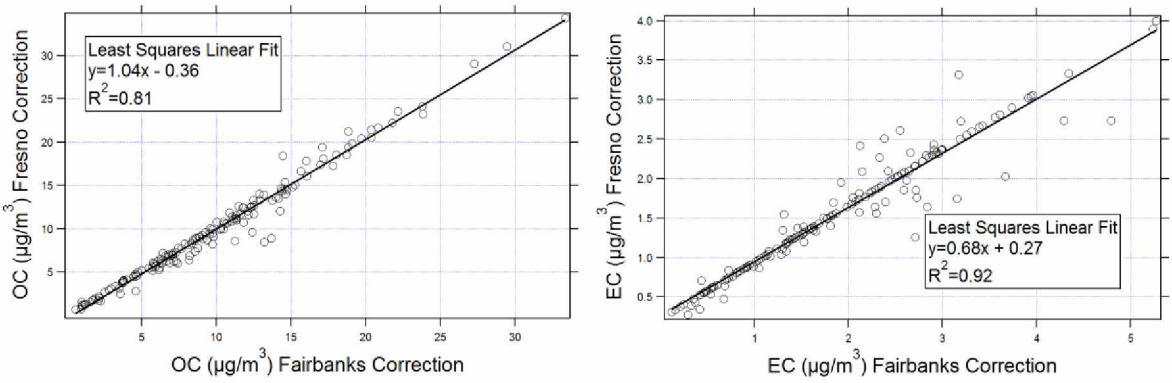

Figure 3.5: Linear fit of URG/IMPROVE OC and EC data corrected using the Fresno and Fairbanks correction methods developed in this work. Data from Fairbanks SOB 2009-2010 through 2013-2014 violation seasons.

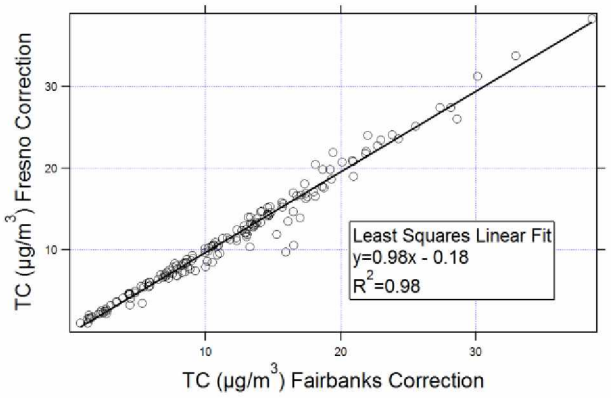

Figure 3.6: Correlation of Fairbanks and Fresno TC corrections. Linear fit of URG/IMPROVE TC data corrected using the Fresno and Fairbanks corrections developed in this work. Fairbanks SOB 2009-2010 through 2013-2014 violation seasons. Original data from (EPA, 2014b).

3.2 Temporal Trends

3.2.1 Meteorological Impacts on $PM_{2.5}$

Figure 3.7 shows the overall $PM_{2.5}$ gravimetric mass concentration at different temperatures for the full 2006-2014 data set, and thus includes data outside of the violation season. A clear trend is apparent with higher $PM_{2.5}$ occurring during colder temperatures. The high $PM_{2.5}$ events observed above +10°C in this data set are the result of summer wildfires, and are removed in this work by selecting data from only November 1 through the end of February.

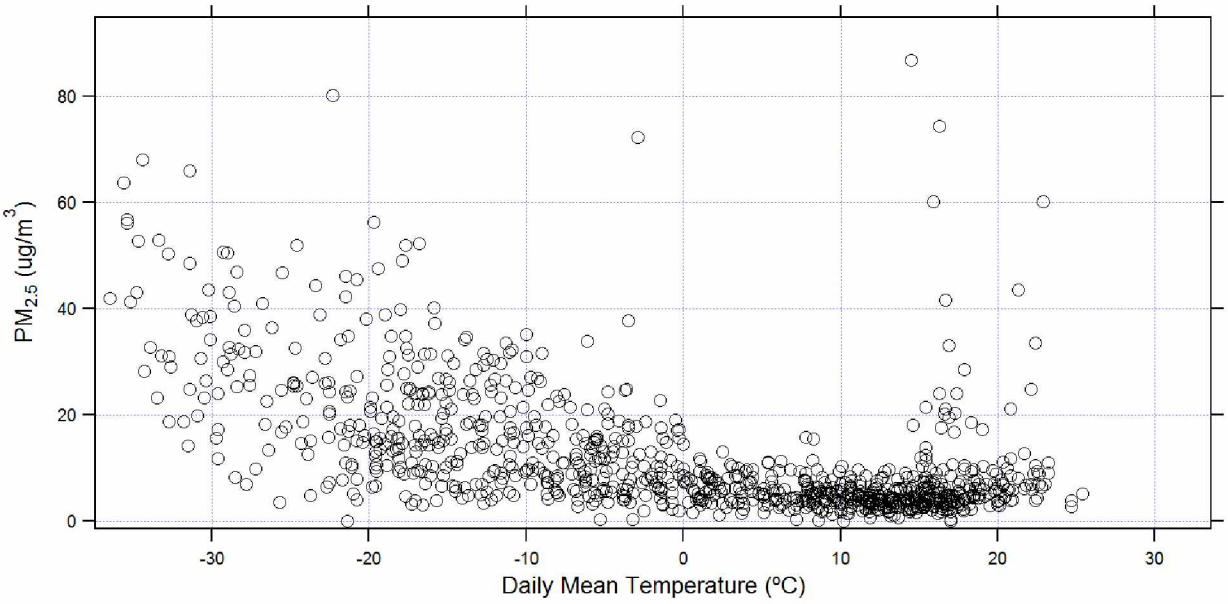

Figure 3.7: $PM_{2.5}$ gravimetric mass concentration at different air temperatures. Fairbanks SOB full year data 2006-2013. Data from (EPA, 2014b).

3.2.2 Component Mass Concentrations in Air

Figure 3.8 shows the violation season mean $PM_{2.5}$ composition and $PM_{2.5}$ mass concentration measurements. High $PM_{2.5}$ component concentrations in ambient air occur with high ambient $PM_{2.5}$ mass concentration, indicating that the particle composition varies little in

comparison to the total amount of particles in the air. The $OC/PM_{2.5}$, $TC/PM_{2.5}$ and $SO_4^{2-}/PM_{2.5}$ ratios were chosen to display in Figure 3.8, however all components analyzed in this thesis show similar trends. Changes in $PM_{2.5}$ mass concentration are anti-correlated with temperature.

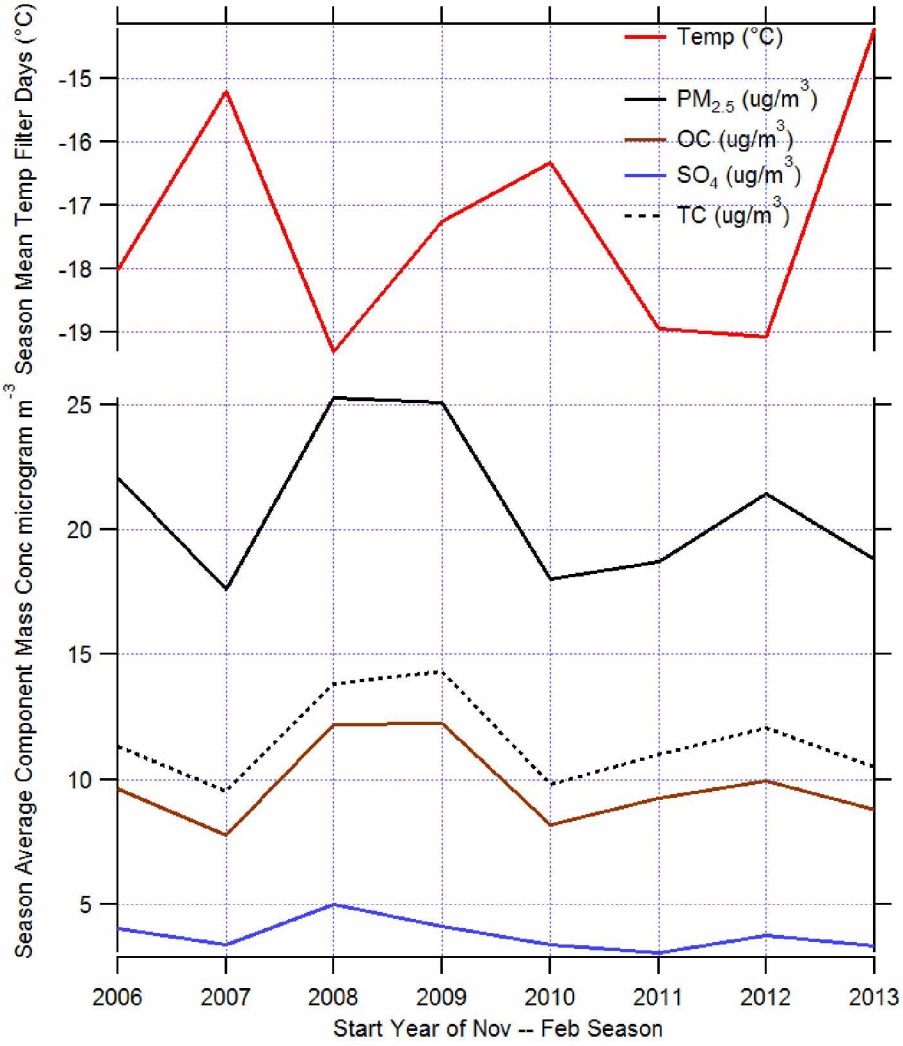

Figure 3.8: Violation season mean component concentrations in ambient air ($\mu g\ m^{-3}$), gravimetric $PM_{2.5}$ mass concentration, and ambient temperature. Fairbanks SOB violation season data 2006-2013. Data from (EPA, 2014b).

3.2.3 Interannual and Daily Variability in Component/$PM_{2.5}$ Ratios

Figure 3.9 shows the mean composition of the SOB particulate data for the full study period used in the temporal analysis was calculated using the carbon multiplier of 1.4. The particles are

composed mostly of OCM, SO_4^{2-}, and other components, in good agreement with previous modeling of the mean particulate composition (Figure 1.4).

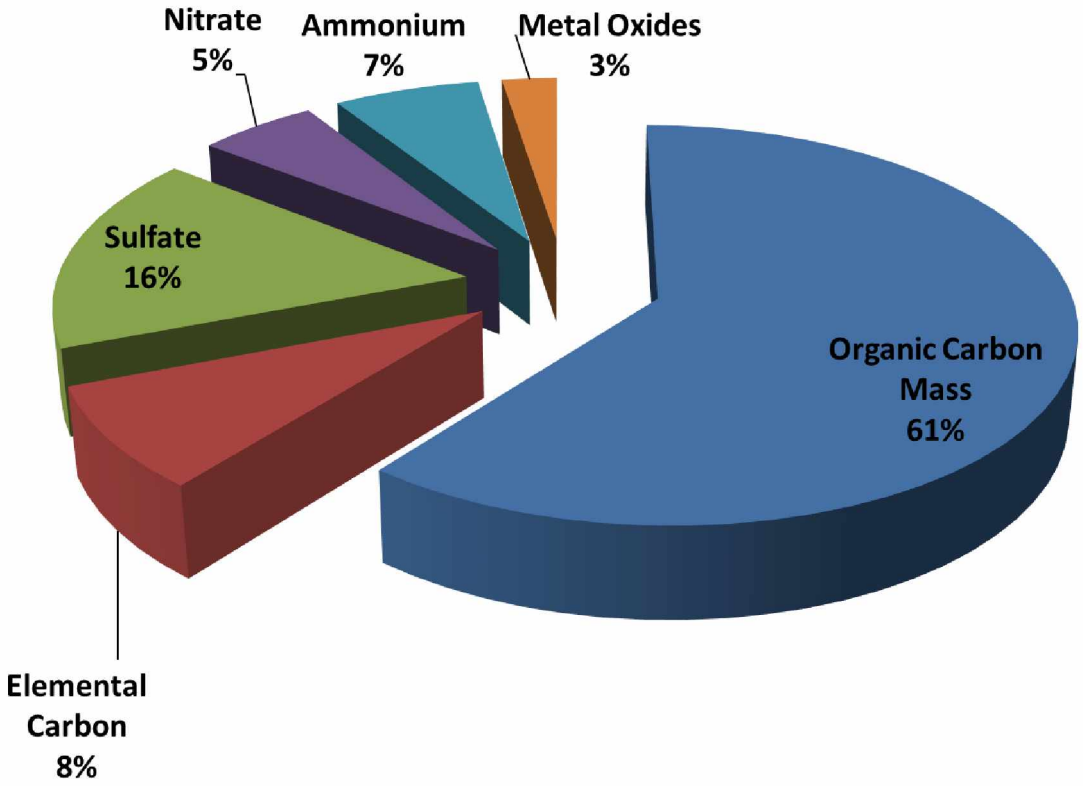

Figure 3.9: 2006 – 2014 mean Fairbanks particle composition based on our analysis using Equation 1-3 to calculate OCM from the OC measurement.

Figure 3.10 shows the interannual variability in the component/$PM_{2.5}$ ratios. $OC/PM_{2.5}$ show the largest absolute interannual variability with a change of 0.07 μg m^{-3} from 2007-2008 to 2008-2009 seasons. OC also has the largest absolute day to day variability, with a standard deviation of 0.2 μg m^{-3} during the 2008-2009 season. However, since OC makes up such a large portion of the $PM_{2.5}$ this does not translate to OC having the largest relative variability. The mean interannual relative variability is shown in Table 3.2 for all component/$PM_{2.5}$ ratios.

Significantly different violation seasons are marked in Figure 3.10 by placing an * next to the seasons average, and the t-scores are shown in Table 3.2. All component/$PM_{2.5}$ ratios except $NO_3^-/PM_{2.5}$ show at least one individual violation season that is significantly different from the mean of the 2006-2007 through 2013-2014 violation seasons. No significantly different individual violation seasons occur simultaneously with $OC/PM_{2.5}$, $EC/PM_{2.5}$ and $SO_4^{2-}/PM_{2.5}$. Figure 3.11 (left plot) shows the interannual variability in mean $NH_4^+/PM_{2.5}$, $SO_4^{2-}/PM_{2.5}$, and the $NO_3^-/PM_{2.5}$ ratios. Figure 3.11 (right plot) shows this interannual variability on a molar basis. The 2011-2012 and 2012-2013 $NH_4^+/PM_{2.5}$ and $SO_4^{2-}/PM_{2.5}$ violation season mean ratios are significantly lower than the 2006-2014 mean for these components. $NH_4^+/PM_{2.5}$ is significantly higher than the mean for three of the four first violation seasons.

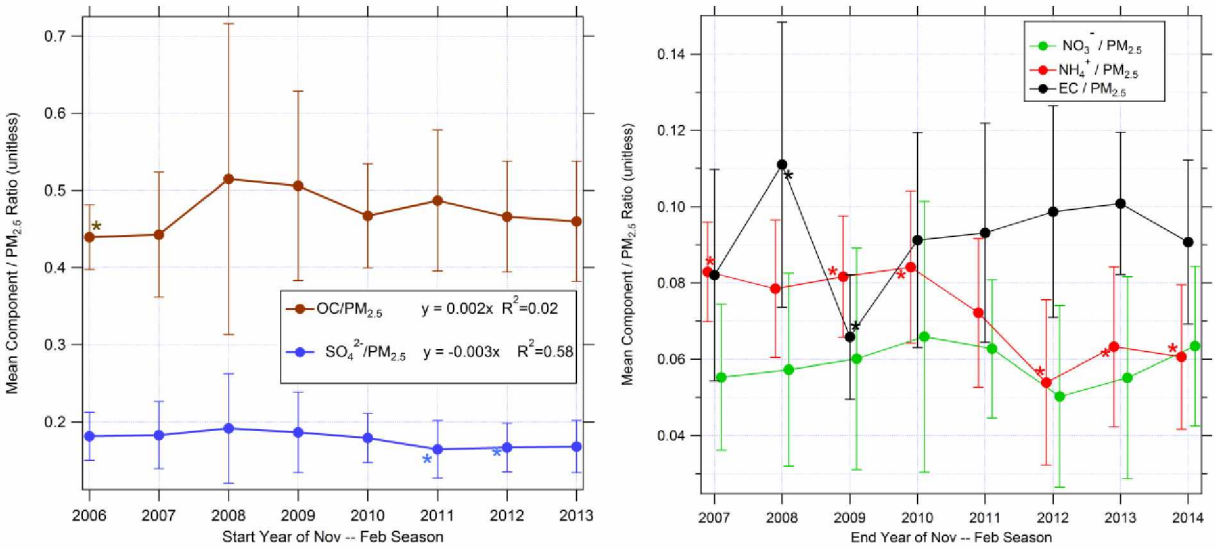

Figure 3.10: Interannual variability in mean component/$PM_{2.5}$ ratios for both the major (larger fraction of the $PM_{2.5}$ mass) and minor components. Fairbanks SOB mean violation season data 2006-2013. Error bars represent standard deviation of the calculation of the mean values.

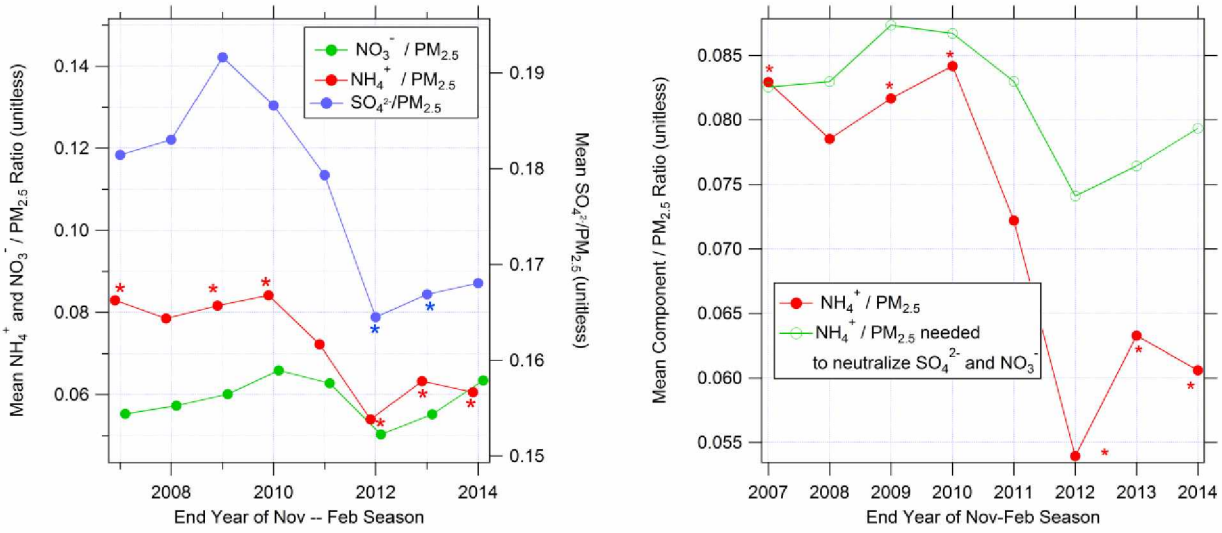

Figure 3.11: Temporal change in the three major particulate ions. Right plot shows the violation season mean component/$PM_{2.5}$ ratios for the major ions, and the left plot shows just $NH_4^+/PM_{2.5}$ ratio and the $NH_4^+/PM_{2.5}$ ratio that would be needed to fully neutralize the particulate NO_3^- and SO_4^{2-}. The standard deviation of all of these mean values is large enough to include the previous and next years' data points for all years and all variables shown, indicating that these trends are not significant. 2006-2007 through 2013-2014 violation season Fairbanks SOB data.

Table 3.2: T-test results for temporal trend analysis. 95% confidence, t-critical is roughly 2. Violation seasons in bold are significantly different from the 2006-2014 mean.

Violation Season	Seasonal Mean	t-stat	Violation Season	Seasonal Mean	t-stat
$OC/PM_{2.5}$			**$K^+/PM_{2.5}$**		
2006-2007	**0.439**	**2.99**	**2006-2007**	**0.00359**	**3.35**
2007-2008	0.443	1.72	**2007-2008**	**0.00355**	**3.34**
2008-2009	0.515	1.32	2008-2009	0.00476	1.07
2009-2010	0.506	1.78	2009-2010	0.00499	1.11
2010-2011	0.467	0.07	2010-2011	0.00507	0.99
2011-2012	0.487	1.10	**2011-2012**	**0.00567**	**2.89**
2012-2013	0.466	0.14	**2012-2013**	**0.00713**	**2.01**
2013-2014	0.460	0.54	2013-2014	0.00660	0.61
2006-2014	*0.473*		*2006-2014*	*0.00517*	
$EC/PM_{2.5}$			**$NO_3^-/PM_{2.5}$**		
2006-2007	0.082	1.94	2006-2007	0.055	0.94
2007-2008	**0.111**	**3.03**	2007-2008	0.057	0.30
2008-2009	**0.066**	**7.78**	2008-2009	0.060	0.29
2009-2010	0.091	0.07	2009-2010	0.066	1.21
2010-2011	0.093	0.24	2010-2011	0.063	0.98
2011-2012	0.099	0.83	2011-2012	0.050	1.91
2012-2013	0.101	0.38	2012-2013	0.055	0.69
2013-2014	0.091	0.98	2013-2014	0.063	1.22
2006-2014	*0.092*		*2006-2014*	*0.059*	
$SO_4^{2-}/PM_{2.5}$			**$NH_4^+/PM_{2.5}$**		
2006-2007	0.181	0.20	**2006-2007**	**0.083**	**3.71**
2007-2008	0.183	0.34	2007-2008	0.079	1.53
2008-2009	0.192	0.91	**2008-2009**	**0.082**	**2.67**
2009-2010	0.187	0.70	**2009-2010**	**0.084**	**3.01**
2010-2011	0.179	0.13	2010-2011	0.072	0.31
2011-2012	**0.164**	**2.27**	**2011-2012**	**0.054**	**5.00**
2012-2013	**0.167**	**2.16**	**2012-2013**	**0.063**	**2.62**
2013-2014	0.168	1.89	**2013-2014**	**0.061**	**3.67**
2006-2014	*0.178*		*2006-2014*	*0.072*	

Figure 3.12 shows the ambient NH_4^+ mass concentration plotted against the NH_4^+ mass concentration needed to neutralize the major particulate acids NO_3^- and SO_4^{2-}. Overall, the

measurements fall very close to the line drawn on the plot with a slope of one and intercept of zero, the line that represents perfect particulate neutralization under the assumption that these three ions are the only major ions in the $PM_{2.5}$. Not all filter measurements fall perfectly onto the idealized line indicating that the NO_3^- and SO_4^{2-} are not perfectly balanced by the NH_4^+. Figure 3.8 shows that the composition of the particles does not change drastically with increasing mass concentration, and thus it can be assumed that the air with a higher concentration of NH_4^+ represents air with a greater $PM_{2.5}$ concentrations. At higher $PM_{2.5}$ concentrations, there is excess NH_4^+, and at lower concentrations there is excess acid.

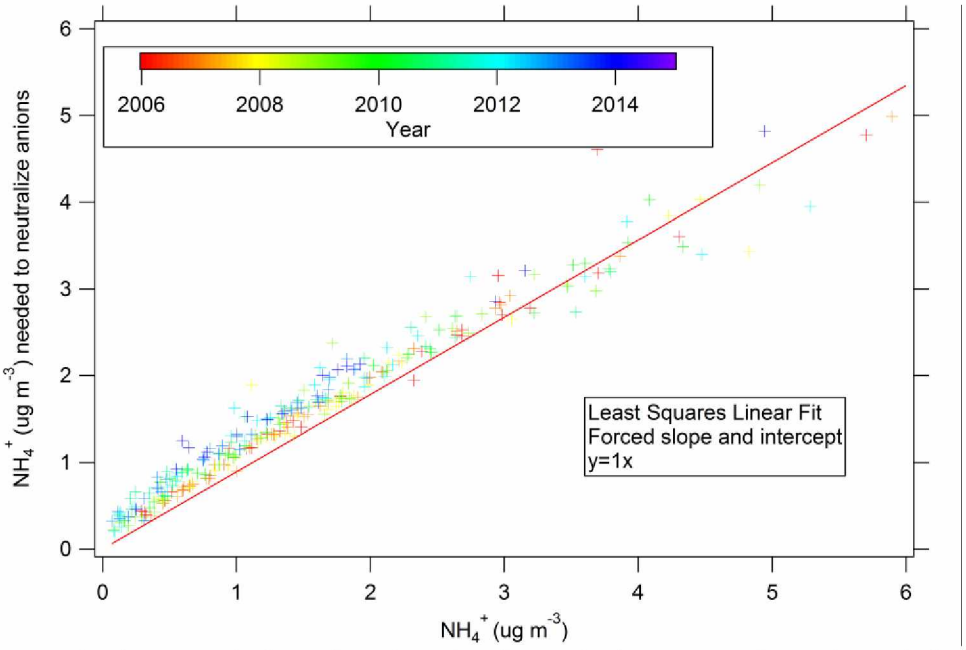

Figure 3.12: Particulate NH_4^+ plotted against the theoretical amount of NH_4^+ needed to neutralize the major particulate acids NO_3^- and SO_4^{2-}. The line represents the forced slope = 1, intercept = 0, line that the data should theoretically fall on assuming that these three components are the only major ions in the particulates. 2006-2007 through 2013-2014 violation season Fairbanks SOB data.

3.2.4 Trends in Component/$PM_{2.5}$ Ratios

Figure 3.13 shows the mean component/$PM_{2.5}$ ratios for the 2006-2007 through 2013-2014 violation seasons, fitted with a least squares linear trend line. Table 3.3 shows that both

$NH_4^+/PM_{2.5}$ and $SO_4^{2-}/PM_{2.5}$ have a significantly different from zero downward trend from 2006 to 2013. A high standard deviation that is often larger than the slope is observed in the trends of other component/$PM_{2.5}$ ratios, and results in non-significant trends in component ratios other than these two. The 2006-2007 violation season $OC/PM_{2.5}$ ratio was significantly lower than the average, and the non-significant trend line is in the upward direction. While not significant, there is a decrease in the $OC/PM_{2.5}$ ratio after the 2011-2012 season. The two violation seasons where the $EC/PM_{2.5}$ ratio was significantly different (high and then low) from the mean both occur at the beginning of the time series.

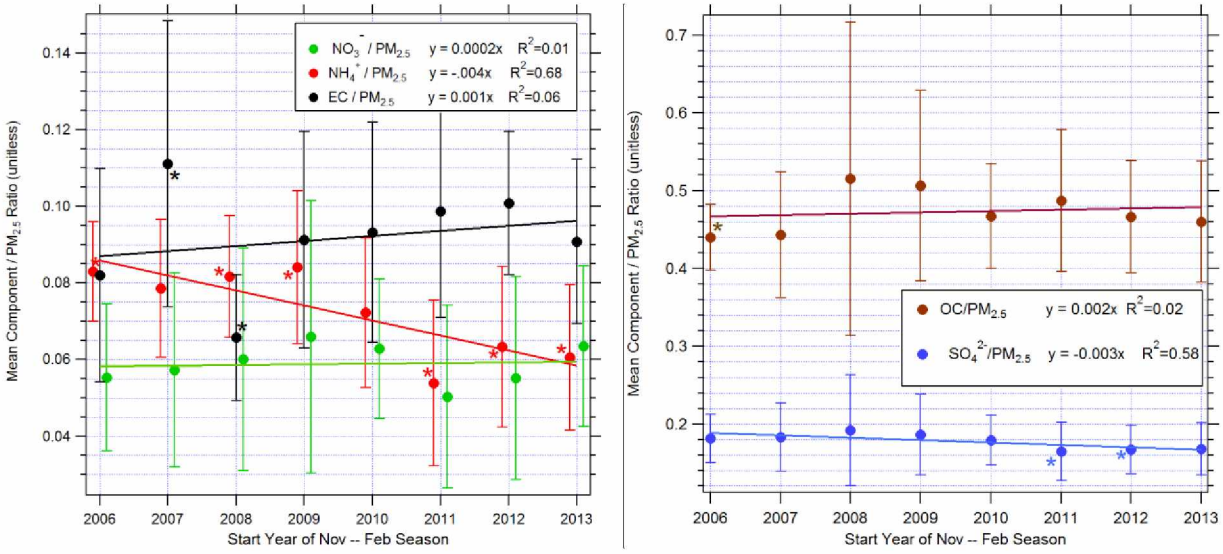

Figure 3.13: Violation season mean component/$PM_{2.5}$ trend fitting. Years that are statistically different from the mean for the full time series are marked with an *. Lines represent least squares linear regression.

Table 3.3: Slope of linear least squares regression of the 2006-2014 violation season mean component/$PM_{2.5}$ ratios, with standard deviation of the regression line. T-test results are a comparison of the observed slope with a zero slope; values above the t-critical of roughly 2 indicate the slope is significantly different from zero.

	Slope (yr^{-1})	stdev	t-stat
$NH_4^+/PM_{2.5}$	-0.0039	0.0012	**9.19**
$EC/PM_{2.5}$	0.0013	0.0022	1.67
$NO_3^-/PM_{2.5}$	0.0002	0.0009	0.52
$OC/PM_{2.5}$	0.0016	0.0045	1.01
$SO_4^{2-}/PM_{2.5}$	-0.0031	0.0011	**7.97**

3.2.5 Correlation of Component/$PM_{2.5}$ Ratios with Temperature

Figure 3.14 illustrates the relationship of the component/$PM_{2.5}$ ratios with temperature. Individual filter measurements are plotted for the entire time series at the SOB, rather than averages. Both $NH_4^+/PM_{2.5}$ and $SO_4^{2-}/PM_{2.5}$ appear to decrease with increasing temperature, while $EC/PM_{2.5}$ increases with increasing temperature. $OC/PM_{2.5}$ remains relatively constant.

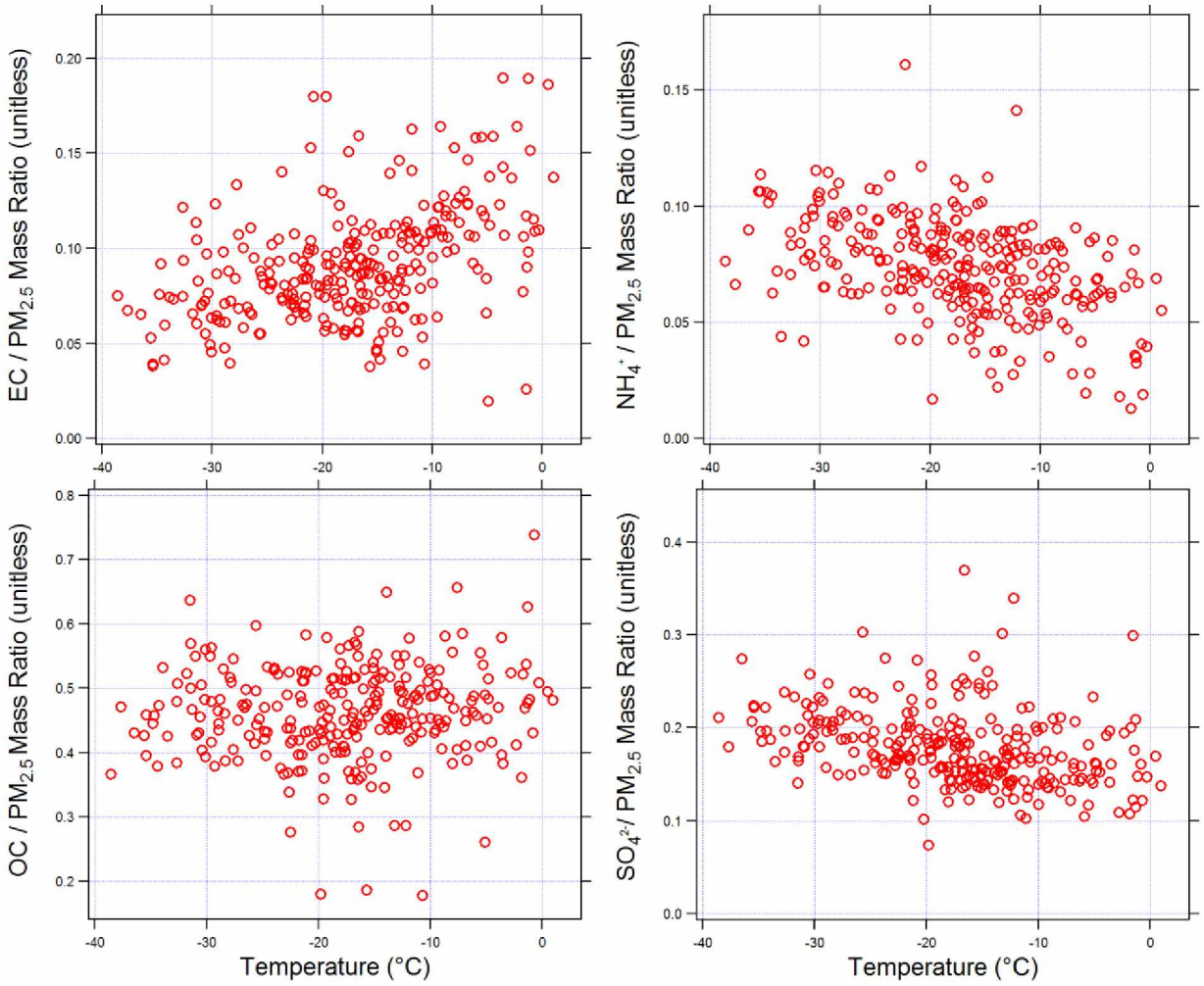

Figure 3.14: Component/$PM_{2.5}$ ratios at different temperatures. Non-significant trends are apparent and may motivate future work. Note that the OC values here represent only carbon, not OCM.

3.3 Spatial Trends

3.3.1 Gravimetric $PM_{2.5}$

Figure 3.15 shows the violation season mean $PM_{2.5}$ gravimetric mass concentration at all four sampling sites. The NPFS3 site measured approximately double the $PM_{2.5}$ mass concentration that was observed at the other three sites. The data used to produce this plot is shown in Appendix B, Table B.1. This table also shows the results of significance testing (paired t-test, log normalized data, 95% conf.) on these values. The NPFS3 site is significantly different from all three other sites, and the other sites are not significantly different from each other. Despite the fact that the mean NPFS3 $PM_{2.5}$ mass concentration is closer to the mass concentration of the NPE site than the Fairbanks site, statistical tests show that NPFS3 is statistically less different from the Fairbanks sites (Appendix B, Table B.1). This statistical discrepancy is likely due to the fact that the NPE site has a smaller number of filters and larger standard deviation than either Fairbanks site.

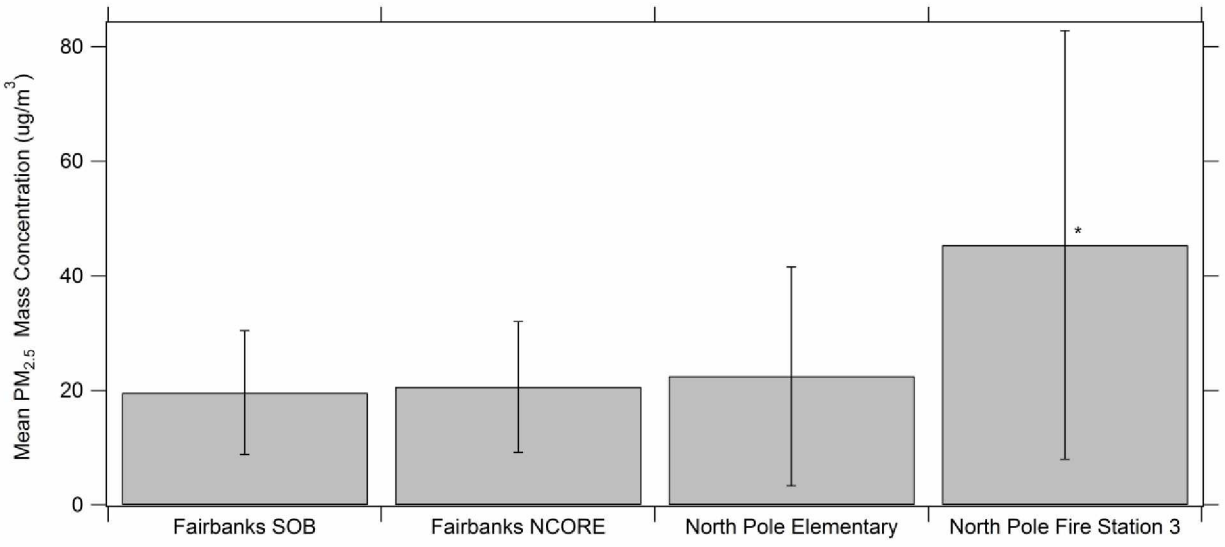

Figure 3.15: Mean gravimetric $PM_{2.5}$ mass concentration at each sampling site. Error bars represent standard deviation. The NPFS3 site is significantly different from all other sites, and is marked with an *. 2011-2012 through 2013-2014 violation seasons.

Figure 3.16 shows the same day filter measurements of gravimetric $PM_{2.5}$ mass concentration. Measurements from different sampling sites are correlated. Correlation of sites that were both in North Pole or Fairbanks always showed a better fit based on a comparison of r^2 values than when sites in Fairbanks were correlated with sites in North Pole.

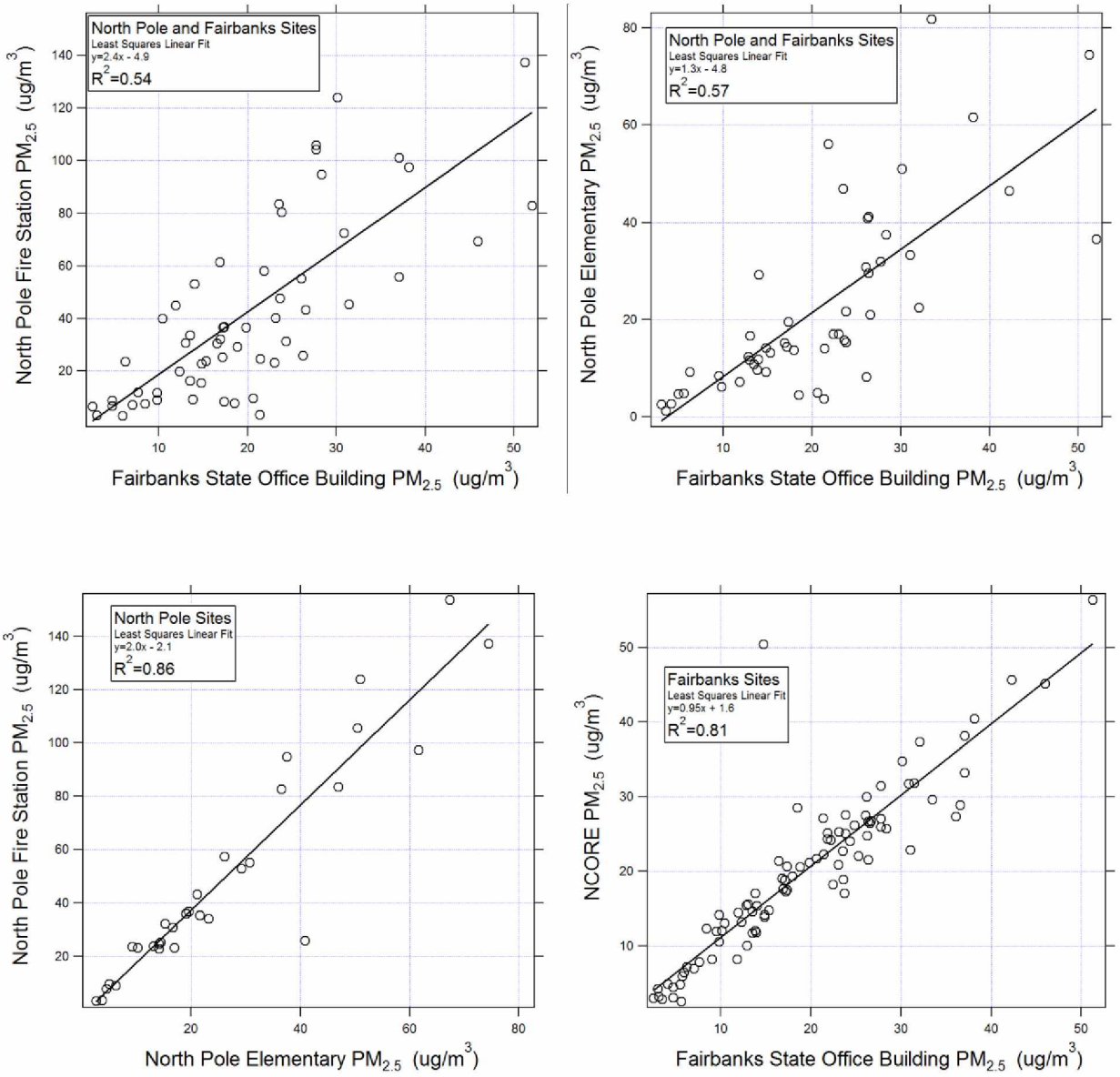

Figure 3.16: Spatial correlation of same day gravimetric $PM_{2.4}$. Sampling sites are correlated with the site within the same city on the bottom row, and correlated with sites in a different city on the top row. 2011-2012 through 2013-2014 violation season data.

3.3.2 Component/$PM_{2.5}$ Ratio Trends

Figure 3.17 shows the mean composition of each sampling site for the 2011-2012 through 2012-2013 violation seasons. The $OC/PM_{2.5}$ ratio is larger at the North Pole sites, the $SO_4^{2-}/PM_{2.5}$ and $Zn/PM_{2.5}$ ratio is larger at the Fairbanks sites. The $K/PM_{2.5}$ and $K^+/PM_{2.5}$ ratios increase from Fairbanks SOB to NPFS3, and EC is smallest at the NPE sampling site.

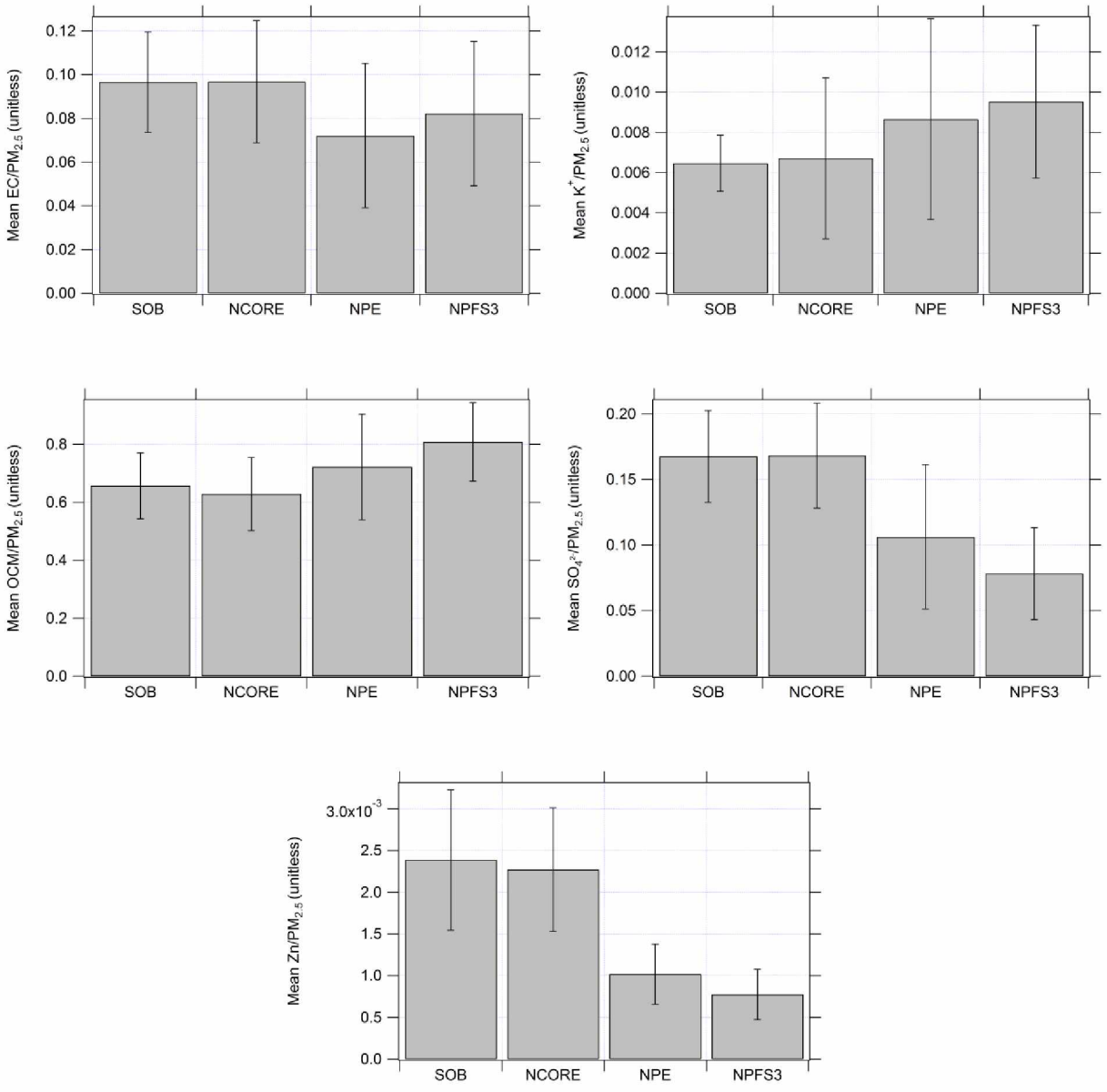

Figure 3.17: Mean composition for the four sampling sites. 2011-2012 through 2013-2014 violation seasons. Note: Paired mean values were used (by pairing each site with the SOB, and the SOB with NCORE), and these values are representative of the mean values for any pairing of these sites (within about 5%). Standard deviations are not included because these values varied by several orders of magnitude between different pairings. See Table 3.4 for the level of significance in compositional differences between sites.

Table 3.4 shows that significant compositional differences exist between some sampling sites. NPFS3 shows significantly different values from nearly all other sites for all components tested with one exception – the EC concentration at NPFS3 is barely significantly different from the concentrations measured at NPE. Fairbanks sites (SOB and NCORE) are not significantly different for all parameters except $OC/PM_{2.5}$, though this value is very close to the level of significance. The smallest statistical differences were observed with the $K^+/PM_{2.5}$ and $EC/PM_{2.5}$ ratios, and the largest with the $SO_4^{2-}/PM_{2.5}$ and $Zn/PM_{2.5}$ ratios. For most components (but not all) the t-values were further from t-critical when sites from different cities were compared than when sites within the same city were compared. For example, with respect to the $OC/PM_{2.5}$ ratio, the SOB site has the same level of significant difference with the NCORE and NPE site. Both the North Pole sites had large standard deviations (Table 3.5), however the NPE site also measured a $OC/PM_{2.5}$ ratio closer to the SOB ratio. The number of valid points for both of these pairings was about 50. The $SO_4^{2-}/PM_{2.5}$ ratio is more significantly different between the SOB site and the NPE site than the SOB and the NCORE site. The $SO_4^{2-}/PM_{2.5}$ ratio has a much smaller standard deviation than the $OC/PM_{2.5}$ ratio, as well as a much larger difference in mean values between Fairbanks and North Pole sites. In addition, significant differences in $Zn/PM_{2.5}$ exist between both Fairbanks sites and both North Pole sites. The two Fairbanks sites are not significantly different, however the North Pole sites are significantly different, though the t-scores are much closer to the level of significance than when sites from different cities are compared.

Table 3.4: Paired t-test (95% significance) results comparing the four sampling sites. Values represent t-scores with a t-critical about 2. Pairing removes non-overlapping data and thus these values all reflect the overlapping subset of 2011-2012 through 2013-2014 violation seasons

$OC/PM_{2.5}$	t-statistic			
$SO_4^{2-}/PM_{2.5}$	SOB	NCORE	NPE	NPFS
SOB		2.1	2.0	7.9
NCORE	0.2		2.6	8.8
NPE	10.9	6.7		5.6
NPFS	19.1	17.6	4.4	
$Zn/PM_{2.5}$				
$K^+/PM_{2.5}$	SOB	NCORE	NPE	NPFS
SOB		1.7	11.7	14.3
NCORE	3.5		11.5	15.5
NPE	4.2	3.6		4.3
NPFS	6.9	3.0	3.4	
$EC/PM_{2.5}$				
	SOB	NCORE	NPE	NPFS
SOB		0.1	5.7	2.8
NCORE			2.0	4.3
NPE				2.0

Table 3.5: Standard deviation from the paired t-test of the $SO_4^{2-}/PM_{2.5}$ of $OC/PM_{2.5}$ ratios comparing the four sampling sites. The first number is the standard deviation of the paired data from the site on the left axis, and the second number is the standard deviation of the paired data from the site on the top axis.

$OC/PM_{2.5}$	Standard Deviation			
$SO_4^{2-}/PM_{2.5}$	SOB	NCORE	NPE	NPFS
SOB		0.08/0.09	0.07/0.13	0.06/0.10
NCORE	0.04/0.04		0.10/0.09	0.09/0.09
NPE	0.05/0.03	0.07/0.03		0.10/0.09
NPFS	0.04/0.03	0.03/0.04	0.04/0.04	

3.4 Sulfur Oxidation

3.4.1 Sulfur Oxidation Ratio (SOR)

Figure 3.18 (left plot) shows the linear least squares regression of the SO_4^{2-} measured in the $PM_{2.5}$ vs the total potential SO_4^{2-} (Section 2.8.1). The slope of this line provides the calculated ambient SOR, which is about 5% of the total potential SO_4^{2-}. This value represents the average SOR for the time period when SO_2 data is available. The coloring of the points based on the $Zn/PM_{2.5}$ ratio indicates that there is no correlation between SOR and particulate Zn. Figure 3.18 (right plot) shows that SOR values were observed up to 10% of the total potential SO_4^{2-}, and the higher SOR values tended to occur on the coldest days, but do not appear to occur more frequently during any particular month during the violation season. The primary SOR was calculated from emission factors to be 0.4%, and approximated from the provided primary SOR values as 2-8%.

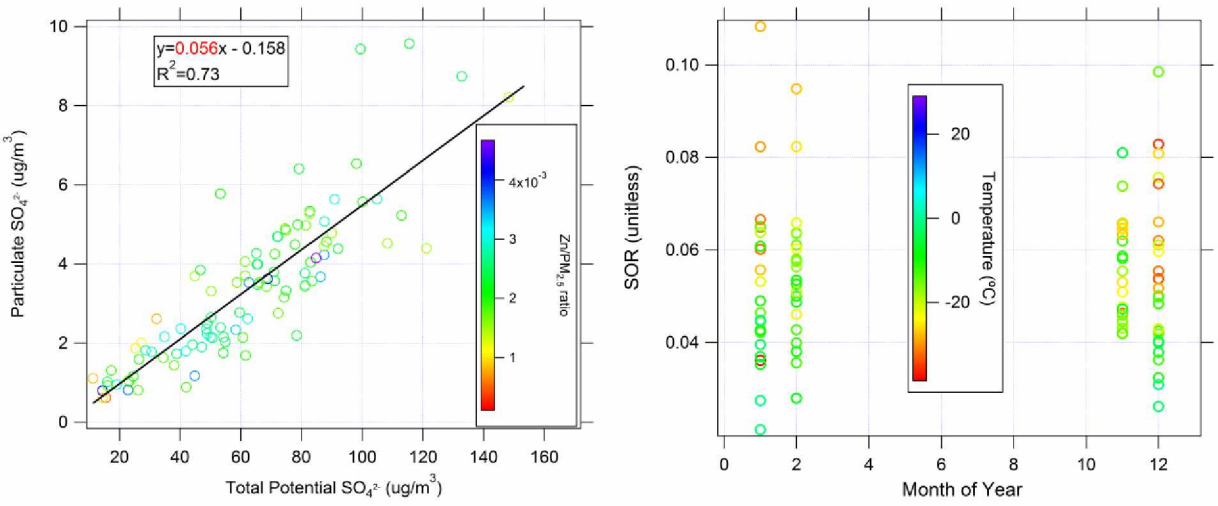

Figure 3.18: SOR at the Fairbanks NCORE site. The left plot shows the measured ambient SO_4^{2-} plotted against the total potential SO_4^{2-}, colored by the concentration of Zn in the $PM_{2.5}$. The line of best fit calculates the average SOR. The right plot shows the SOR plotted for each month of the violation season, and is colored to show the affect that temperature has on the SOR. 2011-2012 through 2014-2015 violation season NCORE data.

3.4.2 Non-Sulfate Sulfur

Figure 3.19 shows the correlation of particulate sulfur measured by two separate methods, XRF and IC. The slope of the line of best fit is about 1.2 for both the Fairbanks SOB and NPFS3 sites, indicating that the XRF sulfur measurements are 20% higher than the sulfur content of SO_4^{2-} measured with IC. Intercepts are negligible.

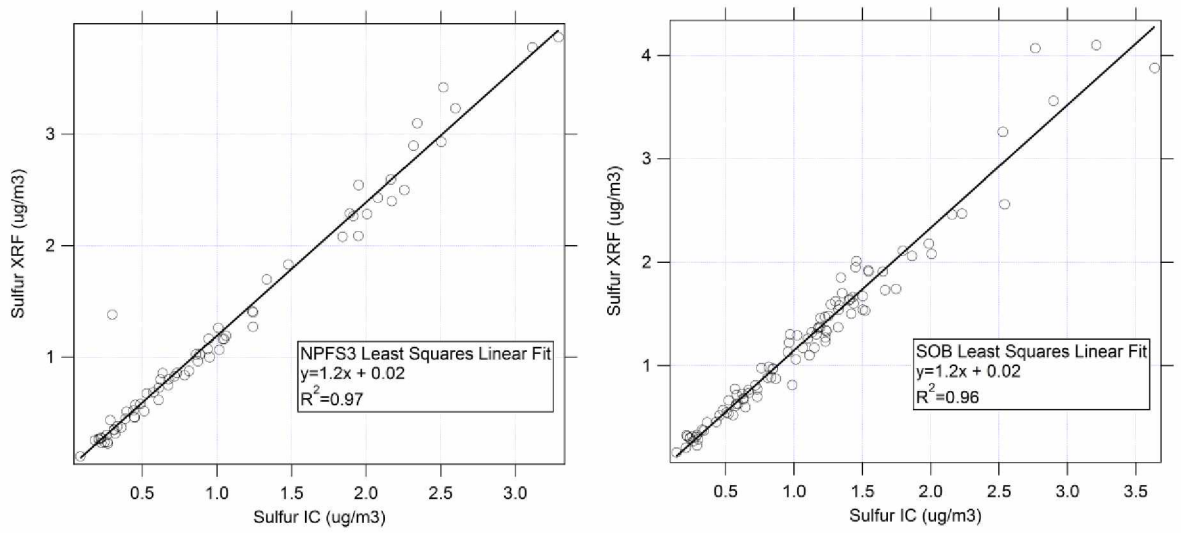

Figure 3.19: Correlation of particulate sulfur measured with XRF and particulate sulfur calculated from the SO_4^{2-} measured with IC. Left plot shows the correlation of NPFS3 data, and right plot shows the correlation of Fairbanks SOB data. 2011-2012 through 2014-2015 violation season data.

3.5 Source Profile Averages

Figure 3.20 shows the result of averaging the selected SPECIATE source profiles, and the Fairbanks specific source profile for #2 fuel oil. The mean and standard deviation of the source profiles that was used to create this plot are shown in Appendix B, Table B.2. Despite attempts to pick profiles that were measured in similar ways, selected profiles from individual emitters within the same source category show high variability in their component/$PM_{2.5}$ ratios. This is expected, because specific emitters within the same category may function differently (Section 4.6). However, several clear compositional differences between the source categories exist. Wood smoke has the highest OCM/$PM_{2.5}$ ratio. Diesel has the lowest OCM/$PM_{2.5}$ ratio and the highest EC/$PM_{2.5}$ ratio. #2 fuel oil is the only significant source of primary SO_4^{2-}. The large standard deviation observed in the OCM/$PM_{2.5}$ ratio of diesel exhaust is likely attributable to the decision to average source profiles from both idling and driving vehicles.

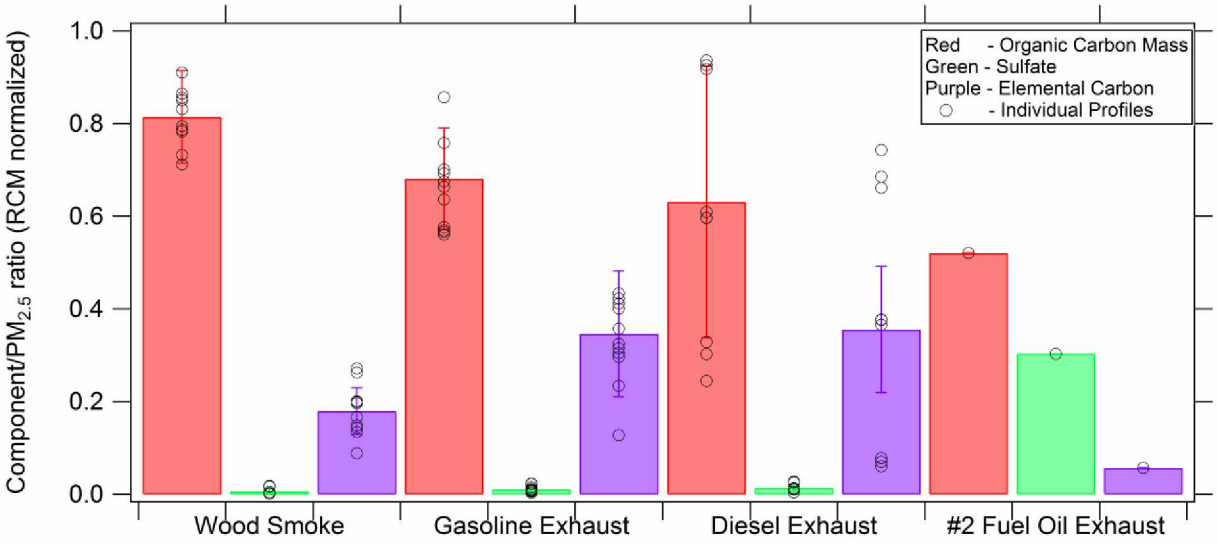

Figure 3.20: Composition of direct emissions from likely sources of breathing level $PM_{2.5}$ in Fairbanks. The averages shown in this bar plot are component/$PM_{2.5}$ ratios (source profile measurements normalized to RCM concentration), error bars represent standard deviation, and black circles represent the individual profiles that were averaged to create the bar plots. Wood, gasoline and diesel are from the EPA SPECIATE database, and the #2 fuel oil is from the Fairbanks specific profiles.

Chapter 4: Discussion

4.1 OC/EC Correction

Section 3.1.1 describes the evidence for how well the OC/EC conversion factor developed from Fairbanks collocated data was able to accomplish the conversion of URG/IMPROVE data to a SASS/NIOSH format. The removal of the visual discrepancy depicted in Figure 3.1 is strong evidence for the success of the correction. The excellent fit found with correlation of RCM concentration and gravimetric mass concentration indicates that the correction method is valid under the assumptions made in calculating the RCM concentration described in Section 2.4.2. This excellent provides evidence that the conversion factor developed using Fairbanks data does not alter the OC measurements excessively.

The good R^2 value obtained from correlation of collocated URG/IMPROVE OC and EC data corrected to a SASS/NIOSH format with collocated SASS/NIOSH data indicates that this OC/EC correction is able to accurately convert the data that was used to create the correction. Converted and measured values are from the same population based on the t-test, with t-scores of 0.03 (OC) and 0.01 (EC). OC is based on TC and EC, and thus represents the performance of both these conversions. This strong agreement is expected since this correction is based on the collocated data, however this agreement does ensure that the correction has been applied correctly.

This correction inherently accounts for the composition of Fairbanks $PM_{2.5}$ better than the correction based on Fresno data that is currently in use. However, Table 3.1 shows that switching methods does not produce significantly different mean $OC/PM_{2.5}$ and $TC/PM_{2.5}$ values. The switch of methods may produce significantly different $EC/PM_{2.5}$ ratios since the t-values were very close to the 95% significance level. If an analysis requires measurements that are more certain than this confidence level, there may be benefit gained from switching to the conversion based on the

collocated Fairbanks data. Measurements of EC would be most affected by a change in correction method. Perhaps the greatest benefit of using the Fairbanks conversion is that it allows correction of SASS/IMPROVE data to a SASS/NIOSH format. Figure 3.1 (left panel) shows a clear decrease in OC/$PM_{2.5}$ ratio when switching from SASS to URG samplers due to increased revolatization of SVOCs. The ability of our conversion method to account for a change in analysis method but no change in sampler, and thus no change in revolatization due to changes in flow and filter surface area, will improve the quality of SASS/IMPROVE data corrected to a SASS/NIOSH-like format.

4.2 Temporal Trends

4.2.1 Meteorological Impacts on $PM_{2.5}$

Figure 3.7 illustrates how colder ambient temperatures increase the $PM_{2.5}$ mass concentration. This increase is due to increased trapping, which is the result of meteorological phenomena that include increased inversion strength and decreased wind speed and is associated with a decrease in temperature. Figure 3.8 shows the correlation of $PM_{2.5}$ mass concentration with all major particle components, and justifies the decision to account for the effect of inversion strength and other meteorological phenomena by using the component/$PM_{2.5}$ ratios (Section 2.5), rather than ambient concentrations, in temporal and spatial analysis of particle composition.

4.2.2 Component Mass Concentrations

Figure 3.8 shows large interannual variability in the particulate mass, but no linear trends. This finding does not indicate that no change in emissions has occurred due to the wood stove changeout program or any other factors. Other metrics, such as the total number of violation days per season, may be better able to assess the impact of policy and weather induced changes in

burning behavior on $PM_{2.5}$ composition. The lack of a decrease in mean $PM_{2.5}$ mass concentration despite a decrease in winter season EPA violations is likely due to a decrease in the amount of particulates experienced during days with bad air quality, without a proportional decrease in the mean $PM_{2.5}$ mass concentration. Tran and Mölders (2012) used predictive models to show that a decrease in the number of violation days, defined as the measurement days that are close to the EPA regulatory limit, could occur due to changing out about 3,000 stoves and 90 hydronic heaters, but would be accompanied by only small changes in mean $PM_{2.5}$. Longer term data analysis such as using the full OC/EC data set with a PMF model, or extending the timeframe of the statistics based analysis used in this thesis, is needed to make a more accurate assessment of the impact of these programs on the ambient $PM_{2.5}$ mass concentration.

Wang and Hopke (2014) claim in their PMF analysis that the WSCP had a "weak impact" on reducing the contribution of wood smoke to breathing level $PM_{2.5}$ after two years of replacements. It is unclear if this analysis actually used particulate carbon data after 2009, since their analysis is missing 42% of the OC and EC data, which is approximately the amount of data collected after the 2009 method switch. Omission of this data would remove any possibility of observing an affect from the WSCP, since this program started in 2010. In addition, Wang and Hopke (2014) did not use significance testing to determine the level of certainty of their claim. The fact that the temporal analysis completed as part of this thesis did not find any significant change after the start of the WSCP despite inclusion of post-2009 carbon data is in clear contrast with the findings of Wang and Hopke (2014).

4.2.3 Interannual and Daily Variability in Component/$PM_{2.5}$ Ratios

Interannual variability, or non-linear temporal changes in particle composition, is both expected and observable in the mean seasonal $PM_{2.5}$ composition data. There are many factors

that contribute to interannual variability in the $OC/PM_{2.5}$, $SO_4^{2-}/PM_{2.5}$, and $NH_4^+/PM_{2.5}$ ratios. These include meteorology, human burning choices, available fuels, public policy and regulation and other factors. The price of fuel oil shows the strongest correlation with the observed interannual variability. After the spike in #2 fuel oil cost in 2007-2008, the reported amount of oil used for heating decreased (Figure 4.3). It is important to note that the wood use data is obtained from the Home Heating Survey, a phone survey that relies on accurate responses from participants. The 2013-2015 surveys found an increase in the anomalous or internally inconsistent responses and either omitted or corrected these responses based on other related survey responses. In 2015 a large under-reporting of hydronic heaters was observed in the North Pole area, however this phenomena should not impact our data set as it does not change the result that more people in North Pole use wood for home heating than in Fairbanks (Carlson and Zhang, 2015). The decrease in reported use of #2 fuel oil is correlated with a drop in the particulate $SO_4^{2-}/PM_{2.5}$ ratio (Figure 4.4) that continues until 2011, despite the return of fuel prices to prior levels and a flattening of the reported use of #2 fuel oil. This is anticipated, since people who purchase wood stoves and chainsaws to increase their capacity to burn wood are likely to continue using wood to heat their home rather than immediately return to using oil when the price of oil drops. The drop in the $SO_4^{2-}/PM_{2.5}$ ratio is not due to volatization since sulfate does not re-volatize the way that NH_4^+ does. While NO_3^- does revolatize, the changes in the $NO_3^-/PM_{2.5}$ have no significantly different years or trends due to small observed changes, and thus do not contribute to the large change in the $NH_4^+/PM_{2.5}$ ratio. Interannual variability was not directly tested for statistical significance, the significance testing used to assess the significance of linear trends shown in Figure 3.13 supports the observed variability, as the year with a significantly low $SO_4^{2-}/PM_{2.5}$ ratio occurs immediately after the sharpest drop in the $SO_4^{2-}/PM_{2.5}$ ratio.

Figure 3.13 shows that the 2006-2007 violation season mean $OC/PM_{2.5}$ is significantly lower than the overall mean, providing statistical evidence that there was an increase in the $OC/PM_{2.5}$ ratio after the 2006-2007 winter. The entire data set after the 2008-2009 season has a higher $OC/PM_{2.5}$ ratio than the first two seasons. The reason that the 2007-2008 violation season is not significantly different is that this season has a much larger standard deviation than the 2006-2007 violation season, leading to less certainty in the mean value and a lesser degree of significance. Figure 4.1 shows an increase in reported wood use following the 2009 spike in fuel oil price (Figure 4.3), which could explain the increase in the $OC/PM_{2.5}$ ratio. ADEC employees report that wood stove sales are high in the Fairbanks area, supporting the survey results. Figure 3.14 shows that no change in the carbon fraction of the particulates occurs with the observed temperature fluctuations. This indicates that the temporal increase in $OC/PM_{2.5}$ is not due to burning behaviors affected by temperature, such as an increase in wood stove emissions relative to oil and other emission sources at lower temperatures. Figure 4.1 (bar plots) shows the reported increase in the amount of heat obtained from wood in the Fairbanks area starting after the 2009 increase in fuel oil cost. Figure 4.2 shows that the percentage of wood stoves reported to be EPA certified has increased from 2006 to 2012, indicating that the increase in emissions from wood stoves is not due to an increase in the use of non-certified devices. One possible confounding factor is that a large decrease in the use of non-certified wood stoves could be offset by a small increase in the use of hydronic heaters (Section 1.8.2) or other highly polluting devices.

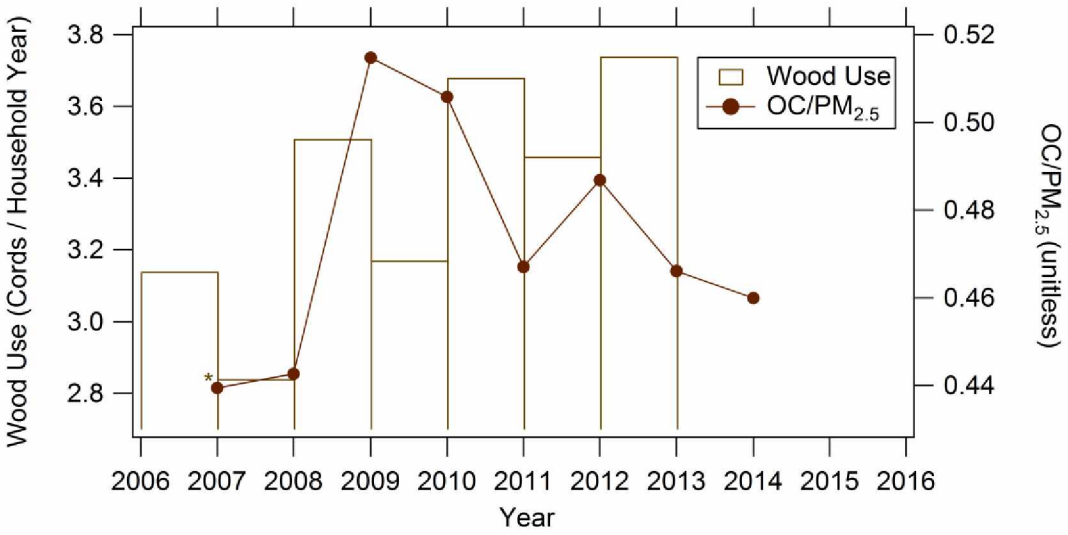

Figure 4.1: Ambient $OC/PM_{2.5}$ ratio plotted with the reported use of wood for home heating. $PM_{2.5}$ speciation from the Fairbanks SOB for the 2006-2007 through 2013-2014 violation seasons. Original data from (EPA, 2014b). Home heating survey results from (Alaska Department of Environmental Conservation, 2015).

Figure 3.14 (right plot) shows that there is a drop in the $NH_4^+/PM_{2.5}$ ratio after 2010 that is not stoichiometrically balanced by a drop in the $SO_4^{2-}/PM_{2.5}$ and $NO_3^-/PM_{2.5}$, and indicates that there is a trend towards a more acidic particle with less NH_4^+ after 2010, or that there is an increase in a particulate anion that is not SO_4^{2-} or NO_3^-. However, this difference might be explained by measurement error, since the MDL for NH_4^+ is 0.017 $\mu g\ m^{-3}$, close to the overall charge imbalance of 0.02 $\mu g\ m^{-3}$. The sampler change in 2009 may also impact the data, since blank values may not account for revolatization of NH_4^+ equivalently between samplers.

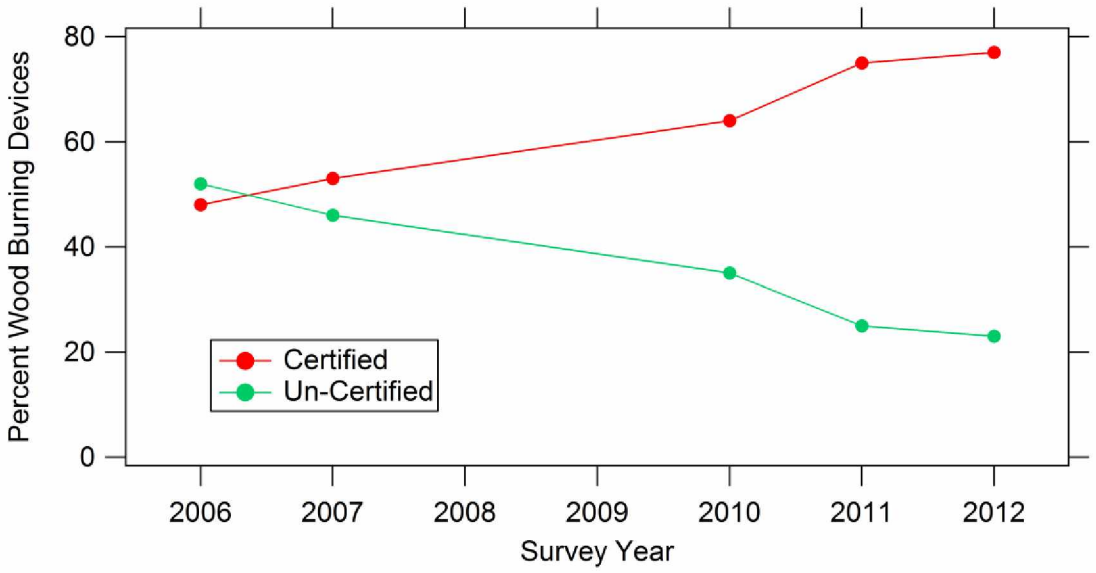

Figure 4.2: Certified and Un-Certified wood heating appliances in use in the Fairbanks North Star Borough. These percentages are calculated from responses to the Home Heating Survey, and represent the number of appliances, not the amount of use these appliances receive during the winter heating season (Alaska Department of Environmental Conservation, 2015).

4.2.4 Trends in Component/$PM_{2.5}$ Ratios

Figure 3.13 and Table 3.3 illustrate that the 2011-2012 and 2012-2013 mean violation season $NH_4^+/PM_{2.5}$ and $SO_4^{2-}/PM_{2.5}$ ratios are significantly lower than the overall mean. Table 3.2 shows that there is a significant downward temporal trend observed in both the $NH_4^+/PM_{2.5}$ and $SO_4^{2-}/PM_{2.5}$ ratios from the 2006-2007 to the 2013-2014 violation seasons. The combination of these findings provides strong evidence that there has been a decrease in the $NH_4^+/PM_{2.5}$ and $SO_4^{2-}/PM_{2.5}$ ratios. There are many possible explanations for this change. A decrease in either the NH_3 or SO_2 emissions, precursor gases for NH_4^+ and SO_4^{2-}, has likely occurred. A decrease in particulate $SO_4^{2-}/PM_{2.5}$ would result in a decrease in the particulate NH_4^+ that is drawn into the particle to neutralize SO_3^- produced from oxidation of SO_2. Figure 4.3 illustrates that one possible cause of the drop in the $SO_4^{2-}/PM_{2.5}$ ratio is the increase in fuel oil cost starting in 2009, which led to a decrease in the reported use of fuel oil starting that year. The drop took a few years to take

full effect, as expected since it takes time for a large number of households to switch to a new heating source. The reported use of oil and the observed particulate $SO_4^{2-}/PM_{2.5}$ did not return to pre-2009 levels by the end of this data set. Interestingly, Figure 4.4 shows that the drop in the $SO_4^{2-}/PM_{2.5}$ ratio did not occur simultaneously with the drop in fuel oil price. This discrepancy is likely due to participants who responded to the home heating survey underestimating their use of #2 fuel oil during the first year after the price spike.

No significant linear trend is observed in the $OC/PM_{2.5}$ ratio. However, a step-like increase occurs after the 2009 fuel oil price increase (Section 4.2.2). The decrease in the $OC/PM_{2.5}$ ratio after the 2011-2012 season despite the increase in the reported use of wood heat might be attributable to the decrease in emissions of stoves exchanged by the wood stove changeout program.

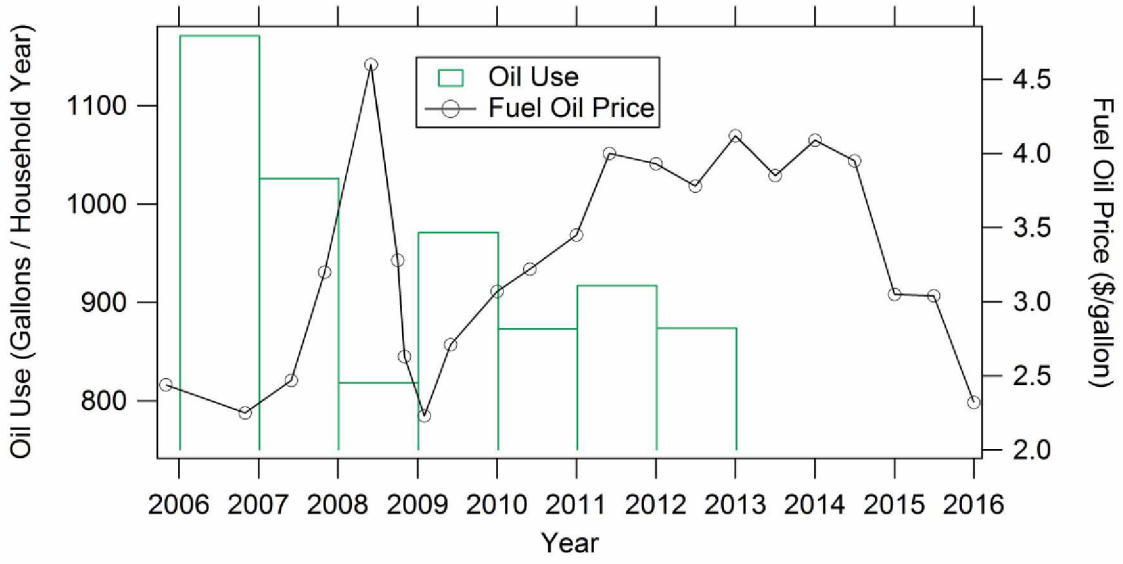

Figure 4.3: Fuel oil price and reported use of fuel oil in Fairbanks area, 2006-2015. Fuel oil prices from (State of Alaska Department of Commerce, 2016), home heating survey results from (Alaska Department of Environmental Conservation, 2015).

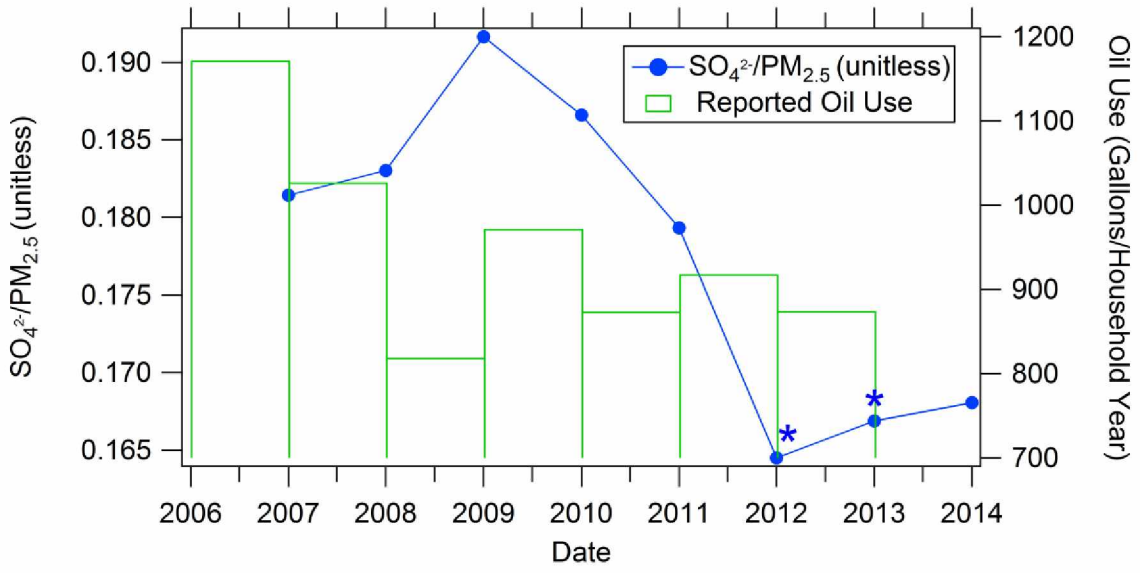

Figure 4.4: Violation season mean particulate $SO_4^{2-}/PM_{2.5}$ at the Fairbanks SOB, and reported gallons of fuel oil used per home in the Fairbanks area. $PM_{2.5}$ speciation from the Fairbanks SOB for the 2006-2007 through 2013-2014 violation seasons. Original data from (EPA, 2014b). Home heating survey results from (Alaska Department of Environmental Conservation, 2015).

While these changes are not statistically significant, the observed drop in $NH_4^+/PM_{2.5}$ and $SO_4^{2-}/PM_{2.5}$ ratios does not reflect a decrease in pure $(NH_4)_2SO_4$, since the stoichiometry of the neutralization reaction differs from the stoichiometry of the observed decrease in these components. Thus, this decrease is not attributable solely to a drop in particulate SO_4^{2-} and subsequent reduction in NH_4^+, nor is it attributable to pure dilution from an increase in another component such as OC. Huff (2014) finds that the Fairbanks system is SO_4^{2-} limited. If this is the case during the 2009-2010 through 2011-2012 violation seasons when the large drop in inorganic salts occurred, then the portion of the decrease in NH_4^+ that is balanced with a decrease in SO_4^{2-} could be attributable to both a decrease in sulfur emissions and dilution of SO_4^{2-} with increased OC due to increased wood stove use. Figure 3.14 shows a non-significant anti-correlation of both SO_4^{2-} and NH_4^+ with temperature, indicating that temperature may also affect emission composition changes or chemical mechanisms responsible for the observed decrease in seasonal

mean $NH_4^+/PM_{2.5}$ and $SO_4^{2-}/PM_{2.5}$ ratios. However, Figure 3.8 shows that there was a non-significant increase followed by a decrease in the mean temperature during this period, indicating the day to day relationship between the $NH_4^+/PM_{2.5}$ and $SO_4^{2-}/PM_{2.5}$ ratios and temperature does not directly explain the observed change in seasonal mean ratios. One possible mechanism is that at warmer temperatures demand for heat from oil decreases, which may have had a larger impact on the daily composition than on the seasonal mean particulate composition. Likely, the cause of the observed decrease in inorganic ions is due to a combination of multiple factors.

The lack of significant trends in the other component/$PM_{2.5}$ ratios (Figure 3.13 and Table 3.2 as well as large observable variability within the significant trends indicate that linear trends are not the best way to understand changes in particulate composition. The lack of significant trends is not surprising, since there are many changes in burning behavior that affect composition and are not expected to show linear change over this time period. These include wood moisture content, the ability for people with both oil and wood to choose their heating source on a daily basis, and other factors. For this reason, interannual variability (Section 4.2.2) is the preferred tool for understanding these changes.

4.3 Spatial Trends

4.3.1 Gravimetric $PM_{2.5}$

Figure 3.15 shows that the NPFS3 site has significantly higher gravimetric $PM_{2.5}$ than the other 3 sites, including the NPE site which is only 2.1 km away. This result indicates that there is little transport of particulates from one city to the other, and also very little transport within the same city. Therefore, sources that are closest to the samplers contribute greatly to the particles measured at that sampler, and the sources located close to the NPFS3 sampling site are producing

significantly more particulates than the sources near the other sites. Ward (2012) found that the North Pole sampling site used in this CMB study had a higher mean gravimetric $PM_{2.5}$ mass concentration than the sites in Fairbanks, supporting our finding. This result does not allow blanket statements regarding the overall differences between air in Fairbanks vs air in North Pole, since the number of sampling sites is so small. Maps of $PM_{2.5}$ mass concentration with higher spatial resolution have been made based on data from the FNSB sniffer car (Alaska State Department of Environmental Conservation, 2013). This data was not used in this thesis as it has a lower data quality than the 24-hour filter data that is the basis for this thesis.

Figure 3.16 illustrates that an R^2 of about 0.8 is observed when daily $PM_{2.5}$ mass concentration measurements are correlated between sites in the same city, and a value of about 0.5 is observed when sites in different cities are correlated. This result provides evidence that the meteorological factors that contribute to the intensity of trapping are more similar between sites in the same city than sites in different cities. The intensity of particle emissions also plays a role in determining the amount of particles measured at a sampling site, and thus this result indicates that the factors that control emission intensity such as burning behavior are more similar between sites in the same city than in sites from different cities. Since the same heating device with a different user can have drastically different emission intensities, the correlation of $PM_{2.5}$ mass concentration does not indicate directly that there are differences in sources. $PM_{2.5}$ composition is a far better indicator of the source of the pollution.

4.3.2 Composition Differences

Table 3.3 shows that many significant differences are observed in $PM_{2.5}$ composition between sampling sites in North Pole and Fairbanks. This provides strong evidence that Fairbanks and North Pole have different sources of $PM_{2.5}$. Specifically, the larger $OC/PM_{2.5}$ ratio and smaller

$SO_4^{2-}/PM_{2.5}$ ratio at the NPFS3 sampling site supports the hypothesis that wood smoke contributes a larger fraction to the particulates in the NPFS3 area, and #2 fuel oil contributes more to the areas near sampling sites in Fairbanks. This result is supported by CMB modeling analysis, which found that for all three winter seasons analyzed, the North Pole site had a higher $PM_{2.5}$ contribution from wood smoke than the Fairbanks sites (Ward, 2012), and is in agreement with the results of the home heating phone survey that found a greater portion of homes in North Pole use wood for heat (Carlson, 2010). The significant difference in the $K^+/PM_{2.5}$ ratio between all sites except the two in North Pole indicates that the source for potassium is dominant in North Pole and highly variable. While potassium is sourced from both fossil and non-fossil sources, it has been used as a tracer for wood smoke (Pachon et al., 2013), and thus this result would support the conclusions drawn from the $OC/PM_{2.5}$ and $SO_4^{2-}/PM_{2.5}$ analysis. Potassium ion (K^+) is sourced from wood smoke, and other forms of potassium are sourced from soil. The soil derived potassium was calculated as the difference of the potassium measured with XRF and potassium ion measured with IC. Soil derived potassium measurements were below the MDL for the IC measurement at all four sampling sites, indicating that most, and possibly all, potassium is in the ion form, and sourced from wood smoke.

It is interesting to note that the SOB measures $EC/PM_{2.5}$ values that are closer to the values at NPFS3 than the NPE site. This indicates that the EC component is not sourced primarily from wood smoke, but rather a source common to the downtown Fairbanks and North Pole residential areas. The source profiles averaged in Figure 3.8 show that diesel exhaust is the most likely source of EC.

The larger standard deviation associated with the $OC/PM_{2.5}$ ratio than the $SO_4^{2-}/PM_{2.5}$ ratio indicates that the intensity of emissions from wood combustion are more sporadic than those from

toyo stoves. A wood stove must be started and fed to function, whereas an oil burning stove works consistently regardless of human behavior.

To determine if the significantly higher $Zn/PM_{2.5}$ ratios measured in Fairbanks sites could be attributed to brake ablation and vehicle oil burning, the traffic counts from the busiest street near the samplers at each location were obtained. Airport Way west of Lathrop Street, a measurement site close to the Fairbanks SOB, reported an average of 17,766 vehicle passes per month in 2013. Badger Rd west of Horseshoe Way, a measurement site close to NPFS3, reported 1,591 vehicle passes per month in 2013 (State of Alaska Department of Transportation, 2014). These results support the possibility that greater vehicle traffic could be responsible for the increased particulate Zn in Fairbanks.

4.4 Sulfur Oxidation

Section 2.8.1 describes how the primary SOR for #2 fuel oil combustion was calculated to be 0.4% using emission factors, and estimated as 2-8% using oxidation ratios provided in the text of the emission factor document. Both primary SOR values were compared to the ambient SOR.

Section 3.4.1 shows that the ambient SOR in Fairbanks is about 5%, and falls inside of the possible range of primary oxidation (2-8%) from the combustion of #2 fuel oil obtained directly from the provided oxidation ratios. Based on this primary SOR, we cannot determine if the observed particulate SO_4^{2-} is attributable to some secondary oxidation or is the result of solely primary oxidation. Under the assumption that the primary SOR is 2-8%, the SOR values above 8% in Figure 3.18 (right plot) could be attributed to secondary oxidation; however, there are many other explanations that could address the excess, such as measurement error or transport of particulate sulfur without the transport of proportional gaseous sulfur from point source pollution emitted above the inversion layer.

Use of the primary SOR calculated from the Fairbanks specific #2 fuel oil source profile and EPA emission factors (0.4%) results in the clear conclusion that secondary oxidation must be taking place.

Shakya and Peltier (2013) report sulfur oxidation ratios in Fairbanks to be 87% (±15%) in the winter and 46% (±29%) in the summer, similar to the finding of Laakso et al. (2003), who report the ambient SOR in Tanzania to be between 8% and 91%. The Fairbanks wintertime SOR reported by Shakya and Peltier (2013) is in strong disagreement with the wintertime SOR calculated in Section 3.4.1 of this thesis, which is unexpected since both analyses used much of the same data. The value reported by Shakya and Peltier (2013) is assumed to be a typo, since less oxidation should be taking place in the Fairbanks winter than in the sunny and moist air of Tanzania.

Use of the SOR to determine if secondary sulfur oxidation is taking place is limited by the inability to obtain the primary SOR for #2 fuel oil combustion from a single source profile measurement. It should be noted that this lack of certainty is not contradictory to the ADEC conclusion that secondary oxidation is taking place (Section 1.4.2).

Figure 3.18 (left plot) shows that there is no relationship between the amount of particulate Zn and the ambient SOR. Due to the possibility that the Zn emissions from waste oil combustion and brake ablation do not effectively mix with air masses that contain large amounts of SO_2, this lack of correlation cannot be used to assess the effect of Zn and other metals on the oxidation of atmospheric sulfur in this airshed. Additionally, it is possible that even when the ambient metal concentrations are at the lowest observed values, their concentrations are still sufficient to catalyze this reaction and increase the oxidized sulfur above primary values, resulting in no observable change in SOR at higher Zn concentrations.

4.5 Non-Sulfate Sulfur (NSS)

Figure 3.19 shows a correlation slope of about 1.2, indicating that about 20% of the particulate sulfur is in a form other than SO_4^{2-}. The good R^2 value indicates that this systematic bias is due to either a source of NSS that occurs consistently throughout the study period or to a systematic measurement error. This result is supported by Ward (2012) which states that there are known winter events with higher measured sulfur than sulfate that are associated with excess positive charge. This implies that there are anions in the particles that are not analyzed as part of the limited IC analysis used in long term air quality monitoring and that occurrence of these anions is correlated with the particulate NSS. The NPFS3 site does not show greater NSS than the Fairbanks SOB site, indicating that the NSS is not sourced from wood smoke, since the NPFS3 site has a greater contribution from wood smoke than the Fairbanks SOB site

4.6 Applications and Limitations of Source Profiles

Source profiles were used to qualitatively assess the sources of ambient particulates by comparing the composition of ambient particles with source profile emissions. Specifically, the high $SO_4^{2-}/PM_{2.5}$ ratio in #2 fuel oil exhaust that is not observed in any other profile indicates that the vast majority of SO_4^{2-} in the airshed is sourced from the combustion of fuel oil. The OCM/EC ratio could also be used to qualitatively assess the contribution of different sources to the ambient particles, however source profiles did not always report which OC/EC sampling and analysis method was used. Since these methods affect the OCM/EC split (Section 2.1.1.1 and 2.1.2.3), the OCM/EC source profile measurements contain a degree of uncertainty. Ambient particle measurements were converted using the correction method in this thesis (Section 2.7.4) however this is not possible with source profile measurements. In addition, the OCM/EC ratios are very

close for different source categories (Table 3.3), and thus separating sources based on the OCM/EC ratio is less effective than separating sources with a more distinct tracer.

Table 4.1: OCM/EC ratios for the source profiles shown in Figure 3.1.

Source Category	OCM/EC Ratio
Woodsmoke	4.5
Gasoline exhaust	2.0
Diesel exhaust	1.8
#2 fuel oil exhaust	8.7

Source profiles depend on a large number of factors, including fuel used, appliance or vehicle type, age and maintenance, and operating/meteorological conditions (Ward, 2013) and (Alaska Department of Environmental Conservation, 2015). These factors can affect the total particulate emissions and composition of wood stove emissions (Kaivosoja et al., 2013). Thus, a set of profiles from the same source type may show large variability. Hays et al. (2008) report that the $PM_{2.5}$ source profile for low sulfur (0.14 ppm sulfur) #2 fuel oil has a SO_4^{2-}/RCM of 0.45, which is more than the SO_4^{2-}/RCM of the higher sulfur fuel oil (2,500 ppm sulfur) from the Fairbanks specific source profile (Figure 3.20).

Disagreement is observed between PM_1 source profiles (Kaivosoja et al., 2013) and $PM_{2.5}$ source profiles (Ward, 2013), and may indicate that the size fraction within $PM_{2.5}$ has an impact on the composition of particulates. This difference could also be attributed to the use of different combustion units in these studies, since the industrial boiler profile obtained in (Kaivosoja et al., 2013) may produce a different particle composition than the industrial boiler profile acquired from the EPA database (Ward, 2013). Poor mass closure, often as high as 50%, is observed in many fossil fuel source profiles. This is likely due to particle bound water associated with particulate SO_4^{2-} (Kaivosoja et al., 2013).

Chapter 5: Conclusions and Future Work

5.1 Conclusions with Regard to the Three Hypotheses

5.1.1 Hypothesis 1: Significant differences in $PM_{2.5}$ composition and mass concentration will exist between North Pole and Fairbanks sampling sites.

We hypothesized that the component/$PM_{2.5}$ mass ratios of major (OC, EC, SO_4^{2-}) and minor (K^+ and Zn) components would differ spatially between sampling sites in North Pole and Fairbanks due to different sources in these cities. Hypothesis 1 is supported based on the results from a comparison of the $PM_{2.5}$ mass concentration and composition at different sites, which is described in Section 4.3.2. Based on source profiles these differences are most likely attributable to a greater contribution of wood smoke to $PM_{2.5}$ in North Pole and #2 fuel oil in Fairbanks. The larger contribution of wood smoke in North Pole is also likely responsible for the higher concentrations of K^+, though there are other sources of this metal which may explain the high spatial variability of particulate K^+. The smaller (but still significant) differences in EC between Fairbanks and North Pole indicate that wood smoke and oil combustion exhaust contribute less to particulate EC than these sources contribute to particulate OC or SO_4^{2-}. This implies that ambient particulate EC is sourced primarily from a non-home heating source. Diesel emissions are the most likely source for this EC based on source profiles (Section 3.5). The significantly larger Zn concentrations in Fairbanks could be attributed to greater waste oil combustion or to greater vehicle traffic from increased brake ablation and vehicle oil burning. The "unknown Zn profile" identified in PMF modeling (Alaska Department of Environmental Conservation, 2014) cannot be identified based on this analysis.

For all components except EC, the NPE site is not as significantly different from the Fairbanks sites as the NPFS3 site. Most importantly, the SOB site has the same level of significant difference of $OC/PM_{2.5}$ ratio with the NCORE and NPE site, indicating that there is a greater similarity in particulate sources between the SOB and NPE site than the NPFS3 and NPE site. Since the NPE site is located in downtown North Pole this is likely due to the larger portion of business and homes that heat with oil in this area. The larger significant difference in the $SO_4^{2-}/PM_{2.5}$ ratio between the NPE site and the Fairbanks sites indicates that oil is a larger fuel source in Fairbanks than downtown North Pole.

5.1.2 Hypothesis 2: A reduction in the $OC/PM_{2.5}$ ratio will be observed after 2010.

We hypothesized that a decrease in wood stove based emissions due to the wood stove changeout program would result in a decrease in the ambient $OC/PM_{2.5}$ ratio after 2010 and a subsequent increase in all other $PM_{2.5}$ components. Since the $SO_4^{2-}/PM_{2.5}$ ratio is the next largest, we hypothesized that increases in this ratio will be largest. Figure 3.13 shows that no significant trends exist in the $OC/PM_{2.5}$ ratio and that the only significantly different violation season (2006-2007) is lower than the average season, implying an increase in the $OC/PM_{2.5}$ ratio occurred during the 2008-2009 season. The trend after the wood stove changeout program started appears to be going down, but was not tested for significance due to the small number of data points. Thus, hypothesis 2 is not supported by this analysis. However, the wood stove changeout and burn wise educational program may have still reduced $PM_{2.5}$ and decreased the $OC/PM_{2.5}$ ratio, but the decrease was obscured in this data set by an increase in wood stove use. As discussed in Section 4.2.2, the increase in #2 fuel oil cost may have increased the use of wood for home heating, and subsequently increased $OC/PM_{2.5}$ ratio. Figure 5.2 shows that the use of un-certified wood heating devices has decreased, however it is unknown if the subsequent decrease in OC emissions has been

offset by the increase in wood use (Alaska Department of Environmental Conservation, 2015), and any conclusion regarding the observed decrease the $OC/PM_{2.5}$ ratio after the 2011-2012 season is not supported with a statistically significant trend. With a longer term data set after the beginning of the WSCP, use of statistical tests would be useful to investigate if the program has decreased the $OC/PM_{2.5}$ ratio.

5.1.3 Hypothesis 3: Secondary sulfur oxidation is taking place during the Fairbanks winter.

It was hypothesized that secondary sulfur oxidation is taking place based on the inability of atmospheric models to predict the observed particulate SO_4^{2-}. Section 4.4 describes how the comparison of the ambient SOR with the primary SOR of oil combustion does not support or contradict this hypothesis.

Figure 3.18 shows that the ambient SOR was not correlated with the tracer Zn (and thus not correlated with other transition metals based on the assumption that these metals are co-emitted). As a result, the SOR does not provide evidence that a metal-catalyzed sulfur oxidation mechanism is taking place. This result does not imply that this mechanism is not taking place, just that this method is not able to determine if it is happening. More accurate analytical methods exist for measuring trace metals in particulates than XRF, and may allow the question of metal catalyzed oxidation to be properly addressed. Flights through the point source emission plumes during the winter could prove useful, since coal power plant plumes are a hypothesized source of particulate transition metals and moisture that could allow sulfur oxidation and observing trends of SOR and transition metals here may show a correlation unlike the measurements taken at ground level. All of these approaches assume that the air masses that contain transition metals also contain sufficient sulfur dioxide to allow this catalytic oxidation, however this may not be the case. Modeling or measurements could aid in understanding air mass transport would be useful in determining if the

mixing of sulfur rich air masses with metal rich air masses is taking place and could allow this oxidation pathway to occur.

5.3 Future Work: Investigating Recent Changes in Emissions

The North Star Borough has passed many regulations that may decrease the particulate pollution in the Fairbanks area, and in 2015 (after the end of the data analyzed in this thesis) prohibited the burning of trash, wet wood, and other highly polluting fuels in home heating appliances (FNSB, 2016). Continued assessment of long-term trends may provide evidence of the efficacy of these most recent regulations, in addition to the effect of education and changeout programs that continued after the 2012-2013 violation season when this analysis ended.

In addition, the company and refinery that produces local #2 fuel oil changed in 2014 when the Flint Hills Refinery in North Pole was closed. The results of our inquiry are not conclusive, however it appears that there may not have been a substantial change in the sulfur content of the #2 fuel oil produced in Fairbanks during the study period. The Flint Hills Refinery in North Pole produced Heavy Atmospheric Gas Oil (HAGO) and home heating oil until its closure in 2014, and were only willing to state that the sulfur content of the fuel was under ASTM specifications (Cook, J.: Personal Communication, email, Flint Hills, 2015). ASTM specifications are 0.5% or 0.05% sulfur for both #2 and #1 fuel oil, based on the sulfur rating (ASTM International, 2010). Current #2 fuel oil sold in Fairbanks is refined by Petro Star in North Pole, and the amount of sulfur in the fuel is unavailable[2]. Lab personnel at the refinery stated that the oil produced by Flint Hills likely had a similar sulfur content since it was coming from the same pipeline. However, future

[2] The reported concentration for this #2 oil was 0.005 % by weight when the website was accessed, and discussion with a representative indicated that this was a typo, and would be fixed. Typo not fixed as of 1/18/16, and Petro Star did not respond to email request for the actual value.

investigations are warranted to see if the change in refinery has affected the sulfur content of fuel used in Fairbanks, and composition of particulate pollution.

5.4 Future Work: Improved Statistics and Trend Analyses

This thesis focused on assessing the average particles encountered during the winter violation seasons. Future work could improve the validity of the statistical tests and trend analyses used here by removing the low concentration outliers not caught with the QC metric. This may improve the normalcy of the log normalized gravimetric mass concentration as well as component/$PM_{2.5}$ ratios.

An alternative approach to understanding these trends that would follow more closely the work done by the ADEC is to only use the upper quartile of measurements. Use of statistical tests and trend analyses used in this thesis on this data would allow a look at the extreme days when the majority of violations occur.

5.5 Future Work: Improved Source Apportionment

The carbon conversion developed as part of this work will allow improved source apportionment using CMB and PMF analysis. By providing a longer data set from multiple sites, models will be able to better calculate the sources of the $PM_{2.5}$. Principal Component Analysis (PCA) is another form of source apportionment, and has been used by the ADEC as part of the SIP. Use of this improved data set could improve the effectiveness of PCA analysis.

A tool that holds promise for assessing the source of the largest $PM_{2.5}$ component (OC) is the use of nuclear magnetic resonance (NMR) spectroscopy to determine the major functional groups in the OCM fraction of the particulates. Preliminary analysis discovered an observable difference in the relative contribution of different functional groups (in particular aromatics) to

$PM_{2.5}$ sourced from ambient filter measurements and from exhaust from a heating oil stove (Hooper, 2016). Further characterization of particulate matter OCM using NMR could allow a new data driven approach to identify the sources of the Fairbanks area $PM_{2.5}$.

5.6 Accessing Data for Future Research

The data and algorithms developed as part of this work are freely available in the IARC data archives and in the Scholarworks data archives. Please contact thesis author Kristian C. Nattinger or advisor William R. Simpson if you need assistance accessing this data or have other questions regarding this thesis.

Kristian Nattinger: kcnattinger@gmail.com

William R. Simpson: wrsimpson@alaska.edu

Literature Cited

Adams, J. R. and Merz, A. R.: Hygroscopicity of Fertilizer Materials and Mixtures, Ind. Eng. Chem., 21(4), 305–307, doi:10.1021/ie50232a003, 1929.

Alaska Department of Environmental Conservation: Alaska State Implementation Plan: Section III.D.5.08 SMAT (Speciated Modeleled Attainment Test). [online] Available from: https://dec.alaska.gov/air/anpms/SIP/SIPhome.htm, 2014.

Alaska Department of Environmental Conservation: Alaska State Implementation Plan: Section 5.6 Emission Inventory Data. [online] Available from: https://dec.alaska.gov/air/anpms/SIP/SIPhome.htm (Accessed 6 May 2015), 2015.

Alaska State Department of Environmental Conservation: The Need and Basis for More Stringent Wood-fired Heating Device Emission Standards Peer Review Draft. [online] Available from: https://dec.alaska.gov/air/anpms/comm/docs/justification_NOV13.pdf (Accessed 7 January 2015), 2013.

Alexander, B., Park, R. J., Jacob, D. J. and Gong, S.: Transition metal-catalyzed oxidation of atmospheric sulfur: Global implications for the sulfur budget, J. Geophys. Res. Atmos., 114(2), 1–13, doi:10.1029/2008JD010486, 2009.

ASTM International: ASTM Fuel Oil Specifications, [online] Available from: https://www.astm.org/ (Accessed 6 September 2016), 2010.

Brandt, C. and van Eldik, R.: Transition Metal-Catalyzed Oxidation of Sulfur(IV) Oxides. Atmospheric-Relevant Processes and Mechanisms, Chem. Rev., 95(1), 119–190, doi:10.1021/cr00033a006, 1995.

Broderick, D. and Houck, J.: PM2.5 Emission Reduction Benefits of Replacing Conventional Uncertified Cordwood Stoves with Certified Cordwood Stoves or Modern Pellet Stoves, Beaverton, OR., 2005.

Cahill, C. F.: Asian aerosol transport to Alaska during ACE-Asia, J. Geophys. Res., 108(D23), 8664–8671, doi:10.1029/2002JD003271, 2003.

Carlson, T.: 2010 Fairbanks Home Heating Survey, Sierra Res. Inc, 95811(SR-2010-06-01) [online] Available from: https://dec.alaska.gov/air/doc/Fbks_2010_HHSurvey.pdf (Accessed 5 August 2015), 2010.

Carlson, T. and Zhang, W.: 2013-2015 Fairbanks Home Heating Survey, [online] Available from: https://dec.alaska.gov/air/doc/Fbks_2013-15_HHSurvey.pdf (Accessed 5 October 2015), 2015.

Cheng, Y., Duan, F. K., He, K. Bin, Zheng, M., Du, Z. Y., Ma, Y. L. and Tan, J. H.: Intercomparison of thermal-optical methods for the determination of organic and elemental carbon: Influences of aerosol composition and implications, Environ. Sci. Technol., 45(23), 10117–10123, doi:10.1021/es202649g, 2011.

Chiappini, L., Verlhac, S., Aujay, R., Maenhaut, W., Putaud, J. P., Sciare, J., Jaffrezo, J. L., Liousse, C., Galy-Lacaux, C., Alleman, L. Y., Panteliadis, P., Leoz, E. and Favez, O.: Clues for a standardised thermal-optical protocol for the assessment of organic and elemental carbon within ambient air particulate matter, Atmos. Meas. Tech., 7(6), 1649–1661, doi:10.5194/amt-7-1649-2014, 2014.

Chow, J. C., Watson, J. G., Pritchett, L. C., Pierson, W. R., Frazier, C. a. and Purcell, R. G.: The dri thermal/optical reflectance carbon analysis system: description, evaluation and applications in U.S. Air quality studies, Atmos. Environ. Part A. Gen. Top., 27(8), 1185–1201, doi:10.1016/0960-1686(93)90245-T, 1993.

Chow, J. C., Watson, J. G., Crow, D., Lowenthal, D. H. and Merrifield, T.: Comparison of IMPROVE and NIOSH Carbon Measurements, Aerosol Sci. Technol., 34(March 2015), 23–34, doi:10.1080/027868201300081923, 2001.

Chow, J. C., Watson, J. G., Chen, L. A., Arnott, W. P., Moosmller, H. and Fung, K.: Equivalence of Elemental Carbon by Thermal / Optical Reflectance and Transmittance with Different Temperature Protocols Equivalence of Elemental Carbon by Thermal / Optical Reflectance and Transmittance with Different Temperature Protocols, Environ. Sci. Technol., (L), 4414–4422, doi:10.1021/es034936u, 2004.

Chow, J. C., Watson, J. G., Louie, P. K. K., Chen, L. W. A. and Sin, D.: Comparison of PM2.5 carbon measurement methods in Hong Kong, China, Environ. Pollut., 137(2), 334–344, doi:10.1016/j.envpol.2005.01.006, 2005.

Chow, J. C., Watson, J. G., Doraiswamy, P., Chen, L. W. A., Sodeman, D. a., Lowenthal, D. H., Park, K., Arnott, W. P. and Motallebi, N.: Aerosol light absorption, black carbon, and elemental carbon at the Fresno Supersite, California, Atmos. Res., 93(4), 874–887, doi:10.1016/j.atmosres.2009.04.010, 2009.

Chow, J. C., Watson, J. G., Chen, L. W. a, Rice, J. and Frank, N. H.: Quantification of PM2.5 organic carbon sampling artifacts in US networks, Atmos. Chem. Phys., 10(12), 5223–5239, doi:10.5194/acp-10-5223-2010, 2010.

Clegg, S. L. and Wexler, A. S.: The Extended Aerosol Inorganics Thermodynamics Model, [online] Available from: http://www.aim.env.uea.ac.uk/aim/aim.php (Accessed 6 June 2016), n.d.

Davies, J., Misiuk, D., Colgan, R. and Wiltse, N.: Reducing PM2 .5 Emissions from Residential Heating Sources in the Fairbanks North Star Borough, , (Cold Climate Housing Research Center) [online] Available from: http://cchrc.org/docs/reports/PM2.5_Final_2-23-09.pdf (Accessed 6 September 2015), 2009.

Desert Research Institute: DRI Model 2001 Thermal/Optical Carbon Analysis (TOR/TOT) of Aerosol Filter Samples - Method IMPROVE_A, Reno. [online] Available from: https://www3.epa.gov/ttnamti1/files/ambient/pm25/spec/DRI_SOPforIMPROVEAFINAL.pdf, 2005.

EPA: Air Quality System Code List, [online] Available from: http://www.epa.gov/aqs/aqs-code-list (Accessed 1 January 2015a), 2014.

EPA: United States Environmental Protection Agency Website, Air Qual. Database [online] Available from: http://www.epa.gov/ (Accessed 9 January 2014b), 2014.

FNSB: Fairbanks North Star Borough Code, [online] Available from: http://www.codepublishing.com/AK/FairbanksNorthStarBorough/?FairbanksNSB08/FairbanksNSB0821.html (Accessed 15 June 2016), 2016.

Frank, N. H.: Retained nitrate, hydrated sulfates, and carbonaceous mass in federal reference method fine particulate matter for six eastern U.S. cities., J. Air Waste Manag. Assoc., 56(3), 500–511, doi:10.1080/10473289.2006.10464517, 2006.

GVEA: Golden Valley Electric Association Webpage, [online] Available from: http://www.gvea.com/, 2015.

Han, Y., Chen, A., Cao, J., Fung, K., Ho, F., Yan, B., Zhan, C., Liu, S., Wei, C. and An, Z.: Thermal/optical methods for elemental carbon quantification in soils and urban dusts: Equivalence of different analysis protocols, PLoS One, 8(12), doi:10.1371/journal.pone.0083462, 2013.

Harris, D.: Quantitative Chemical Analysis, 6th ed., edited by M. L. Byrd, Michelle Russel Julet, New York., 2003.

Hays, M. D., Beck, L., Barfield, P., Lavrich, R. J., Dong, Y. and Vander Wal, R. L.: Physical and chemical characterization of residential oil boiler emissions, Environ. Sci. Technol., 42(7), 2496–2502, doi:10.1021/es071598e, 2008.

Holstius, D. M., Pillarisetti, A., Smith, K. R. and Seto, E.: Field calibrations of a low-cost aerosol sensor at a regulatory monitoring site in California, , 1121–1131, doi:10.5194/amt-7-1121-2014, 2014.

Hooper, M.: 2016 Environmental Chemistry Symposium, Charact. Org. Compd. Inter. Alaska Part. matter using NMR Spectrosc. [online] Available from: http://www.uaf.edu/chem/echemsymposium/, 2016.

Houk, J., Chow, J., Watson, J., Simons, C., Pritchett, L., Goulet, J. and Frazier, C.: Determination of Particle Size Distribution and Chemical Composition of Particulate Matter from Selected Sources in California, Reno. [online] Available from: https://www.dri.edu/images/stories/editors/eafeditor/Houcketal1989CASourceProfilesALL.pdf, 1989.

Hsu, Y., Divita, F. and Dorn, J.: FINAL REPORT EPA / 600 / R-13 / 307 Database Development Documentation., 2014.

Huff, D.: Addressing the Precursor Gases for Fairbanks PM2.5 State Implementation Plan. [online] Available from: https://dec.alaska.gov/air/anpms/SIP/SIPhome.htm, 2014.

Jacob, D.: Atmospheric Chemistry, First., Princeton University Press, Princeton, NJ. [online] Available from: http://acmg.seas.harvard.edu/people/faculty/djj/book/, 1999.

Joyce, P. L., von Glasow, R. and Simpson, W. R.: The fate of NO_X emissions due to nocturnal oxidation at high latitudes: 1-D simulations and sensitivity experiments, Atmos. Chem. Phys., 14(14), 7601–7616, doi:10.5194/acp-14-7601-2014, 2014.

Jung, C.-R., Lin, Y.-T. and Hwang, B.-F.: Ozone, particulate matter, and newly diagnosed Alzheimer's disease: a population-based cohort study in Taiwan., J. Alzheimers. Dis., 44(2), 573–84, doi:10.3233/JAD-140855, 2015.

Kaivosoja, T., Jalava, P. I., Lamberg, H., Virén, A., Tapanainen, M., Torvela, T., Tapper, U., Sippula, O., Tissari, J., Hillamo, R., Hirvonen, M. R. and Jokiniemi, J.: Comparison of emissions and toxicological properties of fine particles from wood and oil boilers in small (20-25kW) and medium (5-10MW) scale, Atmos. Environ., 77, 193–201, doi:10.1016/j.atmosenv.2013.05.014, 2013.

Karanasiou, A., Diapouli, E., Cavalli, F., Eleftheriadis, K., Viana, M., Alastuey, A., Querol, X. and Reche, C.: On the quantification of atmospheric carbonate carbon by thermal/optical analysis protocols, Atmos. Meas. Tech., 4(11), 2409–2419, doi:10.5194/amt-4-2409-2011, 2011.

Kossover, R.: Association between Air Quality and Hospital Visits — Fairbanks , 2003 – 2008, Anchorage, AK. [online] Available from: http://www.epi.hss.state.ak.us/bulletins/docs/b2010_26.pdf, 2010.

Laakso, L., Hussein, T., Aarnio, P., Komppula, M., Hiltunen, V., Viisanen, Y. and Kulmala, M.: Diurnal and annual characteristics of particle mass and number concentrations in urban, rural and Arctic environments in Finland, Atmos. Environ., 37, 2629–2641, doi:10.1016/S1352-2310(03)00206-1, 2003.

Leelasakultum, K., Mölders, N., Tran, H. N. Q. and Grell, G.: Potential impacts of the introduction of low-sulfur fuel on PM 2.5 concentrations at breathing level in a subarctic city, Adv. Meteorol., 2012(2), doi:10.1155/2012/427078, 2012.

Met One Instruments Inc: SASS Specifications, Grants Pass., 2016.

Naeher, L. P., Brauer, M., Lipsett, M., Zelikoff, J. T., Simpson, C. D., Koenig, J. Q. and Smith, K. R.: Woodsmoke Health Effects: A Review, InhalationToxicology, 19(1), 67–106, doi:10.1080/08958370600985875, 2007.

Office of Air Quality Planning and Standards: Fuel Oil Combustion. [online] Available from: http://www.epa.gov/ttnchie1/ap42/ch01/final/c01s03.pdf, 1995.

Ohta, S.: A Chemical Characterization of Atmospheric Aerosol in Sapporo, Atmos. Environ., 24(4), 1990.

Pachon, J. E., Weber, R. J., Zhang, X., Mulholland, J. a. and Russell, A. G.: Revising the use of potassium (K) in the source apportionment of PM2.5, Atmos. Pollut. Res., 4(1), 14–21, doi:10.5094/APR.2013.002, 2013.

Peltier, R. E.: Exploratory Research of Wintertime Aerosol Chemical Composition at a Ground Location in Fairbanks , Alaska, [online] Available from: https://dec.alaska.gov/air/anpms/comm/docs/fbxSIPpm2-5/Peltier_Feb 10 2012 Final report.pdf, 2012.

Peterson, M. R. and Richards, M. H.: Thermal-optical-transmittance analysis for organic, elemental, carbonate, total carbon, and OCX2 in PM2.5 by the EPA/NIOSH method, Proceedings, Symp. Air Qual. Meas. Methods Technol., 1–20 [online] Available from: http://www.rti.org/pubs/oc-ec_paper_83_3b.pdf, 2002.

Sanders, P. G., Xu, N., Dalka, T. M. and Maricq, M. M.: Airborne brake wear debris: size distributions, composition, and a comparison of dynamometer and vehicle tests., Environ. Sci. Technol., 37(18), 4060–9, doi:10.1021/es034145s, 2003.

Scire, J. S., Strimaitis, D. G. and Yamartino, R. J.: A Users Guide for the CALPUFF Dispersion Model, Concord., 2000.

Seagrave, J. C., McDonald, J. D., Bedrick, E., Edgerton, E. S., Gigliotti, A. P., Jansen, J. J., Ke, L., Naeher, L. P., Seilkop, S. K., Zheng, M. and Mauderly, J. L.: Lung toxicity of ambient particulate matter from southeastern U.S. sites with different contributing sources: Relationships between composition and effects, Environ. Health Perspect., 114(9), 1387–1393, doi:10.1289/ehp.9234, 2006.

Seinfeld, J. and Pankow, J.: Organic Atmpospheric Particulate Material, Annu. Rev. Earth Planet. Sci., 31(1), 105–134, doi:10.1146/annurev.earth.31.100901.141329, 2003.

Shakya, K. M. and Peltier, R. E.: Investigating missing sources of sulfur at Fairbanks, Alaska, Environ. Sci. Technol., 47(16), 9332–9338, doi:10.1021/es402020b, 2013.

Solomon, P., Mitchell, W., Tolocka, M., Norris, G., Gemmill, D. and Wiener, R.: Evaluation of PM 2.5 Chemical Speciation Samplers for Use in the EPA National PM 2.5 Chemical Speciation Network, Research Triangle Park., 2000.

State of Alaska Department of Commerce: Fuel Price Survey, [online] Available from: https://www.commerce.alaska.gov/web/dcra/ResearchAnalysis/FuelPriceSurvey.aspx (Accessed 1 January 2016), 2016.

State of Alaska Department of Transportation: Annual Traffic Volume Report. [online] Available from: http://www.dot.alaska.gov/stwdplng/transdata/pub/Regional_Traffic_Reports/trafficdata_reports_nor/NR_2014_Traffic_Volume_Report.pdf, 2014.

Torvela, T., Tissari, J., Sippula, O., Kaivosoja, T., Leskinen, J., Virén, A., Lähde, A. and Jokiniemi, J.: Effect of wood combustion conditions on the morphology of freshly emitted fine particles, Atmos. Environ., 87, 65–76, doi:10.1016/j.atmosenv.2014.01.028, 2014.

Tran, H. N. Q. and Mölders, N.: Investigations on meteorological conditions for elevated PM2.5 in Fairbanks, Alaska, Atmos. Res., 99(1), 39–49, doi:10.1016/j.atmosres.2010.08.028, 2011.

Tran, H. N. Q. and Mölders, N.: Wood-burning device changeout: Modeling the impact on PMconcentrations in a remote subarctic urban nonattainment area, Adv. Meteorol., 2012, doi:10.1155/2012/853405, 2012.

Turpin, B. J. and Lim, H.-J.: Species Contributions to PM2.5 Mass Concentrations: Revisiting Common Assumptions for Estimating Organic Mass, Aerosol Sci. Technol., 35(1), 602–610, doi:10.1080/02786820119445, 2001.

University of Wyoming Department of Atmospheric Science: US Atmospheric Soundings, [online] Available from: http://weather.uwyo.edu/upperair/sounding.html (Accessed 10 January 2015), 2015.

URG Corporation: URG Corporation Webpage, [online] Available from: http://www.urgcorp.com/index.php/maintenance/urg-3000n/cyclone-assembly (Accessed 6 July 2016), 2016.

Wang, Y. and Hopke, P.: Is Alaska Truly the Great Escape from Air Pollution ? – Long Term Source Apportionment of Fine Particulate Matter in Fairbanks , Alaska, Aerosol Air Qual. Res., 14, 1875–1882, doi:10.4209/aaqr.2014.03.0047, 2014.

Ward, T.: Source Apportionment of PM2.5 in a Subarctic Airshed - Fairbanks, Alaska, Aerosol Air Qual. Res., (December 2009), 536–543, doi:10.4209/aaqr.2011.11.0208, 2012.

Ward, T.: Apportionment Research Study Final Report, (406), 1–171 [online] Available from: ftp://209.165.171.132/Air Quality/AQSymposiums/2011 AQ Symposium/Fairbanks CMB Final Report 061510.pdf (Accessed 6 January 2015), 2013.

Watson, J. and Chow, J.: The 1987-88 Metro Denver Brown Cloud Air Pollution Study, Volume II: Measurements., 1988.

Wu, C., Ng, W. M., Huang, J., Wu, D. and Yu, J. Z.: Determination of Elemental and Organic Carbon in PM2.5 in the Pearl River Delta Region: Inter-Instrument (Sunset vs. DRI Model 2001 Thermal/Optical Carbon Analyzer) and Inter-Protocol Comparisons (IMPROVE vs. ACE-Asia Protocol), Aerosol Sci. Technol., 46(6), 610–621, doi:10.1080/02786826.2011.649313, 2012.

Yatkin, S.: IMPRROVE Standard Operating Procedure for the X-Ray Fluorescence Analysis of Aerosol Deposits on PTFE Filters., 2014.

Zanobetti, A., Dominici, F., Wang, Y. and Schwartz, J. D.: A national case-crossover analysis of the short-term effect of PM2.5 on hospitalizations and mortality in subjects with diabetes and neurological disorders., Environ. Health, 13(1), 38, doi:10.1186/1476-069X-13-38, 2014.

Zhang, R.: The Elemental Composition of Atmospheric Particles at Beijing during Asian Dust Events in Spring 2004, Aerosol Air Qual. Res., 67–75, doi:10.4209/aaqr.2009.05.0038, 2010.

Zielinska, B., McDonald, J. and Hayes, T.: Northern Front Range Air Quality Study, Reno. [online] Available from: https://www.dri.edu/images/stories/editors/eafeditor/Zielinskaetal1998NFRAQS.pdf, 1998.

Appendix A: Data and Processing Code Archived with this Thesis

All data were extracted from the AQS database, located in the US EPA web site (EPA, 2014b), or were obtained directly from the ADEC. Extraction was accomplished through the use of python scripts written by William R. Simpson which are archived with this thesis. The full 2006-2014 data is located in one large file. The script pm_calcs.py did the following calculations and output the results into this file:

- Made a violation season flag (szn_flag) that can be multiplied by any wave to select only the violation season data. Parameters of interest that were season selected were named *_szn.
- Made a QC flag that can be multiplied by any wave to select only QC'd data. Parameters of interest that were QC'd were named *_qc.
- Created "collocated data" waves by removing all data except the data collected to develop the carbon conversion. Parameters of interest filtered to include just the colocation period were named *_coloc.
- OPM (other primary material) was calculated for each filter.
- Consistent EC and TC data sets were produced with conversion factors developed from the Fairbanks collocated data set. Parameters of interest corrected with this correction method were named *_corr.
- Consistent EC and TC data sets were produced with the Fresno correction. Parameters of interest corrected with this correction method were named corr_*_fres.
- SO_2 values were converted to the "potential sulfate," and stored in the SO2_tot_pot wave.
- NOy values were converted to the "potential nitrate," and stored in the NO3_tot_pot wave.

- Blank subtracted $PM_{2.5}$, sulfate, nitrate, and ammonia ambient concentrations were calculated.
- OC was determined from TC and EC. OCM, and RCM concentration were calculated.
- SO_2 and temp were added to the file.

Next, these files were analyzed with IGOR using macros written by William R. Simpson. These macros are archived with this thesis. The analysis in IGOR accomplished the following:

- The macro calc_ratios_and_stats utilizes the macros subrange_stats, analyze_season_multiyear, filter_season, filter_jja, stats_intersite, and zap_newyear_2 to accomplish the following:
    - calculates the startyear, count, mean, standard deviation, and median of $PM_{2.5}$ mass and component/$PM_{2.5}$ ratios for each specified parameter
        - runs t-test on these values for the spatial analysis
        - runs t-test on the seasonal trends of these values for the temporal analysis
    - removes January 1 and December 31 K_ion and K data for each year

Analysis at the IGOR command line or through the IGOR interface was done by Kristian C Nattinger to accomplish the following:

- Paired and not-paired t-tests were done in IGOR, and the results were copied to an excel document. The relevant values were referenced to a table in the same excel sheet and these tables were copied into the thesis.
- Figures and trend lines were done in IGOR.

Appendix B: Data Used in Creating Figures

Table B.5.1: Data used to create Figure 3.15. Paired t-test results on $PM_{2.5}$ gravimetric mass data (paired, log normalized data, 95% confidence, t-critical about 2). The t-critical is about 3.9 for the 99.99% confidence intervals. 2011-2012 through 2012-2013 violation season data. Original data from (EPA, 2014b).

Site	# filters	Mean $PM_{2.5}$/(ug/m^3)	stdev	Mean $\log_{10}$ [$PM_{2.5}$/(ug/m^3)]	stdev	t-score	
						NCORE	1.1
SOB	99	19.6	10.8	1.213	0.290	NPE	1.6
						NPFS3	**5.9**
						NPE	1.9
NCORE	104	20.6	11.4	1.231	0.301	**NPFS3**	**4.6**
NPE	61	23.3	19.1	1.207	0.409	**NPFS3**	**11.0**
NPFS3	71	45.4	37.4	1.487	0.423		

Table B.5.2: Data used to create Figure 3.20. Source profile mean and standard deviation values. Number of source profiles used for each average are as follows: n=9 for wood smoke, n=10 for gasoline exhaust, n=9 for diesel exhaust, and n=1 for #2 fuel oil exhaust.

Mean Component/$PM_{2.5}$ Ratios (standard deviation)				
Parameter	**Wood Smoke**	**Gasoline Exhaust**	**Diesel Exhaust**	**#2 Fuel Oil Exhaust**
OCM/$PM_{2.5}$	0.81 (0.10)	.68 (0.11)	0.63 (0.30)	0.52
SO_4^{2-}/$PM_{2.5}$	0.006 (0.006)	0.011 (0.007)	0.014 (0.007)	0.30
EC/PM2.5	.18 (0.05)	0.34 (0.14)	0.35 (0.14)	0.06